

Carbon Monoxide Exchanges between Soils and the Atmosphere

Janet Mary Moxley BSc MSc

Thesis submitted for the Degree of Doctor of Philosophy in the Faculty of Science,
Institute of Ecology and Resource Management.

UNIVERSITY OF EDINBURGH

1996



Declaration

I, Janet Mary Moxley, declare that this thesis was composed entirely by myself, and that the work described herein was carried out by myself except where specifically acknowledged.

Acknowledgements

There are several people who I would like to thank for their involvement in this thesis. Firstly my supervisors, Dr. Keith Smith of the Institute of Ecology and Resource Management, University of Edinburgh, and Dr. Neil Cape, of the Institute of Terrestrial Ecology, Bush Estate, Edinburgh, for their advice and guidance during the work described. I would also like to thank all of the of my colleagues in the Soils Dept. at SAC Edinburgh for their support, in particular John Parker for assistance in carrying out N analyses on my samples, and Dr. Karen Dobbie and Simona Castaldi for allowing me access to their data on methane and nitrous oxide fluxes respectively. Robert Storeton-West and Chris Fletchard of Institute of Terrestrial Ecology, Bush Estate, Edinburgh deserve thanks for their assistance in transporting equipment to the Leadburn field site. The work was funded by the Natural Environment Research Council. Finally I would like to thank Stephen Finney for his support and encouragement while I have been working on this project, and to dedicate this thesis to the memory of my mother.

Abstract

Carbon monoxide (CO) is an important atmospheric trace gas; it is the main sink for the hydroxyl radical which oxidises many other trace gases including methane, and is also involved in the production of tropospheric ozone. Oxidation by soil microorganisms accounts for approximately one fifth of the CO sink, the remainder being removed by reaction with hydroxyl. The size of the soil sink for CO is not accurately known, and the factors which affect the rate of oxidation are not fully understood. In addition, there is evidence that soils may be net sources of CO in some circumstances. This work investigated CO fluxes between soils and the atmosphere at a variety of scales, from laboratory incubations to measurements in the nocturnal boundary layer, to identify the major controlling factors and quantify fluxes.

Laboratory incubations of a wide range of Scottish soils showed that the soil total organic carbon (TOC) content was the main factor influencing CO oxidation. This may reflect increases in microbial biomass with increasing TOC content. Multiple linear regression showed that water content was also important, and further investigation showed that there was an optimum water content for oxidation which was close to the field capacity. Static chamber measurements at arable and woodland sites showed that the most important factor affecting CO oxidation within a site was temperature. In several cases there was a negative linear relationship between CO uptake rate and temperature. This unusual relationship was attributed to simultaneous CO production from dead or senescent plant litter. In contrast, fallow arable land showed an optimum rate at approximately 10 °C. During May-June 1994 continuous measurements were made of the CO concentration in clean air. This followed a diurnal pattern with decreasing during the night, increasing in the early morning, and showing little change in the late morning and afternoon. The decrease in CO concentration at night was thought to be caused by deposition to the ground, and oxidation of CO by soil microorganisms. The mean deposition velocity was $1.1 \times 10^{-3} \text{ m s}^{-1}$, which is in reasonable agreement with values obtained by other methods. At similar experiment in July-Aug 1996 found CO deposition with a mean deposition velocity of $1.8 \times 10^{-3} \text{ m s}^{-1}$.

A series of experiments to investigate CO production found that soils which normally oxidised CO could be converted into sources by drying or sterilising. CO production was further increased by wetting dried or sterilised soils. The rate of CO production was proportional to the soil TOC content. A possible mechanism is the breakdown of large organic acids to smaller ones, such as formic acid, which is known to decompose to yield CO. In this study, both humic and formic acids were shown to produce CO in circumstances similar to those in which soils produced it.

In an area of wet peatland net CO production was observed from some chambers during the wetter months of the year, although CO oxidation occurred in all chambers during dry conditions in the summer. The CO production appeared to occur just above the watertable. No CO production occurred when cores from this site were incubated under aerobic conditions, which suggests that the CO production at this site took place under anaerobic conditions.

Table of Contents

Declaration.....	i
Acknowledgements	ii
Abstract.....	iii
Table of Contents.....	iv
Index of Plates, Figures and Tables.....	ix
Chapter 1: Review of literature on the exchange of carbon monoxide between soil and the atmosphere.....	1
1.1 Atmospheric carbon monoxide.....	1
1.1.1 Introduction	1
1.1.2 Sources of carbon monoxide	2
1.1.3 Sinks for carbon monoxide.....	4
1.1.4 Distribution of carbon monoxide in the troposphere	6
1.1.5 Seasonal variation	7
1.1.6 Long term trends.....	8
1.2 Soil as a sink for carbon monoxide.....	9
1.3 Emission of carbon monoxide from soils.....	15
1.3.1 Carbon monoxide emission from dry soils.....	15
1.3.2 Carbon monoxide emission from waterlogged soils.....	20

2: General experimental methods 23

2.1 Analytical methods23

2.1.1 Carbon monoxide..... 23

2.1.2 Soil analyses..... 26

 i) Ammonium and nitrate-N 26

 ii) Microbial biomass carbon 27

 iii) Moisture content 29

 iv) pH..... 29

 v) Texture..... 29

 vi) Total organic carbon (TOC). 30

**2.2 Laboratory methods for measurement of CO oxidation and
production rates.....31**

2.3 Field measurements33

2.3.1 Chamber measurements of CO fluxes 33

2.3.2 Continuous atmospheric CO measurements 35

2.4 Statistical treatment of data36

2.4.1 Calculation of means and standard deviations. 37

2.4.2 Linear regressions, the correlation co-efficient and curve fitting..... 38

2.4.3 Comparison of means and slopes: t tests..... 40

2.4.4 Analysis of variance (ANOVA) 41

2.4.5 Analysis of factorially designed experiments. 42

Chapter 3: Oxidation of CO by soils: field and laboratory studies..... 45

3.1 Introduction45

3.2 Materials and Methods.....46

3.2.1 Laboratory Studies.....46

3.2.2 Field measurements47

3.2.3 Analytical Methods.51

3.2.4 Statistical Analysis51

3.3 Results51

3.3.1 Laboratory Incubations51

3.3.2 Field Measurements63

 i) Bush.....63

 ii) Gullane.....66

3.4 Discussion.....70

3.5 Conclusions75

3.6 Acknowledgements76

Chapter 4: Factors affecting CO production by soils under aerobic conditions: laboratory investigation..... 77

4.1 Introduction77

4.2 Materials and Methods.....78

4.2.1. Incubations78

4.2.2. Analytical methods.....80

4.3 Results 81

4.4 Discussion..... 89

4.5 Conclusions 93

4.6 Acknowledgement..... 93

Chapter 5: CO production by waterlogged soils. 94

5.1 Introduction 94

5.2 Materials and Methods..... 94

5.2.1 Laboratory studies 94

5.2.2. Field measurements..... 96

5.3 Results 98

5.3.1 Laboratory experiments..... 98

5.3.2 Field measurements..... 100

5.4 Discussion..... 101

5.5 Conclusions 103

5.6 Acknowledgement..... 103

**Chapter 6: Depletion of carbon monoxide from the nocturnal
boundary layer..... 104**

6.1 Introduction 104

6.2 Measurement Procedures 106

6.3 Results 109

6.4 Discussion..... 114

6.5 Conclusions 120

6.6 Acknowledgements 120

**Chapter 7: Attempted measurement of CO fluxes using flux
gradient micrometeorology 121**

7.1 Introduction 121

7.2 Measurement procedures 122

7.3 Results 124

7.4 Discussion..... 127

7.5 Conclusions 128

7.6 Acknowledgements 129

Chapter 8: Discussion and Conclusions 130

Appendix 1: Standard RGA3 Reduction Gas Analyser settings..... 135

**Appendix 2: Results of factorial experiments, to investigate CO
production 139**

Appendix 3: Explanation of meteorological parameters..... 147

Index of Plates, Figures and Tables

Plates

	Title	Page
Plate 2.1	Equipment for measuring CO fluxes in the field: flux chamber, temperature probe and insulated box for transporting syringes.	36
Plate 3.1	The field site at Bush Estate, Midlothian, Scotland showing woodland area on left and fallow arable land on right.	49
Plate 3.2	The field site at Gullane, East Lothian, Scotland showing arable land on extreme left, woodland at back and set aside land on right.	49
Plate 5.1	The field site at Leadburn, Midlothian, Scotland	97
Plate A1.1	The RGA3 Reduction Gas Analyser	136

Figures

	Title	Page
Figure 1.1	Pathway for oxidation of phenolic substances yielding formic acid. Taken from Joglekar <i>et al.</i> (1991)	19
Figure 2.1a	Residuals of regression of reported CO concentration on actual concentration.	25
Figure 2.1b	Residuals of regression of reported CO concentration on actual concentration after repairs 6/2/95.	25
Figure 2.2	Calibration curve for CO monitor after repairs, 6/2/95.	26
Figure 2.3a	Configuration of the autoanalyser for ammonium-N analysis.	28
Figure 2.3b	Configuration of the autoanalyser for nitrate-N analysis.	28
Figure 2.4	Relationship between amount of soil used in jar experiments and measured rate constant for CO oxidation.	32
Figure 2.5	Cylindrical closed chamber. Taken from Smith <i>et al.</i> (1995).	35
Figure 3.1	Arrangement of replicate chambers on the coniferous woodland at Bush.	48
Figure 3.2	Relationship between CO oxidation rate and total organic carbon content of various Scottish soils.	57
Figure 3.3	Relationship between residuals of regression of k_{ox} on TOC and soil water content (omitting peaty loam soils).	58

Figures (cont).

	Title	Page
Figure 3.4	The effect of soil water content on CO oxidation.	59
Figure 3.5	CO oxidation rate constants of soil from 4 sites with contrasting land uses.	59
Figure 3.6	Variation in CO oxidation rate constant with depth in soils from contrasting land uses.	61
Figure 3.7	Variation in microbial biomass carbon with depth for soils from contrasting land uses, Gullane, 1994.	61
Figure 3.8	The effect of acetylene on CO oxidation	62
Figure 3.9	The effect of dicyandiamide (DCD) on CO oxidation	62
Figure 3.10	Decrease in CO concentration with time in the flux chamber on the coniferous woodland soil at Bush.	63
Figure 3.11	Seasonal variation in CO deposition velocity for soils at Bush.	65
Figure 3.12	Relationship between CO deposition velocity and soil temperature at Bush.	66
Figure 3.13	Seasonal variation in CO deposition velocity for soils at Gullane.	67
Figure 3.14	Nitrogen content of Gullane soils during 1995.	68
Figure 3.15	Relationship between rate constant for CO oxidation and soil temperature at Gullane.	69
Figure 3.16	Temperature dependence of CO production by litter from coniferous woodland at Bush.	74
Figure 4.1	Effect of drying and rewetting on soils from 4 sites.	82
Figure 4.2	Relationship between TOC content and rate of CO production by soils air dried at room temperature and not rewetted.	82
Figure 4.3	Effect of sterilising soils on CO production	83
Figure 4.4	Relationship between water content and CO production rate for soils from Bush air dried at ~ 25 °C and rewetted.	85
Figure 4.5	Relationship between water content and CO production rate for soils from Bush air dried at ~ 25 °C and rewetted.	86
Figure 4.6	Change in CO concentration with time over air dried soils without rewetting.	89
Figure 4.7	Change in CO concentration with time over air dried soils without rewetting.	90
Figure 5.1	Variations in CO production rate with depth for peat cores from Springfield Farm, Leadburn, Midlothian, Scotland.	99
Figure 5.2	Relationship between water content and CO production rate for peat cores form Springfield Farm, Leadburn, Midlothian.	99
Figure 5.3	Seasonal variation in CO production rate on peat land at Springfield Farm, Leadburn, Midlothian.	100

Figures (cont).

	Title	Page
Figure 5.4	Change in CO concentration with depth at Leadburn 13/10/95.	101
Figure 6.1	Diurnal variation in CO concentration at Bush, May-June 1994. Average data for whole campaign.	110
Figure 6.2	CO concentration in boundary layer air overnight at Bush. Julian days 165 - 166 1994.	111
Figure 6.3	The relationship between cooling rate and boundary layer height.	112
Figure 6.4	The relationship between windspeed and boundary layer height.	112
Figure 7.1	CO fluxes measured by flux gradient micrometeorology at Springfield Farm, Leadburn, Scotland. Aug-Sept 1996	126
Figure 7.2	CO concentrations at Springfield Farm, Leadburn, Midlothian Scotland, 4/9/96.	126
Figure 7.3	CO concentration profiles	129
Figure A2.1	Results of factorial experiments on CO production by Gullane arable soil.	140
Figure A2.2	Results of factorial experiments on CO production by Gullane woodland soil.	142
Figure A2.3	Results of factorial experiments on CO production by Bush arable soil.	144
Figure A2.4	Results of factorial experiments on CO production by Bush deciduous woodland soil (dry area).	146

Tables

	Title	Page
Table 2.1	Design matrix for a 2 ² factorial experiment	43
Table 3.1	Properties of soils used in incubation experiments to measure CO oxidation rates.	52
Table 3.2	Rate constants for CO oxidation during laboratory incubations for Scottish soils.	56
Table 3.3	Variation in soil properties with depth at Gullane.	60
Table 3.4	Mean CO oxidation rate constants from soils under different vegetation types determined in the field at Bush.	64
Table 3.5	Activation energies for CO production by soils.	73
Table 4.1	CO production rates from dried soil.	80
Table 4.2	Design matrix for factorial experiments to investigate CO production by soils.	81
Table 4.3	Summary of results of factorial experiments to investigate CO production by dry soils.	88
Table 6.1	Literature values of the deposition velocity of carbon monoxide into soil.	105
Table 6.2	Nocturnal boundary layer parameters and CO deposition velocities at Bush Estate, Midlothian, Scotland during May and June 1994.	113
Table 6.3	Nocturnal boundary layer parameters and CO deposition velocities at Springfield Farm, Leadburn, Midlothian, Scotland during August and September 1996.	115
Table 6.4	Calculated and actual overnight CO concentration minima at Bush during May and June 1994.	118

Chapter 1: Review of literature on the exchange of carbon monoxide between soil and the atmosphere

1.1 Atmospheric carbon monoxide

1.1.1 Introduction

Carbon monoxide is a trace gas present in the troposphere at concentrations ranging from about 50 nl l⁻¹ in unpolluted areas in the southern hemisphere to more than 1000 nl l⁻¹ in locations subject to anthropogenic emissions (Section 1.1.4).

When interest in atmospheric CO first arose in the 1950s, it was thought to be purely the product of human activity (Bates and Witherspoon, 1952). There was concern because of rising anthropogenic emissions and its toxicity to humans. The only natural sink known was the soil, which was thought to be small sink compared with CO production. It is now known that CO has natural sources and other sinks, and interest is directed towards the important roles it plays in tropospheric chemistry.

CO affects the oxidising power of the troposphere by its interaction with the hydroxyl radical, OH•, which in turn affects the concentration of other trace gases including methane, CH₄, and ozone, O₃, which contribute to the greenhouse effect (Wofsy *et al*, 1972; Levy, 1973; Sze, 1977; Logan *et al*, 1981; Thompson and Cicerone, 1986 a,b). Ozone production can occur in locations where concentrations of CO and nitric oxide, NO, are high. Elevated concentrations of tropospheric ozone can damage vegetation and the human respiratory system.

Direct radiative forcing from CO was thought to be negligible (Shine *et al*, 1990) but recent evidence (Evans and Puckrin, 1995) suggested that CO itself is a minor

radiatively active gas. However, Sinha and Toumi (1996) point out that Evans and Puckrin's calculations are based on changes in irradiance at the surface rather than the tropopause, and ignore the effect of clouds and the non-uniform distribution of CO. Sinha and Toumi conclude that the radiative forcing from CO is likely to be small compared to that from chlorofluorocarbons (CFCs).

1.1.2 Sources of carbon monoxide

As well as anthropogenic production from fossil fuel and biomass burning (*e.g.* Bates and Witherspoon, 1952; Crutzen *et al*, 1979; Greenberg *et al*, 1984; Watson, C.E *et al*, 1990), CO is produced naturally in the troposphere from the oxidation by OH• of methane (McConnell *et al*, 1971) and non-methane hydrocarbons, NMHCs, (such as terpenes and isoprenes from plants) (Greenberg *et al*, 1990, 1992). Small amounts of CO are produced by photolytic decomposition of organic materials in sea (Swinerton *et al*, 1970) and pond water, by plants (Conrad 1988), asphalt (Tyler *et al*, 1990) and in certain circumstances, by soils (Section 1.3).

Although there is some doubt as to the exact strength of each source, estimates by various authors give reasonable agreement (Table 1.1).

The reaction of OH• radicals and methane is described below, and that with NMHCs is similar.

The OH• radical is produced when ozone is broken down photolytically to give oxygen molecules, and excited oxygen atoms:



Table 1.1 Estimated carbon monoxide source strengths

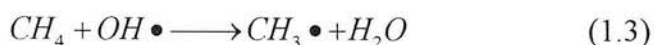
Source	Production (Tg year ⁻¹)(1)	Production (Tg year ⁻¹)(2)	Production (Tg year ⁻¹)(3)
Fossil fuel burning	425-1150	440-840	383
Biomass burning	310-1250	400-1600	730
Vegetation	50-200	50-100	165(4)
Ocean	20-80	20-180	165
Soil	-	2-32	-
Oxidation of methane	400-1000	300-900	800
Oxidation of non-methane hydrocarbons	280-1380	400-400	480
Total	1485-5060	1610-5050	2500-3000

(1) Logan *et al.* 1981 (2) Conrad 1988 (3) Müller 1992 (4) Total direct biogenic emissions

The excited oxygen atom reacts with water to give OH•:



The hydroxyl radical reacts with methane to produce a methyl radical:



This is followed by reaction with oxygen to give peroxyethyl radicals:



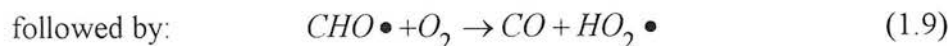
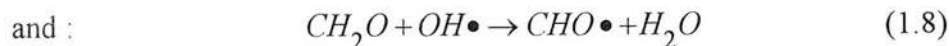
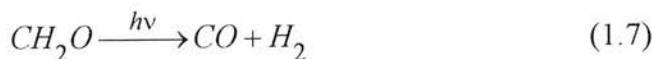
The peroxyethyl radicals then participate in a series of reactions, which in the presence of NO lead to formaldehyde, which breaks down by one of three routes to give CO (Crutzen and Zimmermann, 1991). The major path, accounting for 40 % of the breakdown is:



followed by:



Other routes are:



1.1.3 Sinks for carbon monoxide

There are two main sinks for CO: oxidation by OH• (McConnell *et al*, 1971), and oxidation by soil microorganisms (Section 1.2). Oxidation by OH• is the main sink (1400-3000 Tg y⁻¹), with oxidation by soil microorganisms accounting for 10 - 20 % of the total (240-530 Tg y⁻¹) (Conrad, 1988; Khalil and Rasmussen, 1990a).

Oxidation of CO by OH• produces CO₂:



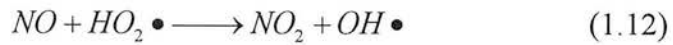
This would seem to lead to a loss of OH•, which could then lead to an increase in methane concentration due to a reduction in the rate of reaction (1.3). However, in areas where the concentration of nitric oxide is greater than the natural marine background concentration of approximately 150 pl l⁻¹, OH• is eventually regenerated, in a series of reactions which also result in the production of

tropospheric ozone (Fishman and Crutzen, 1978). In the northern hemisphere, this appears to have led to an increase in the average OH• concentration since preindustrial times (Crutzen and Zimmermann, 1991). The reactions proceed as shown below.

Firstly the H• produced in reaction (1.10) reacts with oxygen to produce a peroxy radical:



This then oxidises NO to NO₂ and regenerates OH• :



Ozone can then be generated via the photolysis of NO₂:



1.1.4 Distribution of carbon monoxide in the troposphere

The balance of the source and sink strengths of CO mean that its lifetime in the atmosphere is fairly short, about 0.3 year (Weinstock, 1969; Cicerone, 1988), and therefore its distribution is uneven.

Early studies of CO distribution by Robbins *et al.* (1968) in North America and the Pacific found considerable spatial variation in CO concentration, with concentrations of up to 900 nl l⁻¹ over Greenland, and only 90 nl l⁻¹ over Alaska. They also found appreciably lower concentrations of CO over the Pacific (about 50 nl l⁻¹) than over land. There were considerable variations in CO concentration in short periods of time depending on the wind direction and the origin of the air masses.

Seiler and Junge (1970) and Seiler (1974) measured CO concentrations in both the upper and lower troposphere. Seiler and Junge (1970) found that concentrations in the upper troposphere (8000-10,000 m) remained almost constant at 100-150 nl l⁻¹ in both the northern and southern hemispheres. Measurements of CO in the upper troposphere (Seiler, 1974) showed increased concentrations in the mid-latitudes, especially in the northern hemisphere. This suggested that the main sources of CO were in this region, with sinks in the stratosphere and the southern hemisphere. In support of this concept, Seiler and Fishman (1981) found evidence of inter-hemispheric transport of air with high concentrations of CO from the northern to the southern hemisphere.

All of the above workers found a marked difference between hemispheres when they examined the lower troposphere over the Atlantic. South of the intertropical convergence zone (ITCZ), the zone which divides the air masses of the southern hemisphere from those of the north, CO concentrations at sea level remained between

100 and 120 nl l⁻¹, but north of this point they reached 170-250 nl l⁻¹. Seiler and Junge (1970) took the increased CO concentration in the lower troposphere of the northern hemisphere as evidence that the sea is a source of CO. This was confirmed by measurements on samples of sea water, which showed supersaturation in all cases. However, they did not observe a comparable effect in the southern hemisphere, even though the water there was also supersaturated with CO. In contrast to Robbins *et al.* (1968), Seiler and Junge (1970) found little variation in CO concentration with time in the free troposphere, although Seiler (1974) did find large variations due to the transport of polluted air masses from Europe over the Atlantic.

Smaller scale variations have been found in areas which act as sources of CO, such as cities (Seiler and Zankl, 1976; Parrish *et al.*, 1991; Derwent *et al.*, 1994). The polluted air masses from such sources are able to travel considerable distances. The sources of the high CO concentrations in these air packets are clearly anthropogenic, as they also contain high concentrations of other pollutant gases such as chlorofluorocarbons and nitrogen oxides.

1.1.5 Seasonal variation

Seasonal variations in CO concentration have been observed in both hemispheres (Seiler *et al.*, 1984; Derwent *et al.*, 1994). Seiler *et al.* (1984) found that the CO concentration rose to a maximum in the southern hemisphere during the winter. Models showed that this could not be explained by decreased solar radiation leading to a decrease in the hydroxyl radical concentration, and hence decreased CO destruction during the winter. They suggested that the maximum could be due to changes in the position of the ITCZ. During the southern winter the ITCZ moves northwards, allowing larger areas of Africa, Asia, and America to influence the southern atmosphere. These land masses include areas which give rise to considerable

anthropogenic emissions of CO, and hence the CO concentration in the southern hemisphere increases.

Derwent *et al.* (1994) found that a similar maximum occurs in the northern hemisphere during the months of January to March.

1.1.6 Long term trends

Until recently the concentration of CO in the atmosphere of the northern hemisphere was thought to have been increasing at 1-2% per year since the start of industrial times, based on long-term monitoring work covering the period from 1950 onwards (Dianov-Klokov and Yurganov, 1981; Khalil and Rasmussen, 1984, 1988; Rinsland and Levine, 1985). No such increasing trend was detected in the southern hemisphere (Brunke *et al.*, 1990). Recent work (Bakwin *et al.*, 1994; Khalil and Rasmussen, 1994; Novelli *et al.*, 1994) shows that since 1988 CO concentrations have been decreasing by 2-6 % per year in both hemispheres. The reason for this decrease is not clear, but decreases in anthropogenic emissions and increased tropospheric oxidation have been suggested. Increased oxidation may occur as decreased stratospheric ozone allows more high energy radiation to reach the troposphere. This would generate more hydroxyl radicals. However, an increase in the hydroxyl radical concentration would also lead to increased oxidation of methane to form CO, which would tend to cancel out increased removal of CO. It would be expected that this effect would only be significant at high latitudes, but reductions in CO concentration of similar magnitude have been noted at all latitudes, reinforcing the view that decreased emissions, particularly from fossil fuels and biomass burning, could also be important (Khalil, 1995).

Data from before 1950 is extremely sparse. Robbins *et al.* (1973) attempted to measure the concentration of CO trapped in bubbles in polar ice cores, and found

concentrations of up to 400 nl l⁻¹. They concluded that these high concentrations were due to the production of CO from methane oxidation in the bubbles, and that CO concentrations may have been approximately 100 nl l⁻¹ for several centuries, with no marked increase with the onset of industrialisation. Recent analysis of CO in ice core bubbles suggests that the northern hemisphere CO concentration in 1802 may have been as high as 92 nl l⁻¹ (Haan *et al*, 1996): much higher than the concentration obtained by back-extrapolating the increase in carbon monoxide concentrations observed since 1950, which suggests concentrations of about 40 nl l⁻¹ at the start of the industrial era. Southern hemisphere CO concentrations appear to have remained constant at around 55 nl l⁻¹.

Many factors interact to govern the concentration of CO in the atmosphere. Whilst some of these are fairly well understood, more work needs to be done in many areas. The next sections focus on just one of these: the exchange of carbon monoxide between the soil and the atmosphere.

1.2 Soil as a sink for carbon monoxide

Several authors have observed removal of various pollutant gases, including CO, from the atmosphere by a variety of soils.(e.g. Frye *et al*, 1992; Smith *et al*, 1973). This removal of CO does involve incorporation directly into the soil, so the phrase " CO uptake", which is sometimes used is misleading. Bartholomew and Alexander (1979, 1982) found that ¹⁴CO is oxidised by microorganisms to ¹⁴CO₂, and not incorporated into the microbial cellular material. They also found that the presence of CO did not promote the uptake of CO₂. Duggin and Cataldo (1985) also found little incorporation of labelled carbon from CO into the soil, but almost complete oxidation of CO to CO₂.

The role of microorganisms has been shown in several experiments. When the soil is sterilised by autoclaving or irradiation (Inman *et al*, 1971; Bartholomew and Alexander, 1979) or treated with antibiotic solution (Inman and Ingersoll, 1971; Conrad and Seiler, 1980) the ability to oxidise CO is lost, although it can be restored to autoclaved soil by inoculating the sample with untreated soil (Inman and Ingersoll, 1971). An optimum temperature for CO oxidation of 40 °C has been found (Inman and Ingersoll, 1971; Bartholomew and Alexander, 1981), which again points to the biological nature of the CO oxidation process.

The term "oxidation" is used in this thesis to refer to the removal of CO from the atmosphere by soils, although no experiments were carried out to confirm the results mentioned above.

In contrast to Bartholomew and Alexander's (1979, 1982) results, Spratt and Hubbard (1981) found an increased assimilation of CO₂ into the soil organic matter in the presence of CO, but again no direct incorporation of CO. They also found increased CO oxidation by samples which had previously been exposed to high levels of CO. A similar result was obtained by Conrad and Seiler (1982a). This is reflected in the finding that roadside soils, which are exposed to high CO levels, show higher CO oxidation rates than those of other soils (Spratt and Hubbard, 1981; Ingersoll *et al*, 1974).

Studies have shown that CO oxidation follows first order kinetics, i.e. the rate of CO oxidation, R_{ox} is given by:

$$R_{ox} = k_{ox}[CO] \quad (1.15)$$

Where k_{ox} is the first order rate constant for CO oxidation (Heichel, 1973; Duggin and Cataldo, 1985).

Deviations from first order behaviour have been observed in some soils. In some experiments at high CO concentrations the Michaelis constant, K_m was exceeded, and the reaction became zero order with respect to CO (Inman *et al*, 1971). Heichel (1973) reported an exponential relationship between CO concentration and oxidation rate for soils with high water contents, which may have arisen due to reduced diffusion rates through the soil.

Although the oxidation of CO is well documented, the organisms responsible, and the benefits they derive from metabolising CO, are not fully understood. Much of the work, both with soils and with laboratory cultures of bacteria, is of limited applicability to the actual situation in natural soils, owing to the high concentrations of CO used (up to $130 \mu\text{l l}^{-1}$ (Inman *et al*, 1971)). To simulate realistic conditions in the soil, CO concentrations in the order of a few hundred nl l^{-1} should be used. Ambient CO concentrations in clean air are approximately 100 nl l^{-1} , although concentrations can reach $10 \mu\text{l l}^{-1}$ in urban air (Bower *et al*, 1995). Unfortunately, much of the earlier work in this area used detection systems which were not sufficiently sensitive to allow work at these concentrations, and higher ones were used.

Inman and Ingersoll (1971) suggested that fungi were the organisms responsible for the oxidation of CO, as they were able to extract several types of fungi from soil which were capable of oxidising CO, but they did not succeed in finding any bacteria which were able to do this. Further evidence that fungi are at least partly responsible for CO oxidation comes from Conrad and Seiler (1980), who found that CO oxidation was reduced in soil treated with streptomycin (which inhibits prokaryotic organisms i.e. bacteria). CO oxidation was completely halted by treating the soil with both

streptomycin and cycloheximide (which inhibits eukaryotic organisms e.g. fungi). They found the proportions of bacterial and fungal activity were dependent on the soil type.

Oxidation of CO occurs under aerobic conditions (Inman *et al*, 1971; Conrad and Seiler, 1980), and is halted (Inman *et al*, 1971) or inhibited (Conrad and Seiler, 1980) by anaerobicity. The latter authors suggested that pre-incubating the soil under anaerobic conditions can increase the rate of oxidation of CO.

Experiments with laboratory cultures of bacteria have isolated several types which are able to use CO as either a carbon source or an energy source, but the concentrations of CO used in these experiments were generally high ($0.5\text{--}500,000\ \mu\text{l l}^{-1}$) (Conrad *et al*, 1981, Daniels *et al*, 1977). Organisms which can grow on CO as sole carbon and energy source are known as carboxydobacteria. The oxidation is catalysed by a dehydrogenase enzyme (Meyer, 1985). Conrad (1984) calculated that to obtain enough energy for maintenance and growth from CO oxidation alone, they must have K_m values much lower than those exhibited by the bacteria in natural soil samples (i.e. have a greater affinity for CO). Few carboxydobacteria have been isolated which are capable of utilising ambient concentrations of CO. However, *Pseudomonas carboxydovorans*, as a suspension, or mixed with sterilised soil, has been found to remove CO from an atmosphere which initially contained $700\ \text{nl l}^{-1}$ CO (Conrad and Seiler, 1980). This removal was approximately four times more rapid in aerobic than anaerobic conditions.

There is evidence to suggest that methanotrophs and nitrifiers are able to oxidise CO, although the mechanism of oxidation is different from that in carboxydobacteria. Both methanotrophs and nitrifiers contain mono-oxygenases with CO oxidising activity (Bédard and Knowles, 1989). CO oxidation by pure cultures of nitrifiers and

methanotrophs has been observed in the laboratory (Ferenci, 1976; Jones and Morita, 1983; Jones *et al*, 1984), but again, the work has been done using very high CO concentrations. Conrad and Seiler (1982a) found that incubating soil in an atmosphere containing $1 \mu\text{l l}^{-1}$ CO, but no methane, did not lead to enhanced oxidation of added methane. This shows that methanotrophs gain no benefit from oxidising CO. Bender and Conrad (1994) have made an extensive investigation of the ability of methanotrophs, nitrifiers and carboxydobacteria in soil to utilise each others' preferred substrates. They found that both nitrifiers and methanotrophs can oxidise CO, but that this does not promote their own growth. However, carboxydobacteria cannot oxidise any other substrate. The size of the nitrifier population appeared to have more influence on CO oxidation rates than the size of the carboxydobacteria population. Carboxydobacteria were more effective at oxidising elevated concentrations of CO ($2,300 \mu\text{l l}^{-1}$) than ambient concentrations. This suggests that nitrifiers may be the main CO oxidising organisms in soil. In the short term addition of ammonium slightly inhibited CO oxidation, presumably as it was oxidised in preference to CO as it is the nitrifiers' preferred substrate.

Ingersoll *et al.* (1974) found that soils with high organic matter contents, such as those covered by natural vegetation, could oxidise CO more efficiently than those with lower organic matter contents, such as agricultural soils. Increased oxidation of CO was obtained by increasing organic matter in the soils, for example by adding manure or leaf mould. They also investigated another possible cause of the slow CO oxidation by the agricultural soil, namely the effect of herbicides, insecticides, and fungicides. Although the range of chemicals examined was fairly small, they only found one, the herbicide Triox, which reduced the ability of the soil to oxidise CO. Ingersoll *et al.* (1974) and Duggin and Cataldo (1985) examined the effect of organic matter and pH on CO oxidation rates and both studies found that oxidation was increased by high organic matter content, and low pH.

Spratt and Hubbard (1981) found that soil water content also affected the oxidation of CO by soils. They found that maximum removal rates were observed when the soil had been stored for several days at 100 % humidity. There was little CO oxidation by soils stored at less than 90 % humidity, but moistening the samples with water reduced the CO oxidation rate, a fact which they attributed to the increased resistance to gaseous diffusion in soils which contained waterlogged regions. Heichel (1973) also examined the effect of the soil water content, and concluded that gaseous diffusion is hampered by excess water. The optimum amount of water depends on the soil type. Comparing a field and a forest soil, he found that not only did the water content affect the rate of CO oxidation by both soils, but that the form of the dependence of the rate on the CO concentration changed too. At low water contents the rate was directly proportional to the CO concentration, whereas at high water contents there was an exponential relationship between the CO concentration and the rate of its removal. The field soil reached a plateau of maximum uptake when the water content exceeded about 10 % on a weight basis, whereas the forest soil showed a maximum in the CO destruction rate at a water content of about 55 %. The forest soils oxidised CO faster at all water contents.

The influence of vegetation cover on CO oxidation, using the same soil which has different vegetation, or which has been subjected to different management, has not been extensively examined. However, differences in land use could lead to changes in soil chemistry, biology and biochemistry which could in turn lead to changes in the efficiency of CO oxidation. Bartholomew and Alexander (1981) found that for two soils, a Brookston silty clay loam and a Holopaw sand, the CO oxidation rate was larger under hardwood forest than under cropland.

Sanhueza *et al.* (1994a,b) found that ploughing savannah soils led to increased CO oxidation, probably because the loosening allowed CO to diffuse further into the soil. This effect has not been explored for other soils.

1.3 Emission of carbon monoxide from soils

Although soil generally acts as a net sink for CO, there are certain circumstances in which soils can be a source of CO: i) in arid environments, especially after rewetting, and ii) in anaerobic, waterlogged conditions.

1.3.1 Carbon monoxide emission from dry soils

Production of carbon monoxide by dry soils has been observed both in the laboratory (e.g. Smith *et al.*, 1973; Conrad and Seiler, 1980, 1985c) and in the field (e.g. Marengo and Delaunay, 1980; Conrad and Seiler, 1982b, 1985 a,b).

In laboratory incubations (Conrad and Seiler, 1980), irrespective of whether the initial atmosphere contained no CO, or elevated concentrations, the same equilibrium value was reached. This showed that conditions existed where removal of CO was balanced by production.

Conrad and Seiler (1980) suggested that the CO production was non-biological, because when the soil was treated with antibiotics there was no CO removal, but its production continued. Ingersoll *et al.* (1974) found that CO was produced by soils which had been autoclaved.

Conrad and Seiler (1980) found that the CO production rate observed, R_p , in the absence of any removal appeared to be independent of the CO concentration, i.e.:

$$R_p = k_p \quad (1.16)$$

where k_p is the rate constant for CO production.

Combining equations 1.15 and 1.16 shows that, at equilibrium:

$$k_p = k_{ox} [CO] \quad (1.17)$$

Thus in theory, the gross CO production rate can be determined by preventing microbial oxidation of CO. However, in practice many methods of preventing microbial activity may also affect CO production rates, giving misleading results.

Seiler and Zankl (1976) also found that net CO production in unsterilised soils was enhanced at temperatures above 40 °C, but it is unclear whether this was a result of increased production of CO, or of reduced microbial oxidation.

In field studies, it is more difficult to prevent microbial oxidation of CO by sterilisation. To calculate gross reaction rates Conrad and Seiler (1985a) covered the field site with a sealed box and the CO concentration inside was allowed to come to equilibrium. The atmosphere inside the box was then injected with a slightly higher concentration of CO, and the removal rate of this surplus CO measured. This was used to calculate the constant k_{ox} , as the equilibrium CO concentration was known. The rate of CO production was then calculated.

This methodology was used in several field experiments (Conrad and Seiler 1985a), most of which were in arid areas. In an experiment at three sites in sub-tropical regions, they found that there was a net emission of CO from the soil. This emission still occurred when the sampling boxes were covered with metal foil to reduce

temperature fluctuations, and to keep out light. This suggests that the CO production process is not photochemical. The soils acted as a net sink for CO at night, and a net source in the day time. Similar diurnal patterns have been observed at other locations (Marenco and Delaunay, 1980; Scharffe *et al*, 1990; Sanhueza *et al*, 1994a,b). Conrad and Seiler (1985a) found that the rate of CO production increased exponentially with soil temperature, giving activation energies of 57-110 kJ mol⁻¹. They also found that wetting of the soil by heavy rainfall promoted CO production and that the production rate was proportional to the soil organic carbon content.

However, on the basis of laboratory work on a small set of soils, Conrad and Seiler (1985c) suggest that CO production rates are independent of soil organic matter content, but depend on the type of organic matter present. They suggest that CO may be produced from humic acids and other phenolic compounds by a reaction discovered by Miyahara and Takahashi (1971) who found that CO was produced by various phenolic compounds and aminophenols at high pHs (25 % KOH) in the presence of oxygen. They did not carry out experiments at other pHs to see whether the high pH was required for CO production. There was no relationship between oxygen consumption and CO production. The greatest CO evolution was from pyrogallol (1,2,3,-trihydroxybenzene), and the least from phloroglucinol (1,3,5-trihydroxybenzene). Pyrogallol produced an order of magnitude more CO than any other compound tested. It is not known which carbon from the ring is lost as CO. Miyahara and Takahashi (1971) suggest that the carbon monoxide may be produced by those phenols which polymerise in a complex manner during oxidation. If the high pH is a prerequisite for this decomposition, this reaction is not likely to occur in soils. However, a mechanism for the breakdown of phenols in the presence of water and oxygen at lower pH to yield a mixture of low molecular weight acids, including formic acid has been proposed by Joglekar *et al* (1991) (Figure 1.1). The reaction is used to remove phenols from wastewaters, where high temperatures and pressures

increase the rate. However, it may occur at lower rates at ambient temperature and pressures. An alternative pathway in the presence of light and a photocatalyst is proposed by Tseng and Huang (1990). Formic acid is known to decompose, to CO and water (Drury, 1994). It has been estimated that a full 2.5 l bottle of formic acid, could develop a pressure of 700 kPa over a one year period at 25 °C (Drury, 1994), and a warning is printed on the packaging of formic acid containers of the danger of CO build-up. Under strongly acidic conditions, the decomposition is fast enough to be one of the standard methods of laboratory scale CO production. Quantitative conversion to CO can be achieved by acidifying formic acid with concentrated sulphuric acid (Cotton and Wilkinson, 1980; Bartholomew and Alexander 1981, 1982). It is not known whether dehydration of formic acid occurs in soils.

Hendrickson and Kubiseski (1991) suggest that sucrose may enhance CO production by soils, and Conrad and Seiler (1980) found that CO production was promoted by adding glucose to the soil, or by prolonged (40-60 days) drying in air, followed by re-wetting.

Sanhueza *et al.* (1994a) found that degrading, dry, dead vegetation produced CO. This may contribute to emissions of CO from the ground. Tarr *et al.* (1995) also found emission of CO from dry plant matter, but that light was required. This would not explain the production of CO in the dark observed by Conrad and Seiler (1985a).

More work is needed to discover the range of soils which produce CO when dry, the effect of this process in the field and to determine the mechanism of CO production.

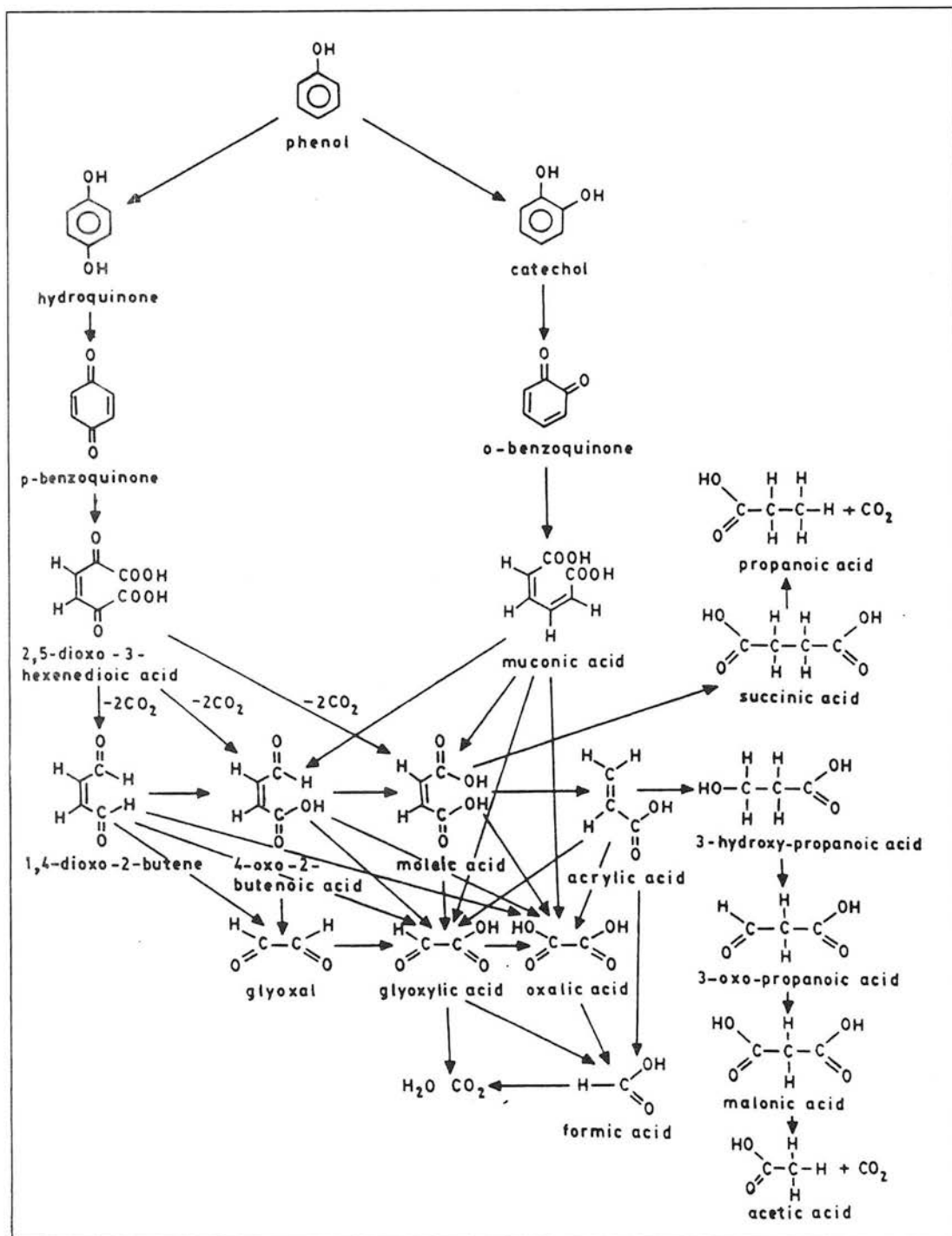


Figure 1.1 Pathway for oxidation of phenolic substances yielding formic acid.

Taken from Joglekar *et al.* (1991).

1.3.2 Carbon monoxide emission from waterlogged soils

Data on CO production from waterlogged soils is extremely limited. Most field data are the result of airborne measurement campaigns which suggest a source of CO close to the ground in wet areas such as the Amazon basin during the wet season (Harriss *et al.* 1990a; Kirchoff and Marinho, 1990; Ritter *et al.* 1990) and the north American tundra (Gosink and Kelley, 1979; Ritter *et al.* 1992,1994). Ritter (1994) reported CO sources of up to $30 \mu\text{g CO m}^{-2} \text{ h}^{-1}$ over the North American tundra, which showed a diurnal cycle corresponding to that of methane. These measurements did not allow the source of the emission to be identified, but models suggest that oxidation of hydrocarbons does not account for the amount of CO produced (Harriss *et al.* 1990b; Jacob and Wofsy, 1990). Thus the CO is likely to come either from direct emission by vegetation or the soil. Funk *et al.* (1994) reported that taiga bog cores with the water-table level with the top of the core are sources of CO, and suggest that waterlogged peatlands could be locally important sources of CO. They found mean CO fluxes from waterlogged cores of $37 \mu\text{g CO m}^{-2} \text{ h}^{-1}$ over a 130 day period, although there was considerable variation between cores. They state that CO emissions from peatlands may be responsible for up to 13 % of global CO production. This figure is very high, and appears to be based on a misinterpretation of a model by Khalil and Rasmussen (1990b) which apportions the CO source strength at each latitude. Funk *et al.*'s figure of 13 % of CO being produced by peatlands is based on the assumption that all CO north of 50° N is emitted directly from peatlands rather than produced by human activities or oxidation of methane. Taking Funk *et al.*'s CO emission rate, and an area of nonforested bog in the northern hemisphere of $897 \times 10^9 \text{ m}^2$ (Matthews and Fung, 1987), the CO emission from northern nonforested bog, based on a 130 day season for emissions, is calculated to be approximately 0.1 Tg y^{-1} , which is a tiny proportion of global emissions. Even if the $2 \times 10^{12} \text{ m}^2$ of forested bog in the northern hemisphere (Matthews and Fung, 1987) were assumed to emit CO at a similar rate,

the total northern hemisphere emission would still be only 0.3 Tg y⁻¹ based on a 130 day emission season.

Conrad *et al.* (1988) measured CO production from submerged rice paddies, and found that there was net production of CO, which showed a diurnal cycle, with fluxes ranging from 12 µg CO m⁻² h⁻¹ to 110 µg CO m⁻² h⁻¹, with peak production in the early afternoons. They calculated that CO emissions from rice paddies were about 0.3 Tg y⁻¹, which is negligible compared to the global CO budget. Emission of CO appeared to be limited by slow diffusion through the standing water. They reported that most transport from the soil was through the plants, and CO emission was greatly reduced when the rice plants were cut below the water-line. Khalil *et al.* (1990) found daytime CO fluxes from rice paddies of 100 µg m⁻² h⁻¹, equivalent to global emissions of 2 Tg y⁻¹. Very high rates of CO production (approximately 6100 µg m⁻² h⁻¹) have been reported following the application of cheese whey to soil, although the data should be treated with caution as very high ambient CO concentrations (up to 7.1 µl l⁻¹) are also reported (Bullock *et al.*, 1995). The whey had a large chemical oxygen demand of about 60 g l⁻¹, which would promote the formation of anaerobic zones in the soil. The hypothesis that the soil became anaerobic when CO production occurred was confirmed by the simultaneous production of methane.

Further evidence to suggest CO production by anaerobic zones in the soil comes from fieldwork which showed that CO concentration in the soil increased with depth in sites where the water-table was close to the surface, reaching a maximum just above the water level. (Liebl and Seiler, 1976; Seiler *et al.*, 1977).

Microbiological evidence supports the idea of biological CO production under anaerobic conditions. CO has been reported as a by-product of acetogenesis from CO₂ and H₂ (Diekert *et al.* 1984, 1986) and methanogenesis from a variety of

substrates including CO_2/H_2 , acetate and methanol (Conrad and Thauer, 1983; Hickey *et al.*, 1987). Bae and McCarty (1993) reported increased CO production when formate was added to an anaerobic digester during the methane fermentation of glucose. In the cases of both acetogenesis and methanogenesis the evolution of CO is thought to be linked to the action of carbon monoxide dehydrogenase (CMDH), and the formation of bound carbonyl compounds. In the case of acetogenesis, CO_2 is reduced to a bound form of CO by CMDH, which then goes on to be inserted into acetate as the carbonyl carbon (Diekert *et al.* 1984, 1986). However, in some cases the bound CO is able to exchange with free atmospheric CO until an equilibrium concentration is reached. CO concentrations of up to $1000 \mu\text{l l}^{-1}$ have been reported in some cases over cell suspensions of *Acetobacterium woodii* grown in a H_2/CO atmosphere (Diekert *et al.* 1984), although the concentration over growing cells is only about one tenth of this, as CO is assimilated into cell material (Diekert *et al.*, 1984; Eikmanns *et al.*, 1985). In the case of methanogenesis the exact mechanism depends on the substrate, but in all cases it is suggested that a bound form of CO is produced either which can be released into the atmosphere up to an equilibrium concentration. Concentrations of $2\text{-}250 \mu\text{l l}^{-1}$ are reported (Hickey *et al.*, 1987; Bae and McCarty, 1993).

Thus while there is some evidence that waterlogged soils can produce CO, much more work is needed before the factors affecting this source, and hence its possible significance, are clear.

2: General experimental methods

2.1 Analytical methods

2.1.1 Carbon monoxide

Carbon monoxide was measured using an RGA3 reduction gas analyser (Trace Analytical, Menlo Park, California, USA) (Appendix 1, Plate A1.1). This uses gas chromatography to separate CO from other gases which may interfere, and then detects the mercury vapour produced as the CO passes over a heated mercuric oxide bed.

CO was separated from other gases by passing through 2 chromatographic columns in series. These were both 77 cm long, the first packed with Unibeads 1S (60/80 mesh), and the second with molecular sieve 5A (60/80 mesh). The chromatographic columns were maintained at 105 °C. Zero grade air (BOC Speciality Gases, Guildford, UK), was used as the carrier gas at a flow rate of 30 ml min⁻¹. After separation, the CO passed over a mercuric oxide bed at 265 °C (Robbins *et al*, 1968; Seiler and Junge, 1967; Seiler *et al*, 1980), where the CO reduced mercuric oxide to mercury. The mercury vapour produced was detected by its absorption in the UV. The instrument's integrator electronics compared the size of the absorbance peak with that of calibration standards (BOC Speciality Gases, Guildford, UK), and displayed the concentration. The calibration standards were certified as 1.0 µl l⁻¹ CO in air. However, large variations were found between cylinders (up to 12 %), so each cylinder supplied was calibrated against the previous one, with the first cylinder being taken as having a CO concentration of 1000 nl l⁻¹. None of the cylinders were calibrated against primary standards, as the later were prohibitively expensive (P. Novelli, *pers. comm*; National Physical Laboratory, *pers. comm.*), and in any case differences in the concentrations of primary standards produced by different groups have been found (Novelli *et al*, 1991). The standard deviation of the CO

concentration between cylinders was 110 nl l^{-1} ($n = 5$). The concentration of CO in the original cylinder was measured on the RGA3 when it had been calibrated used a cylinder belonging to the University of East Anglia (supplied by Air Products Ltd Basingstoke, UK) which had a certified CO concentration of 1020 nl l^{-1} CO. The concentration of CO in the cylinder belonging to SAC provided by BOC, and certified as 1000 nl l^{-1} was found to be 1112 nl l^{-1} when measured against the Air Products cylinder. Standards of lower concentrations were made by diluting the 1000 nl l^{-1} standard with purified compressed air (BOC zero grade), which was purified by passing over Sofnocat (Molecular Products, Thaxted, Essex), a proprietary catalyst to remove CO. The standard error in the repeated measurement of the same sample was 4.5 %. The combined standard error in an individual measurement due to the combined uncertainties in the concentration of the standard and the measurement is 12 %.

The instrument was operated with a 1 ml sample loop. To ensure that the loop and connecting piping were completely flushed with sample, at least 3 ml sample was injected for each analysis. To avoid the build-up of CO observed when using greased-glass syringes, gas-tight syringes with PTFE plungers were used.

Between 18/10/93 and 6/2/95 the instrument responded in a slightly non-linear manner, and data were corrected empirically on the basis of the measured calibration curve. The deviations from linearity were small compared to the CO concentrations, but the deviation from linearity became clear when the residual error of the regression of the reported concentration against the actual concentrations was plotted. If there was no deviation from linearity, the points would be randomly distributed, but in fact a pattern was found (Figure 2.1a), with the instrument reading high at both ends of the range (0 and 1000 nl l^{-1} CO), and low in the middle. Following repairs by the manufacturer on 6/2/95, no pattern was observed in the residuals (Figure 2.1b), and a linear response was obtained (Figure.2.2), and corrections were no longer necessary.

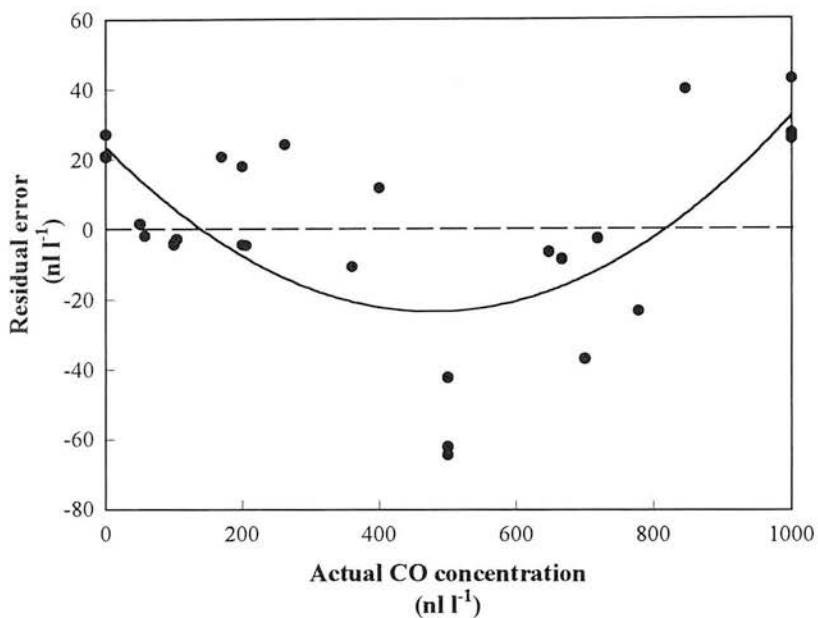


Figure 2.1a Residuals of regression of reported CO concentrations on actual concentration.
 r^2 for fitted curve = 0.46

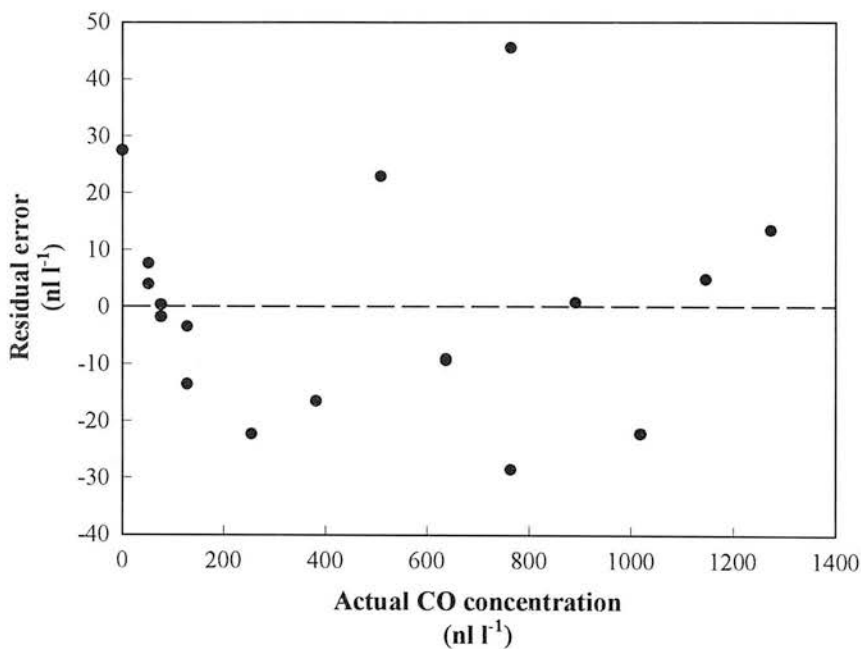


Figure 2.1b Residuals of regression of reported CO concentration on actual concentration after repairs 6/2/95.

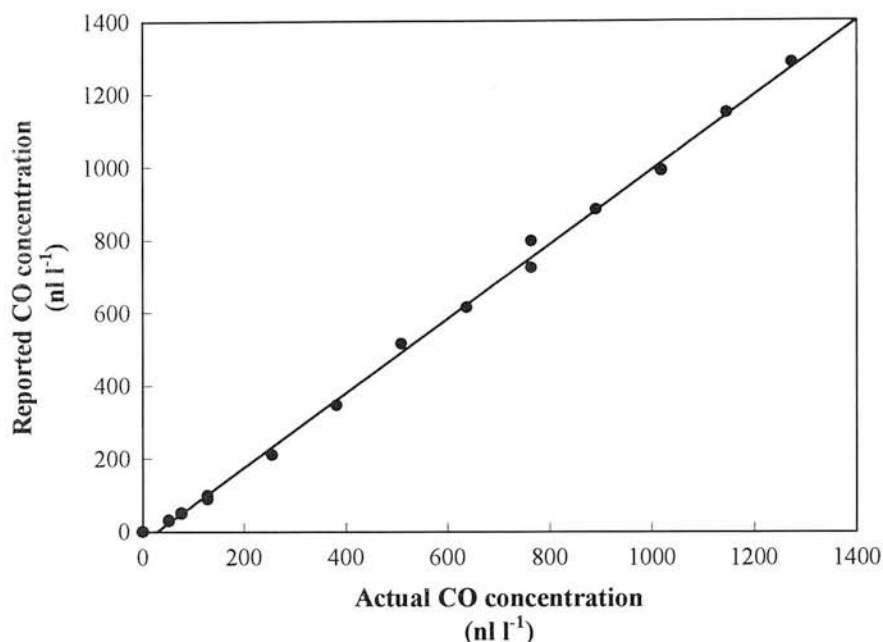


Figure 2.2 Calibration curve for CO monitor after repairs, 6/2/95
 $r^2 = 0.998$, slope = 1.021, intercept = -27.4 nl l⁻¹

A full list of operating parameters for this instrument is included in Appendix 1

2.1.2 Soil analyses

i) Ammonium and nitrate-N

10 g fresh soil was extracted with 50 ml 1.0 M KCl solution by shaking on an orbital shaker for 1 h, then filtering. $\text{NH}_4^+\text{-N}$ and $\text{NO}_3^-\text{-N}$ in the extract were determined colorimetrically. The ammonium-N analysis was based on the reaction of sodium salicylate (34 g l⁻¹) and hypochlorite with ammonia in the presence of a nitroprusside catalyst (0.4 g l⁻¹ sodium nitroprusside dihydrate added to the salicylate solution) to give a blue indophenol which absorbed at 650 nm. A citrate buffer (40 g l⁻¹ trisodium citrate hydrate with 1 ml l⁻¹ Brij-35 (30 % w/v)) was used to buffer the reaction mixture. Because hypochlorite solutions are unstable, hypochlorite was generated *in situ* from sodium dichloroisocyanurate (0.8 g l⁻¹ in 10 g l⁻¹ NaOH), which decomposes in alkaline conditions to give hypochlorite (Crooke and Simpson, 1970).

The analysis of nitrate was based on the reduction of nitrate to nitrite by hydrazine-copper reagent (1.6 g l⁻¹ hydrazine sulphate and 12 mg l⁻¹ copper sulphate pentahydrate), followed by determinations of the nitrite by the formation of an azo dye which absorbed at 520 nm by reaction with sulphanilamide and naphthylethylenediamine (10 g l⁻¹ sulphanilamide and 0.5 g l⁻¹ N-1-naphthylethylenediamine dihydrochloride in 100 ml l⁻¹ phosphoric acid). To remove interferences, the KCl solution extracted from the soil was mixed with NaOH (0.4 M), and passed over a dialysis membrane, which allowed the nitrate through, before mixing with the copper-hydrazine and sulphanilamide solutions (Best, 1976). The initial nitrite contents were measured by using distilled water in place of the hydrazine-copper reagent, but were found to be negligible. The autoanalyser used was a Chemlab Mark III multichannel autoanalyser (Chemlab Instruments Ltd, Hornchurch, Essex, UK). For both analyses, sample and wash times of 50 s were used. The configurations used are shown in Figures 2.3a and b.

ii) Microbial biomass carbon

The analysis was based on the fumigation-extraction method of Vance *et al.* (1987), except that the carbon content of the extract was measured using a carbon analyser, rather than by titration with dichromate.

Duplicate 10 g samples of soil were weighed out. One sample was extracted immediately with 0.5 M K₂SO₄ and the extract filtered through Whatman no. 42 filter paper. The other sample was placed in a vacuum oven with a beaker containing 50 ml ethanol-free chloroform. The oven was evacuated, and left for 24 h. After this, air was allowed into the oven. The oven was evacuated and refilled 4 more times to remove all the chloroform. This sample was then extracted in the same way as the unfumigated sample.

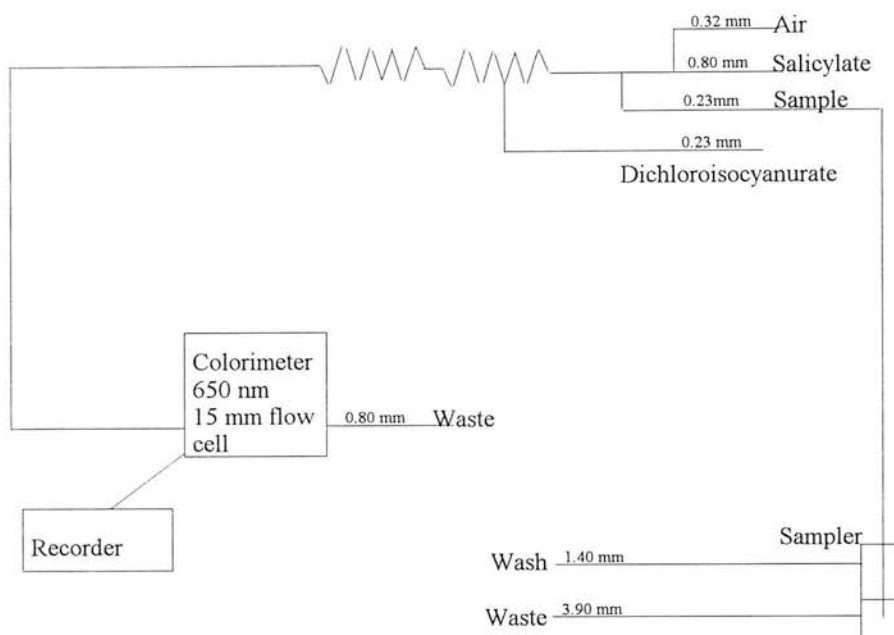


Figure 2.3a Configuration of autoanalyser for ammonium-N analysis.
Tubing internal diameters shown in mm.

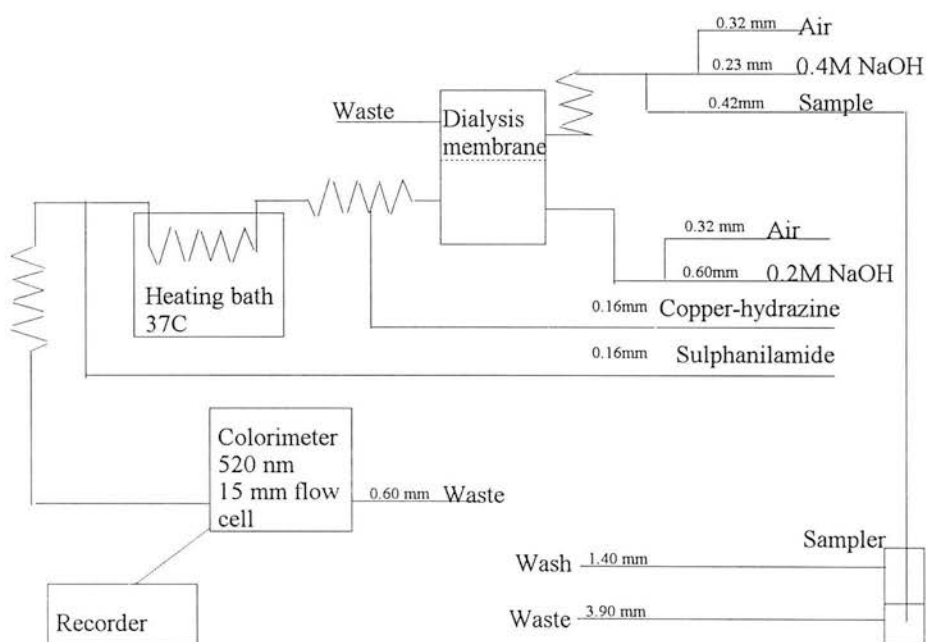


Figure 2.3b Configuration of autoanalyser for nitrate-N analysis.
Tubing internal diameters shown in mm.

The amount of carbon in the extract was determined by injecting 200 ml of extract into a Dohrman DC-50 Carbon Analyser. This determined carbon by using a combination of persulphate and UV light to oxidise all the carbon in the sample to CO₂ which was swept into an infra-red cell by a stream of nitrogen. The infra-red absorbance of the CO₂ was measured. This was proportional to the amount of carbon present in the sample.

The carbon analyser was calibrated at least once per day with a solution of 400 mg l⁻¹ C as potassium hydrogen phthalate solution.

iii) Moisture content

The moisture content was determined gravimetrically by weighing out a 10 g sample of soil, drying for 24 h at 104 °C, and reweighing. The weight difference before and after drying was assumed to be due to water loss.

iv) pH

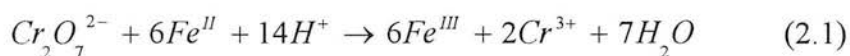
10 g fresh soil was shaken with 25 ml deionised water. The pH of the resulting slurry was then determined using an Orion Research 501 digital ion analyser equipped with an Orion Sureflow Ross combined pH electrode, which was calibrated before and after use with pH 4 and 7 buffers prepared from buffer tablets (Fisher Scientific, Loughborough, UK).

v) Texture

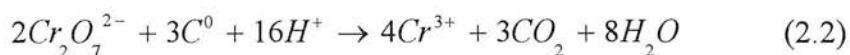
Texture was determined by hand according to the soil texture (85) system. (MAFF, 1985).

vi) Total organic carbon (TOC).

This was measured using the dichromate oxidation method (Kalembasa and Jenkinson, 1973). A small amount of dry soil (< 0.5 g) was weighed out. 20 ml 0.4 N $K_2Cr_2O_7$, 20 ml H_2SO_4 and 10 ml H_3PO_4 were added. The mixture was refluxed for 2 h, cooled, and the remaining dichromate back-titrated with 0.4 N ammonium iron (II) sulphate. Hot and cold blanks were determined for each batch of analyses. The cold blank titration was used to calculate the normality of the ammonium iron (II) sulphate solution from the following reaction of Fe(II) with $Cr_2O_7^{2-}$:



The difference in volume between the hot blank and a sample is due to Cr (VI) being used to oxidise organic C (assumed to be in the zero oxidation state) to CO_2 according to:



The whole calculation of amount of TOC can be simplified to:

$$TOC = \frac{2.4(HB - titre)}{Mass \times CB} \quad (2.3)$$

where TOC is in %; HB is hot blank titre in ml; mass is mass of soil in g; and CB is cold blank titre in ml.

2.2 Laboratory methods for measurement of CO oxidation and production rates

CO oxidation and production rates were measured in the laboratory by placing small amounts of soils into 1.5 l gas-tight Kilner jars. There were three 8 mm holes drilled in the lid of each jar; a "Subaseal" septum was placed in one of these holes, through which samples of gas could be removed using a gas-tight syringe. The other two holes were fitted with rubber grommets, through which pieces of tubing passed to allow the jar to be purged with CO standard or zero air if required. The outside ends of the tubing were fitted with 3-way taps which could be closed to seal off the jar. Tests showed that with no soil in the jar, and a starting concentration of $1 \mu\text{l l}^{-1}$, the rate of change of CO concentration was less than $0.5 \text{ nl l}^{-1} \text{ h}^{-1}$.

Prior to use, the soil samples were passed through a sieve with a 4 mm mesh to remove stones, large pieces of vegetation, worms etc. No additions of water or chemicals were made except where stated.

During experiments on CO oxidation or production, gas samples were removed from the jars at 30 min or 1 h intervals, and the CO content analysed. The reaction was first order with respect to CO concentration i.e.

$$\frac{d[\text{CO}]}{dt} = k_{ox} [\text{CO}]. \quad (2.4)$$

Integration gives $\ln[\text{CO}] = k_{ox} t,$ (2.5)

so k_{ox} can be determined from the slope of a graph of $\ln[\text{CO}]$ against time, which has units of time^{-1} . However, for amounts of soil up to a few hundred g, the CO oxidation rate was proportional to the amount of soil used but when more than about 300 g soil was used, the rate of increase in oxidation rate with amount of soil decreased (Figure 2.4), probably as diffusion in the soil began to control the overall rate. Smaller amounts than this (20-30 g) were generally used, to give rates which were convenient

to measure (i.e. slow enough for several measurements of CO concentration to be made before the concentration became too low to measure). Therefore, to compare different soils removing CO at different concentrations it is best to use the rate constant, k_{ox} (h^{-1}). To allow for the amount of soil used a modified rate constant, $k_{ox}' ((g \text{ dry soil})^{-1} h^{-1})$ was calculated from the change in CO concentration per g dry soil per unit time,

where
$$k_{ox}' = \frac{k_{ox}}{w}, \tag{2.6}$$

and w is the dry weight of soil used in grams. Although this is in terms of dry soil, the soil used was not dried except where stated, but the water content was later determined, and the equivalent weight of dry soil calculated.

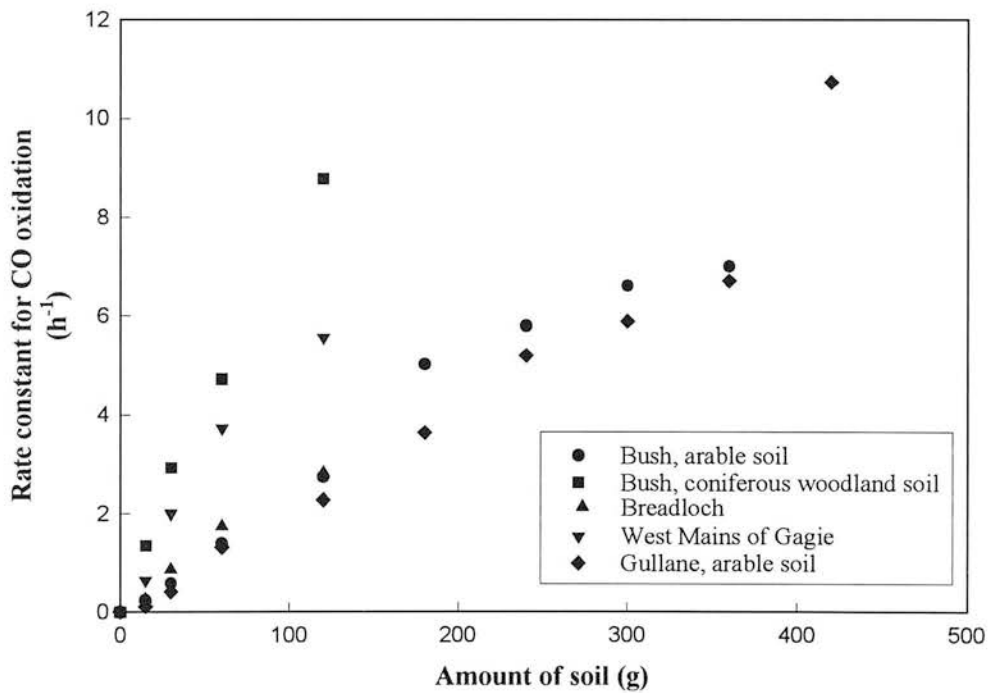


Figure 2.4 Relationship between amount of soil used in jar experiments and measured rate constant for CO oxidation.
See Table 3.1 for details of soils.

Uncertainty in the concentration of the standard will not affect the size of flux measured, as if, for example the concentration of the standard is 10 % higher than

stated, all concentrations will read 10 % too low, but the slope of the $\ln[\text{CO}]$ against time graph used to calculate the rate constant, and hence the flux, will be unchanged. However, errors in making an individual measurement may lead to errors in the flux. The standard error of a individual measurement was 4.5% If the initial concentration is read as being 4.5 % too high, and the final one 4.5% too low, this would lead to the flux being over-estimated by 4.5%.

2.3 Field measurements

2.3.1 Chamber measurements of CO fluxes

Chambers made of opaque PVC drainage pipe (38.5 cm internal diameter, and 16 cm in height), with a horizontal flange to support a lid, were pressed into the ground so that 6 cm of pipe was embedded in the ground (Figure 2.5) (Clayton *et al*, 1994; Smith *et al*, 1995). Vegetation was not cleared from within the chambers. Owing to limited numbers of chambers and syringes and to reduce analysis time only small numbers of chambers were used within each area of vegetation. The exact number of chamber used at each site are detailed in the appropriate chapters (Chapter 3, Section 3.2.2; Chapter 5 Section 5.2.2.) The chambers were randomly positioned by throwing a marker onto the area, and positioning the chamber where the marker landed, then throwing the marker again to position the next chamber. However, areas of the woodland where large roots made it impossible to insert the chamber to the required depth were rejected. Once positioned, the chambers were left in place between measurements.

When measurements were taken, an aluminium lid was put on each chamber, and held in place with plastic clips. The lid had a draught-excluder seal, which rested on the chamber flange. Samples could be withdrawn from the chamber through a piece of tubing in the lid equipped with a 3-way tap. Normally the samples were taken using 5 ml gas-tight syringes. In cold weather, these were stored in an insulated box with a

hot water bottle, to ensure that they remained gas-tight. (At temperatures below 10 °C the plunger shrinks sufficiently that there is no longer a gas-tight seal between it and the syringe barrel.). The maximum rate of change of the CO concentration in the syringes could change by up to 5 nl l⁻¹ h⁻¹. These changes in concentration could be either positive or negative, and were thought to be due to leaks. Samples were normally analysed within 3 hours of collection, so the maximum change in CO concentration was 15 nl l⁻¹. For measurements at the Gullane site, where fluxes of gases other than CO were also being measured, larger samples were removed using a 500 ml gas-tight syringe, which was emptied into a "Tedlar" bag. In the dark, samples were stable for at least 24 hours, but in the light there was a gradual build-up of CO at a rate of 0.7 nl l⁻¹ h⁻¹. Although the bag sampling method appeared to give greater sample stability, it required samples to be taken which were a large proportion of the chamber volume (16.3 l), and the bags tended to develop leaks when taken to the field. It is possible that differences in CO oxidation rates between sites may have been due at least in part to differences in the sampling method, but as the same method was always used at each site comparisons of flux rates made at different times at each site should be valid. Whichever sampling method was used, the samples were returned to the laboratory, and analysed for CO. Where net CO oxidation velocity, v_d was calculated from the rate of CO oxidation at each chamber, as this is independent of both the initial CO concentration and the area of the chamber. $v_d = k_{ox} h$ where k_{ox} is the oxidation rate constant, and h is the height of the chamber.

The soil temperature at 10 cm depth was measured within 5 cm of the side of the chamber during each sampling session using an electronic probe. Plate 2.1 shows the equipment used for making field measurements. In addition to the flux and temperature measurements, several small soil samples were taken from within 1 m of each chamber, bulked and returned to the laboratory for analysis.

As with measurements in jars (Section 2.2), uncertainties in the concentration of the standard will not affect the flux, but measurement uncertainties could lead to errors of 4.5%.

2.3.2 Continuous atmospheric CO measurements

Samples were pumped to the RGA3 reduction gas analyser from a sampling point 4 m above the ground. Both the pump and the RGA3 were controlled from a Campbell datalogger. This was programmed to start the RGA3 analysis cycle once every 5 min. The pump was switched off 1 min before the RGA3 run cycle was started, to allow the sample in the loop to re-equilibrate at atmospheric pressure. The pump was restarted 1 min into the cycle to purge the sampling loop. The integrator was interrogated by the datalogger once per minute. The average integrator output for each 5 min run cycle was calculated, and hence the CO concentration. The RGA3 was calibrated once a day with 1000 nl l⁻¹ standard, as tests had shown that the drift in calibration over a 24 h period was less than 1 %.

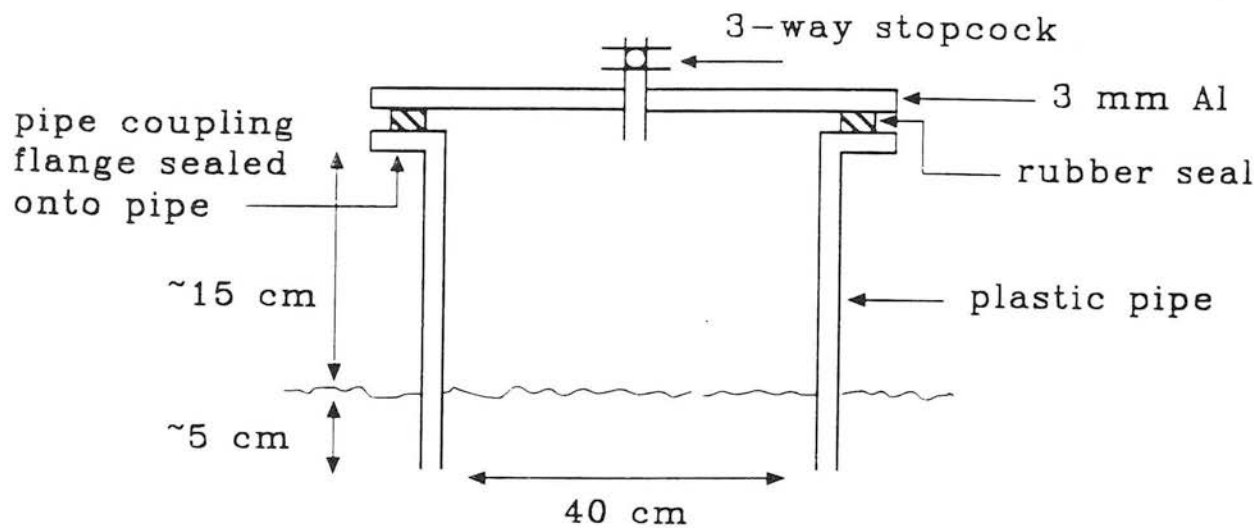


Figure 2.5 Cylindrical closed chamber. Taken from Smith *et al.* (1995).

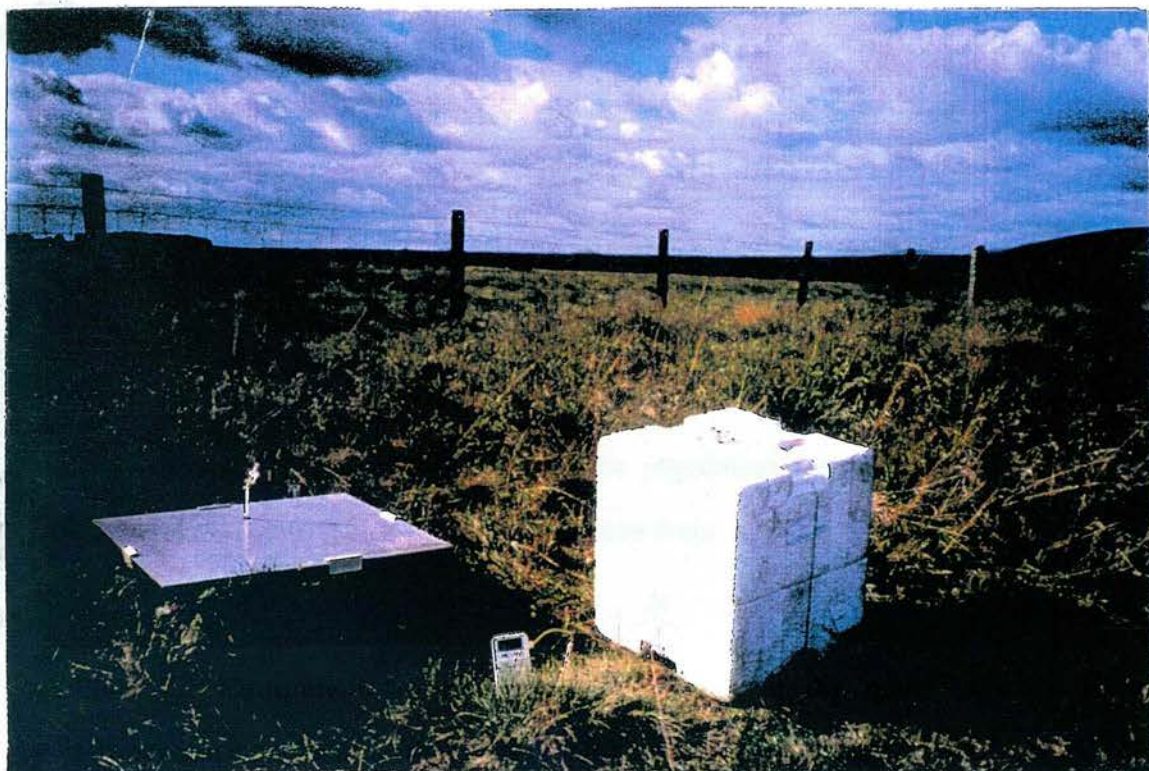


Plate 2.1 Equipment for measuring CO fluxes in the field: Flux chamber, temperature probe and insulated box for transporting syringes.

2.4 Statistical treatment of data

The data were assumed to follow a normal distribution as in most cases the numbers of samples were not great enough to establish whether or not the data were actually normally distributed. Exceptions to this were when there were enough data to test for normality, or when there was an *a priori* reason why a non-normal distribution could be assumed. The data for the continuous atmospheric monitoring campaigns (Chapter 6) were expected to be log-normally distributed, and the results from the campaign at Bush also showed signs of being bi-modal. However, these data were not subjected to statistical tests which require normality. Sections 2.4.1-2.4.4 describe standard statistical analyses, which are mentioned in many statistical textbooks, e.g Fisher (1970); Miller and Miller (1988); Statistics for Industry (1990a).

2.4.1 Calculation of means and standard deviations.

Means calculated from the data were the arithmetic means, \bar{x} , i.e. the sum of the measurements divided by the number of measurements, or

$$\bar{x} = \frac{\sum x}{n} \quad (2.7)$$

This is the sample mean, but because of random variations in sampling and measurement, it is not the true mean of the population from which samples were taken. The population mean, μ can be estimated from \bar{x} , as

$$\mu = \bar{x} \pm \frac{ts}{\sqrt{n}} \quad (2.8)$$

where s is the standard deviation given by equation 2.9.

$$s = \sqrt{\frac{\sum (\bar{x} - x_i)^2}{n - 1}} \quad (2.9)$$

a measure of the spread in the measurements; n is the number of samples; and t is a value taken from tables to reflect the confidence in the value of the standard deviation. For an infinite number of samples, $t = 2$, at the 95 % confidence level, as in a normally distributed population 95 % of values fall within 2 standard deviations of the mean. The smaller the number of samples, the larger t becomes. The quantity $\frac{s}{\sqrt{n}}$ is known as the standard error of the mean, as is shown on many of the results graphs to give an idea of the variation in the measurements. Conventionally the population mean is quoted with 95 % confidence limits unless otherwise stated (i.e limits such that the population mean will be within the stated limits on 95 % of occasions), and this convention was followed here.

2.4.2 Linear regressions, the correlation co-efficient and curve fitting.

Linear regression provides a method for finding the best line through a set of points, where the x values are those of the independent variable (i.e the variable whose values are controlled), and y is the dependent variable (i.e the variable whose values are measured, and which are thought to depend on x). There are several assumptions behind linear regression which should not be violated. Firstly, it is assumed that the relationship between x and y is linear. Secondly, all errors are assumed to be in the measurement of y. Other assumptions concern the residuals (the values obtained when the predicted values of y are subtracted from the actual values). These are assumed to be normally distributed, independent of each other, and not increase in magnitude with increasing y. While minor violations of these assumptions are almost inevitable, data displaying gross violations, e.g obvious curvature, are not suitable for linear regression analysis. Data where linear regression showed that the residuals were not independent of each other, but showed a linear relationship was subjected to further analysis using multiple linear regression when more than one independent variable had been measured (see below).

For any best-fit line,
$$\bar{y} = m\bar{x} + c \quad (2.10)$$

where \bar{x} and \bar{y} are the mean values of x and y respectively, m is the slope of the line, and c the intercept. The slope can be calculated as

$$m = \frac{\sum (x_i - \bar{x})(y_i - \bar{y})}{\sum (x_i - \bar{x})^2} \quad (2.11)$$

This value of m can then be inserted into equation 2.10 to calculate c.

Where it was suspected that more than one factor was affecting a measurement, stepwise multiple linear regression was carried out. In this procedure the correlation coefficients (see below) between each independent variable and the measured variable

were calculated, and linear regression of the measured variable on the independent variable with the largest significant correlation carried out. Next, correlation coefficients were calculated for the correlation between the residuals of this regression and the remaining independent variables. The variable with the strongest significant correlation was included in a second linear regression, this time including two independent variables. The process of including variables which showed significant correlations with the residuals was continued until no more significant correlations were found. Multiple linear regression calculations were carried out using either Excel or Genstat software.

The degree of correlation between x and y was quantified using the correlation coefficient, r.

$$r = \frac{\sum (x_i - \bar{x})(y_i - \bar{y})}{\sqrt{\sum (x_i - \bar{x})^2 \sum (y_i - \bar{y})^2}} \quad (2.12)$$

If the regression line exactly fits the data, then $r = 1$ if the slope is positive, or -1 if it is negative. Smaller values of r denote weaker correlations. If the value of r is larger than the tabulated value, then the correlation is significant.

Fitting of curves which were obviously non-linear was carried on using the curve fitting facilities in the Sigma-Plot programme, which finds the coefficients of polynomial or other specified curves using the Marquardt-Levenberg algorithm to minimise the size of the residuals. Accurate fitting of curves to non-linear data normally requires some prior knowledge of the type of relationship expected between dependent and independent variables.

2.4.3 Comparison of means and slopes: t tests

Student's t tests were used when two means were compared or when a mean result was compared with a known value. t tests were also used to compare the slope of graphs. When comparing means, the value of t was given by equation 2.13.

$$t = \frac{(\bar{x}_1 - \bar{x}_2)}{s\sqrt{1/n_1 + 1/n_2}} \quad 2.13$$

where s is the pooled standard deviation of the two measurements given by:

$$s = \sqrt{\frac{(n_1 - 1)s_1^2 + (n_2 - 1)s_2^2}{(n_1 + n_2 - 2)}} \quad 2.14$$

When comparing a mean value with a known value equation 2.13 becomes:

$$t = \frac{(\bar{x} - \mu)\sqrt{n}}{s} \quad 2.15$$

For comparison of slopes, the residual standard deviation of the slope (RSD) was used in place of the standard deviation. Equation 2.16 shows the most straightforward way of calculating the RSD.

$$RSD = s_y \sqrt{\frac{(n-1)}{(n-2)}(1-r^2)} \quad 2.16$$

where s_y is the standard deviation of the y values.

The t test assumes that the standard deviations of the sets of data compared are not significantly different. This was checked using the F test (see section 2.4.4).

Generally the t tests used were two tailed i.e to see if A differs significantly from B, where A could be either larger or smaller than B. However, on a few occasions it was appropriate to use one-tailed t-tests e.g. comparing a quantity such as concentration which cannot be negative with zero.

2.4.4 Analysis of variance (ANOVA)

While t tests can be used to compare two independent samples, larger numbers of independent samples can be compared using ANOVA. This avoids the possibility that random error leads to one t-test out of a large number incorrectly showing a significant difference between samples when none exists (Samuels, 1989). When only two treatments are being compared ANOVA and a t-test will always give the same result. ANOVA compares the random variation which occurs within each treatment with the variation between treatments. One way ANOVA examines the effects of one variable, applied at different levels or "treatments". The first quantity calculated is the total sum of squares, SS_{total} .

$$SS_{total} = df_{total} * s_{total}^2 \quad (2.17)$$

where df_{total} is the total number of degrees of freedom of all of the measurements, and s_{total} is the standard deviation of all of the measurements. The next quantity calculated is the within sample or residual sum of squares, SS_{within} .

$$SS_{within} = \sum df_{within} * s_{within}^2 \quad (2.18)$$

where df_{within} is the number of degrees of freedom with a given treatment, and s_{within} is the standard deviation within a treatment.

The total sum of squares is the sum of the between-sample and within-sample sums of squares i.e.

$$SS_{total} = SS_{within} + SS_{between} \quad (2.19)$$

so once SS_{total} and SS_{within} have been calculated the between-sample sum of squares, $SS_{between}$ can be calculated using equation 2.19. The sums of squares are then converted to mean squares by dividing by the appropriate number of degrees of freedom. The total number of degrees of freedom, df_{total} , is the number of total

samples minus one. The number of between-treatments degrees of freedom, df_{between} , is the number of treatments minus one, and the number of within sample degrees of freedom, $df_{\text{within}} = df_{\text{total}} - df_{\text{between}}$.

An F test can then be used to compare MS_{between} and MS_{within} .

$$F = \frac{MS_{\text{between}}}{MS_{\text{within}}} \quad (2.20)$$

If the value of F calculated is larger than that given in tables, then the treatments have a significant effect.

Two-way ANOVA is similar, except that two variables are investigated at two or more levels each, and the total sum of squares is obtained by adding the between-sample sums of squares for variables 1 and 2 and the within-sample sum of squares. Similarly the total number of degrees of freedom is the sum of those for each between-sample degrees of freedom for each variable and the within-sample degrees of freedom. Value of F are then calculated for each variable.

The ANOVA analysis assumes that the samples are randomly distributed within treatment; that the population standard deviation is the same for all treatments; and that the residuals are randomly distributed.

2.4.5 Analysis of factorially designed experiments.

Factorially designed experiments (Box *et al*, 1978; Statistics for Industry, 1990b, Garcia-Diaz and Phillips, 1995) allow the efficient investigation of factors which may affect a process. Experiments are designed so that there are no correlations between any of the factors or their interactions so that all factors and interactions can be investigated in relatively few trials. For an experiment in which two levels of each factor are used, the analysis of the results is relatively straightforward. A design matrix is produced, in which each combination of the factors to be investigated is

included as a separate trial (see Chapter 4, Table 4.2), with a "+" showing that a particular treatment is applied (or is at the higher of two levels) in that trial, and a "-" that it is not applied (or is at the lower of two levels). The levels of the interactions for each trial can be calculated by multiplying the levels of the corresponding factor (+ = +1; - = -1). Therefore for a simple 2^2 experiment where 2 factors are investigated at 2 levels, the complete design matrix, including the interactions, is as shown in Table 2.1 below:

Table 2.1 Design matrix for a 2^2 factorial experiment

Trial number	Level of A	Level of B	Level of interaction AB
1	+	+	+
2	+	-	-
3	-	+	-
4	-	-	+

Thus for trial 1, the level of interaction AB is +1 = +1 x +1, for trial 2 it is -1 = +1 x -1 etc.

To decide which factors and interactions significantly affect the dependent variable (CO production rate in the case of Chapter 4), the response for each trial is measured, and stepwise multiple linear regression is used to identify which factors and interactions significantly affect it. The results can also be displayed graphically (Daniel, 1959). The effect of each factor (or interaction) is calculated. (The effect is the mean value of the response from all the trials in which the factor is positive minus the mean value of the response from all the trials in which the factor is negative). The effects are ranked in order of increasing magnitude, and the magnitude of the effect plotted against its rank (the effect with the smallest magnitude has a rank of one; the next smallest, two etc.) on a half-normal plot (i.e. a plot with one axis, the one showing the rank of the effects, plotted on a probability scale). Effects which comprise only random variation appear on a straight line through the origin (if the line

does not go through the origin, this suggests that the result of at least one trial is an outlier - this will affect all of the calculated effects, and so shift the line). Effects which are significant do not appear on this line. The more significant an effect is, the further from the line it is.

Chapter 3: Oxidation of CO by soils: field and laboratory studies¹

3.1 Introduction

The importance of carbon monoxide as an atmospheric trace gas is discussed in Chapter 1, Section 1.1, and literature on its oxidation by soils is reviewed in Chapter 1 Section 1.2.

Although it has been known for some time that soils can oxidise CO, the soil factors affecting the rate of oxidation have not been fully investigated. Investigations have been carried out to determine the response of CO oxidation rate to changes in individual soil variables, but generally only one variable at a time has been examined. A better understanding of the principal factors affecting CO oxidation by soil would help to predict changes in the strength of the soil sink for CO caused by changes in land use and agricultural practice.

Although field measurements have been made of CO fluxes between the land surface and the atmosphere, they have tended to concentrate on a few regions, particularly on arid (Conrad and Seiler, 1982b, 1985a,b) and savannah soils (Scharffe *et al*, 1990; Sanhueza *et al*, 1994 a,b). Two studies have been made in temperate regions (Ingersoll *et al*, 1974; Seiler *et al*, 1977) but only one of them included measurements of fluxes on agricultural land (Ingersoll *et al*, 1974), and examined the effect of land use. It was found that CO oxidation was significantly faster in soil under natural vegetation than from agricultural soils in all the climatic zones examined. Very little field work has been carried out on time scales of more than a few weeks. Whilst

¹Based on Moxley, J.M. and Smith, K.A. Oxidation of atmospheric CO by soils: field and laboratory studies of soil factors affecting oxidation rates. Accepted for publication in Soil Biology and Biochemistry, 1997.

diurnal patterns of CO fluxes have been reported (e.g. Conrad and Seiler, 1982b, 1985,a,b; Sanhueza *et al*, 1994a,b), there are no data on their seasonal variation.

This study consisted of two elements. The first was a series of laboratory experiments on a range of Scottish soils taken from sites under woodland, grassland pastures and arable fields, to determine the factors which have the greatest influence on CO oxidation by soils. The soils used were selected to represent as great a range of properties as possible. The second element of the study involved long-term field work to assess the importance of these factors on uptake rates under natural conditions.

3.2 Materials and Methods

3.2.1 Laboratory Studies

Except where otherwise stated, the soil samples used for measurements of CO oxidation rates in the laboratory were from 0-10 cm depth. The soils were incubated as described in Chapter 2, Section 2.2. Rate constants were determined from three sets of measurements on each soil sample except where otherwise stated. Chapter 2, Section 2.2 gives details of how the rate constants were calculated.

To assess the effect of different land uses on the same soil, samples were taken from 4 sites with adjacent areas under different land uses: at Bush there was arable land, coniferous woodland, and wet and dry areas of deciduous woodland (soils 8-11 in Table 3.1); there was grassland and woodland at Cowpark (soils 15 and 16); arable land, grassland and woodland at Kitleyknowe (soils 30-32), and arable land, woodland, and set-aside land at Gullane (soils 21-24).

To investigate the dependence of the CO oxidation activity on depth, samples were taken from 3 depths from each of the 3 areas at the Gullane site in January 1994 (woodland, arable, and set aside). The arable soil received 75 kg N ha⁻¹ as NH₄NO₃

in February, and a second application of 150 kg N ha⁻¹ in April. It was sampled 1 week after this second application.

The role of microorganisms containing a monooxygenase which is inhibited by acetylene (i.e. methanotrophs and nitrifiers) was investigated by incubating soils from Bush and Gullane under an atmosphere containing 1 ml l⁻¹ acetylene (Bédard and Knowles, 1989). The effect of nitrification inhibitors was investigated further using dicyandiamide (DCD). In this case, 1 ml DCD solution containing 3 g l⁻¹ DCD was added to fresh 30 g fresh soil, giving a soil DCD concentration of 100 µg g⁻¹ fresh soil. The rate constant for CO oxidation with DCD added was compared to that for 30 g fresh soil with 1 ml water added.

To test the hypothesis that the organic layer was responsible for CO production, samples of the litter from the coniferous woodland at Bush, which was several cm thick in places, were collected and incubated at various temperatures in the laboratory.

3.2.2 Field measurements

Field measurements were made on the Bush Estate, Midlothian, Scotland, UK (55 ° 51 ' N, 3 ° 12 ' W, Ordnance Survey grid reference NT 243637) from January to December 1995, and at Gullane, East Lothian, Scotland, UK (56 ° 2 ' N, 2 ° 49 ' W, Ordnance Survey grid reference NT 483814) from January to July 1995. Each site had adjacent areas under different land uses. At both sites, measurements of CO fluxes were made approximately once a fortnight during this period, using the method described in Chapter 2, Section 2.3.1.

At Bush (Plate 3.1), the main comparison was between an area of arable land left fallow during the study, mainly supporting pineapple mayweed (*Chamomilla suaveolens*); and an area of mixed deciduous woodland containing English oak (*Quercus robur*), beech (*Fagus sylvatica*), hazel (*Coryllus avellana*), downy birch

(*Betula pendula*), mountain ash (*Sorbus aucuparia*), and sycamore (*Acer pseudoplatanus*) with a ground covering of wood meadow-grass (*Poa nemoralis*). Two flux chambers were placed on each of these areas. On the deciduous woodland soil, an additional chamber was located on a small patch which was much wetter than the remainder. One further chamber was installed to follow temporal variations in a neighbouring area of coniferous woodland (mainly larch (*Larix decidua*), Sitka spruce (*Picea abies*) and Scots pine (*Pinus sylvestris*) which had very little ground-covering vegetation).

To check the spatial variability of the CO fluxes in the coniferous woodland, measurements were made on the coniferous woodland using 5 chambers in an area of 17 m². The arrangement of the chambers in relation to trees and to the arable field is shown in Figure 3.1

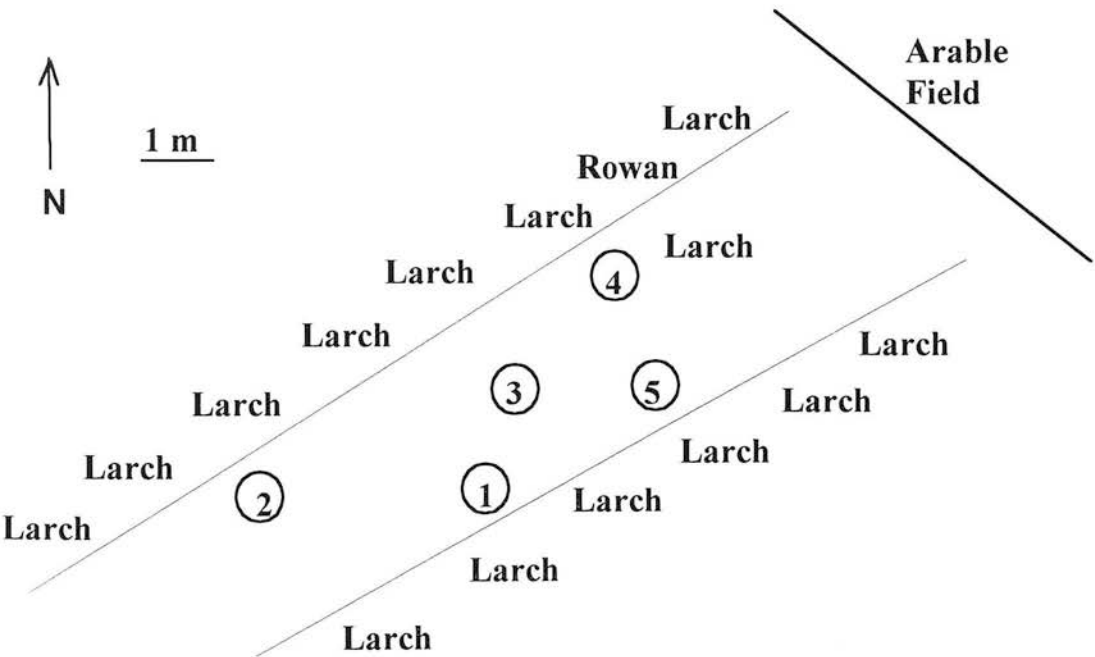


Figure 3.1 Arrangement of replicate chambers on the coniferous woodland at Bush.



Plate 3.1 The field site at Bush Estate, Midlothian, Scotland showing woodland area on left, and fallow arable land on right.



Plate 3.2 The field site at Gullane, East Lothian, Scotland showing arable land on extreme left, woodland at back and set aside land on right.

At Gullane (Plate 3.2), there was an arable field with a crop of winter wheat, an area of deciduous woodland, mainly beech (*Fagus sylvatica*), sycamore (*Acer pseudoplatanus*) and ash (*Fraxinus excelsior*), and an area of set aside land with a patchy vegetation consisting mainly of field horsetail (*Equisetum arvense*), groundsel (*Senecio vulgaris*), cleavers (*Galium aparine*), forget-me-nots (*Myosotis spp.*), hairy bittercress (*Cardamine hirsuta*), barren brome (*Bromus sterilis*), scentless mayweed (*Matricaria perforata*), long-headed poppy (*Papaver dubium*) and common storks-bill (*Erodium cicutarium*). Two chambers were placed on each of these areas.

No meteorological measurements were made at either of these sites, but measurements of soil temperature at 10 cm depth, and soil water content were made whenever CO fluxes were measured (Chapter 2, Section 2.3.1).

At Gullane, comparisons were made of the rate constants for CO oxidation with those for methane oxidation (data from Dr. Karen Dobbie) and nitrous oxide emission (data from Simona Castaldi), which were also measured using the closed chamber method. Methane concentrations were measured using a gas chromatograph fitted with a flame ionisation detector, which operated at 120 °C. The column used was 1.5 m long, and 6 mm in diameter, and was packed with alumina and maintained at 36 °C. Nitrogen at a flow rate of 40 ml min⁻¹ was used as the carrier. The sample loop held 1 ml; 5 ml of each sample was flushed through the loop to ensure that it was completely filled. Nitrous oxide concentrations were measured using a Unicam 610 series gas chromatograph fitted with 4.5 m long stainless steel column with a 0.5 cm diameter filled with Poropak Q and heated to 60 °C. The detector was an electron capture detector, which operated at 320 °C. Argon at a flow rate of 40 ml min⁻¹ was used as the carrier gas. The sample loop held 1 ml.

3.2.3 Analytical Methods.

Carbon monoxide concentrations were measured using an RGA3 Reduction Gas Analyser (Trace Analytical, Menlo Park, California, USA), as described in Chapter 2, Section 2.1.1.

Duplicate samples of each soil were analysed for $\text{NH}_4^+\text{-N}$ and $\text{NO}_3^-\text{-N}$ content; microbial biomass carbon; TOC; pH; and water content using the methods in Chapter 2, Section 2.1.2.

3.2.4 Statistical Analysis

Statistical analyses were carried out using the methods described in Chapter 2, Section 2.4.

3.3 Results

3.3.1 Laboratory Incubations

The first set of incubations aimed to discover the most important variables affecting CO oxidation rates. Forty one Scottish soils were used, representing a wide range of properties (Table 3.1). 30 g soil was used per 1.5 l jar. Initial CO concentrations of 1000 nl l⁻¹ were obtained by purging the jars with 1000 nl l⁻¹ CO standard. In all cases a first order decay in CO concentration was observed. Given enough time the concentration fell to below the limit of detection (5 nl l⁻¹). The rate constants for CO oxidation are given in Table 3.2.



Table 3.1 Properties of soils used in incubation experiments to measure CO oxidation rates

Soil No.	Location	Landuse	Total organic C(1) (% dry weight)	Biomass C(1) (mg C kg ⁻¹)	pH(3)	Nitrate N (2) (mg N kg ⁻¹)	Ammonium N (2) (mg N kg ⁻¹)	Texture(4)	Water content (% fresh weight)	Dry Bulk Density (1) (kg l ⁻¹)
1	Alford	Agricultural (arable)	3.8	373	6.4	9.4	1.1	OSZL	24.	0.9
2	Ardishian	"	5.3	1360	6.0	4.9	4.0	OSL	28	0.7
3	Auchenriuoeh	"	4.8	689	5.8	7.1	2.0	OZL	49	0.6
4	Balquhatsone	"	5.3	1030	6.3	5.4	2.1	OSL	45	0.7
5	Banff	"	4.4	493	5.6	14.	3.6	OSCL	17	0.9
6	Bield	"	3.8	529	5.9	18	1.9	OCL	22	0.8
7	Breadloch	"	2.1	394	6.7	3.1	2.3	SC	22	0.8
8	Bush, arable	Agricultural (fallow)	1.7	102	6.5	1.8	0.3	SL	15	0.9
9	Bush, coniferous woodland	Woodland (coniferous)	7.6	841	4.0	1.0	2.1	OSL	28	0.7
10	Bush, deciduous woodland (dry area)	Woodland (deciduous)	7.3	933	4.0	0.7	0.7	OSL	42	0.6
11	Bush, deciduous woodland (wet area)	Woodland (deciduous)	2.0	403	4.3	1.1	0.9	SL	45	0.7

Table 3.1 (cont)

Soil No.	Location	Landuse	Total organic C(1) (% dry weight)	Biomass C(1) (mg C kg ⁻¹)	pH(3)	Nitrate N (2) (mg N kg ⁻¹)	Ammonium N (2) (mg N kg ⁻¹)	Texture(4)	Water content (% fresh weight)	Dry Bulk Density (1) (kg l ⁻¹)
12	Chirnside	Agricultural (arable)	1.0	287	7.0	0.1	0.3	C	6.7	1.1
13	Coldstream	"	1.8	234	6.9	7.3	1.1	ZL	10	1.0
14	Conon Bridge	"	1.7	170	6.7	3.3	0.7	SC	14	1.0
15	Cowpark, grassland	Agricultural (grassland)	3.3	570	6.7	2.6	0.3	SCL	16	0.7
16	Cowpark, woodland	Woodland (mixed)	6.0	732	6.7	0.2	1.2	OSCL	22	0.5
17	Culbokie	Agricultural (arable)	4.3	602	5.5	11	1.0	OCL	26	Not measured
18	Cupar	"	2.2	230	7.0	9.4	2.4	ZC	18	1.0
19	East Gogar	"	3.6	795	5.9	2.7	5.0	OCL	22	0.7
20	Gott	"	20	3110	6.0	10	3.3	Peaty Loam	55	0.3
21	Grange	"	1.3	99	6.6	3.2	12	ZCL	12	0.9
22	Gullane, arable	"	1.1	108	8.7	3.7	0.9	LS	14	0.9
23	Gullane, set aside	Set aside	1.5	211	7.6	4.6	1.0	LS	22	1.1

Table 3.1 (cont)

Soil No.	Location	Landuse	Total organic C(1) (% dry weight)	Biomass C(1) (mg C kg ⁻¹)	pH(3)	Nitrate N (2) (mg N kg ⁻¹)	Ammonium N (2) (mg N kg ⁻¹)	Texture(4)	Water content (% fresh weight)	Dry Bulk Density (1) (kg l ⁻¹)
24	Gullane, woodland	Woodland (deciduous)	3.1	806	8.3	7.0	1.4	LS	29	0.8
25	Hadden	Agricultural (arable)	1.5	202	6.4	5.7	2.5	ZL	6.5	1.1
26	Halerow	"	14	1010	6.7	8.8	2.8	Peaty Loam	58	0.5
27	Harpertown	"	2.2	476	6.3	13	11	ZC	10	1.0
28	Humbie	"	2.5	287	6.7	17	1.3	SL	16	1.0
29	Inverurie	"	3.4	357	6.6	5.8	1.8	SCL	20	1.0
30	Kitleyknowe, arable	"	3.4	Not measured	6.4	27	6.0	CL	65	Not measured
31	Kitleyknowe, grassland	Agricultural (grassland)	6.2	1240	6.1	0.1	1.2	OZL	60	0.8
32	Kitleyknowe, woodland	Woodland	6.2	Not measured	7.6	31	3.5	OZL	21	0.6
33	Macbie Hill	Agricultural (arable)	7.0	2460	6.7	Not measured	Not measured	SZL	52	0.5
34	Mertoun, field 1	"	1.5	295	7.1	5.9	1.0	SCL	14	0.9
35	Mertoun, field 2	"	2.6	699	5.8	17	21	CL	22	0.9
36	Methlick	"	4.2	278	6.9	8.5	1.6	OCL	13	1.0
37	Reidhall	"	1.2	185	6.2	9.3	0.9	SCL	17	0.8
38	Strathmore	"	1.7	235	6.5	2.6	0.5	ZL	12	1.0

Table 3.1 (cont)

Soil No.	Location	Landuse	Total organic C(1) (% dry weight)	Biomass C(1) (mg C kg ⁻¹)	pH(3)	Nitrate N (2) (mg N kg ⁻¹)	Ammonium N (2) (mg N kg ⁻¹)	Texture(4)	Water content (% fresh weight)	Dry Bulk Density (1) (kg l ⁻¹)
39	Stuartfield	"	2.9	251	6.5	6.5	2.6	ZL	11	1.1
40	Turriff	"	2.3	352	6.8	4.3	2.3	SCL	9.0	1.2
41	West Mains of Gagie	"	4.0	271	6.5	20	0.7	OC	13	0.9

All data are the mean of duplicate measurements

- 1) On a dry weight basis
- 2) On a fresh weight basis
- 3) In water

4) According to the MAFF Soil (85) System (MAFF, 1985). The prefix O denotes an organic soil (6 - 20 % organic matter).

Table 3.2

Rate constants for CO oxidation during laboratory incubations of Scottish soils

Soil No.(1)	Mean first order rate constant $k_{ox}^{(2),(3)}$ (kg ⁻¹ dry soil h ⁻¹)	Standard deviation of k_{ox} (kg ⁻¹ dry soil h ⁻¹)	Soil No.(1)	Mean first order rate constant $k_{ox}^{(2),(3)}$ (kg ⁻¹ dry soil h ⁻¹)	Standard deviation of k_{ox} (kg ⁻¹ dry soil h ⁻¹)	Soil No.(1)	Mean first order rate constant $k_1^{(2),(3)}$ (kg ⁻¹ dry soil h ⁻¹)	Standard deviation of k_1 (kg ⁻¹ dry soil h ⁻¹)
1	62	7	15	27	8	29	77	14
2	120	36	16	83	14	30	14	1
3	29	5	17	58	4	31	72	3
4	63	1	18	71	3	32	149	12
5	68	12	19	20	2	33	106	15
6	44	7	20	129	9	34	40	4
7	26	6	21	33	3	35	48	8
8	30	5	22	39	30	36	69	5
9	147	21	23	5	4	37	20	3
10	132	10	24	25	7	38	41	10
11	15	0	25	1	1	39	67	18
12	19	12	26	80	6	40	23	7
13	51	5	27	18	2	41	55	18
14	36	3	28	26	6			

1) Site numbers as in Table 1

2) Mean of 3 determinations

3) Mean for 6 hour measurement period, or until CO concentration reached zero.

The soil variable most strongly correlated with CO oxidation rate constants was TOC content ($r^2 = 0.36$, $p < 0.01$) (Figure 3.2). The TOC content was strongly correlated with the microbial biomass carbon content ($r^2 = 0.69$, $p < 0.01$). The two peaty loam soils (20 and 26 in Table 3.1) in the set of soils used did not appear to follow the same regression on TOC as the other soils. When the peaty loam soils were included in the analysis, stepwise multiple linear regression showed that no other variables significantly affected the CO oxidation rate. However, when the peaty loams were not included, the relationship between the oxidation rate constant and TOC was highly significant ($r^2 = 0.66$, $p < 0.01$), and there was also a negative correlation with water content ($p < 0.01$) (Figure 3.3).

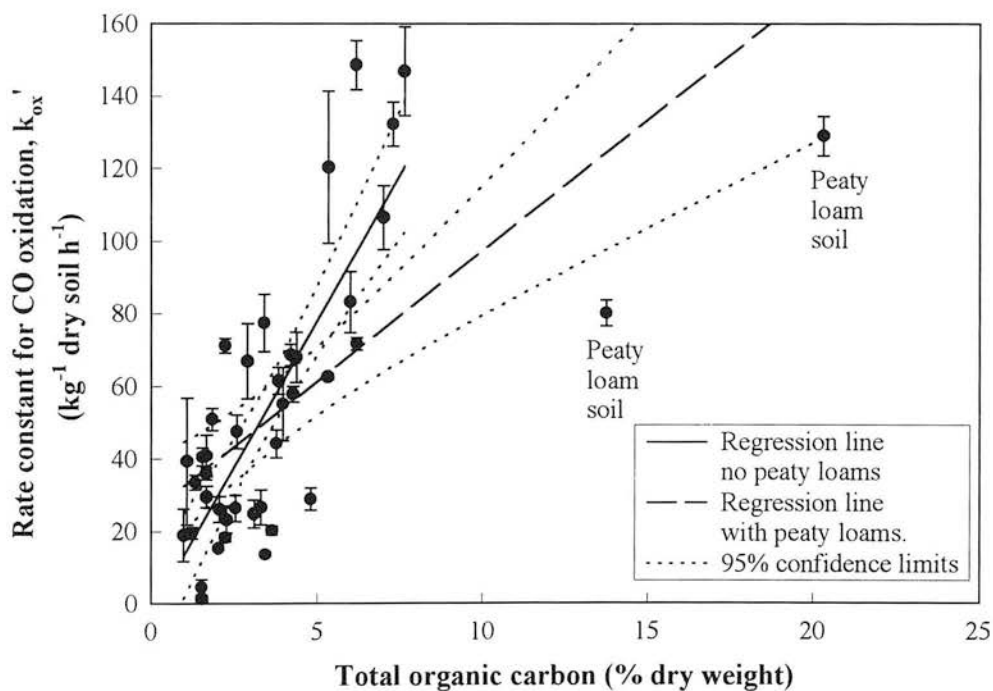
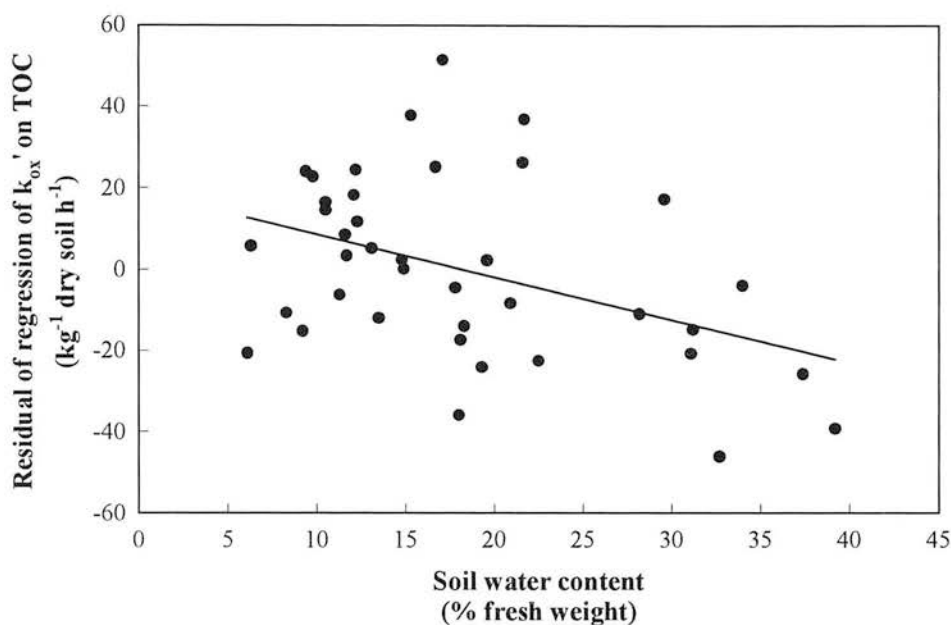


Figure 3.2 Relationship between CO oxidation and total organic carbon content of various Scottish soils. Error bars show 1 standard error. n = 3.



**Figure 3.3 Relationship between residuals of regression of k_1 on TOC and soil water content (omitting peaty loam soils).
 $r^2 = 0.17$, $n = 39$, $p < 0.05$.**

A more detailed study of the effect of water content was made using three soils from two sites (the arable soil from Gullane (soil 22), and arable and coniferous woodland soils from Bush (soils 8 and 9)). Samples as collected from the field were either air dried or wetted with deionised water to give a range of water contents for each soil. The CO oxidation rate constant was then determined for each soil at each water content. This showed that there was an optimum water content for CO uptake for each soil (Figure 3.4).

Generally, the rate constant for CO oxidation by the woodland soils was significantly faster than that of the corresponding arable or grassland soil, but at Gullane the woodland soil had a slightly smaller oxidation rate constant than the arable land, with the rate constant for the set aside land lower still (Figure 3.5).

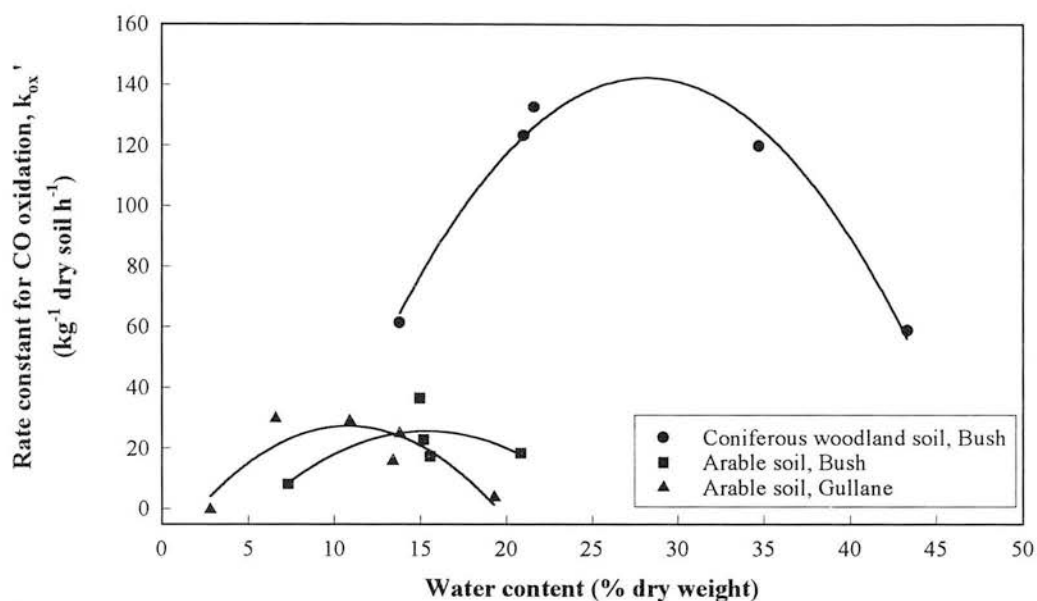


Figure 3.4 The effect of soil water content on CO oxidation.
Only one set of measurements was made for each soil.
Errors assumed to be similar to those in Figure 3.1 i.e +/- ~10 kg⁻¹ dry soil h⁻¹.

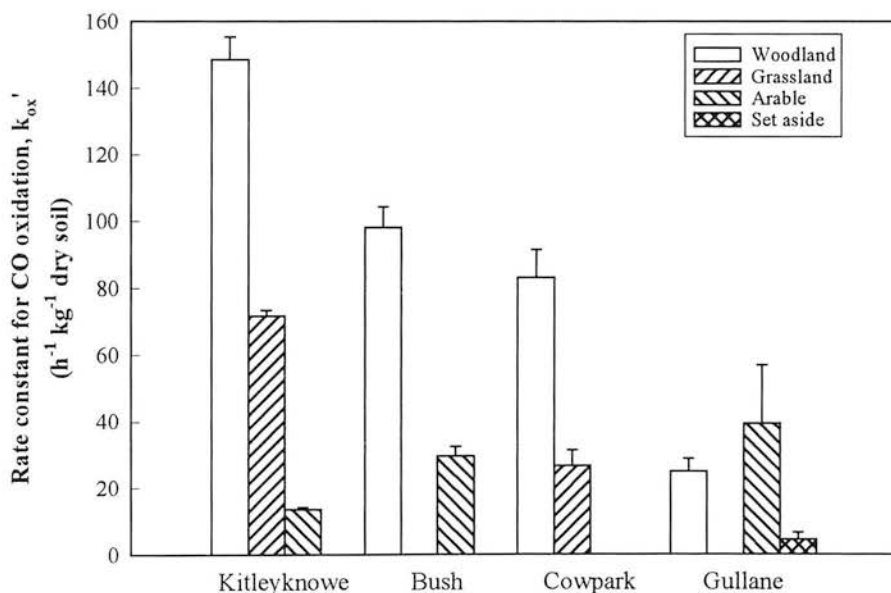


Figure 3.5 CO oxidation rate constants of soil from 4 sites with contrasting land uses.
Error bars show 1 standard error. n = 3.
Data for Bush woodland is mean value for woodland types in Tables 3.3 and 3.4.

The properties of the soils from each depth at Gullane are shown in Table 3.3. In each case the soil from the top 10 cm showed the largest rate constant for CO oxidation (Figure 3.6). Analysis of variance (ANOVA) showed that both depth and vegetation type had a significant effect on the rate constant. The amount of microbial biomass

carbon also decreased with depth in the woodland soil, and in the arable soil in April (Figure 3.7) but the pattern was not identical to that for the rate constant ($r^2 = 0.06$, $p > 0.1$). There was a reduction in the CO oxidation rate constant in the top 10 cm of the arable soil after the fertiliser was applied in April, but the difference was not significant at the 95 % confidence level.

In all cases net CO oxidation was converted to net CO production by the addition of acetylene (Figure 3.8). Although CO oxidation was inhibited by DCD in all of the soils tested it was not completely halted, except in the arable soil from Bush, which had the lowest CO oxidation rate of the soils examined. No CO production was observed when jars containing 1 ml l⁻¹ acetylene or 1 ml DCD solution, but no soil, were incubated (Figure 3.9).

Table 3.3 Variation in soil properties with depth at Gullane.

Land use	Depth (cm)	Water content ⁽¹⁾ (%)	Nitrate N content ⁽²⁾ (mg kg ⁻¹)	Ammonium N content ⁽²⁾ (mg kg ⁻¹)	pH	Biomass C ⁽²⁾ (mg kg ⁻¹)	Total organic carbon ⁽²⁾ (%)
Woodland	0-10	22.5	9.0	1.8	8.3	806	3.1
Woodland	10-20	20.3	8.6	1.0	8.5	509	2.4
Woodland	20-30	19.5	6.4	1.0	8.6	313	1.8
Set aside	0-10	18.1	5.7	1.2	7.6	211	1.5
Set aside	10-20	19.0	4.5	1.2	7.8	182	1.7
Set aside	20-30	21.7	4.1	1.3	7.9	167	1.7
Arable (Jan. 1994)	0-10	12.2	4.2	1.0	8.7	108	1.1
Arable (Jan. 1994)	10-20	15.9	4.3	1.0	8.5	94	1.1
Arable (Jan. 1994)	20-30	18.0	2.9	Not measured	8.4	55	0.7
Arable (Apr. 94)	0-10	10.6	4.7	8.0	8.1	179	1.6
Arable (Apr. 94)	10-20	13.1	8.8	0.6	8.1	93	1.3
Arable (Apr. 94)	20-30	18.0	3.4	0.6	8.3	101	1.4

(1) On a fresh weight basis; (2) On a dry weight basis

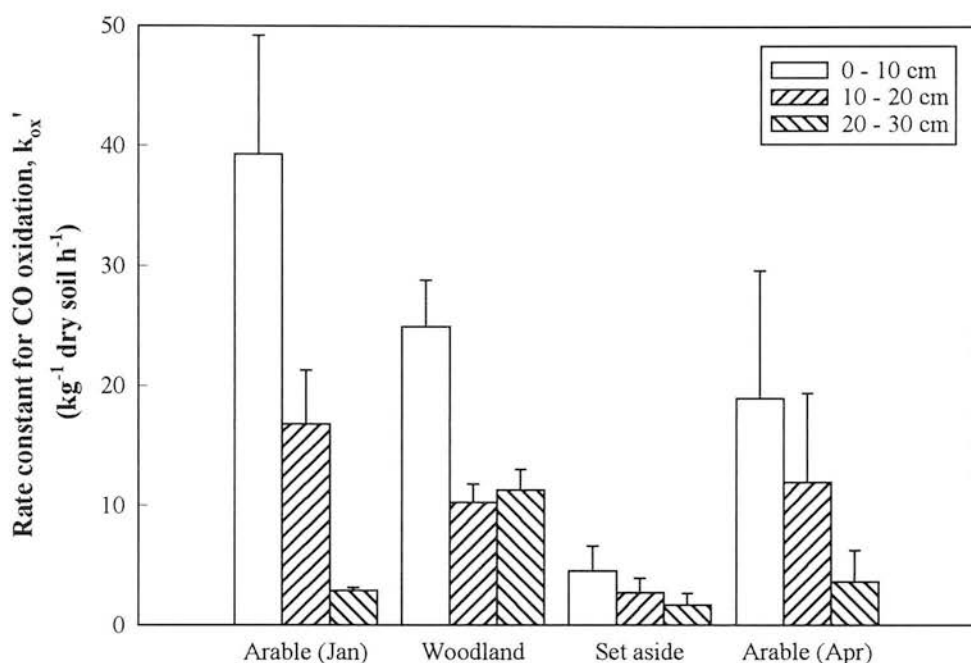


Figure 3.6 Variation in CO oxidation rate constant with depth in soils from contrasting land uses, Gullane, 1994.
Error bars show 1 standard error. n = 3.

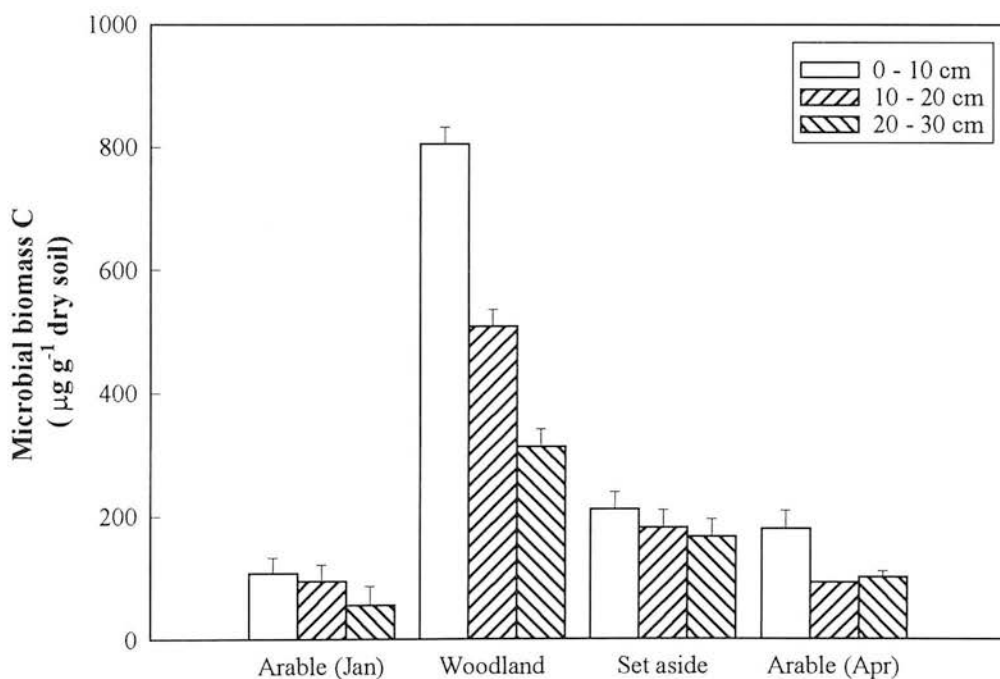


Figure 3.7 Variation in microbial biomass carbon with depth for soils from contrasting land uses, Gullane, 1994.
Error bars show 1 standard error. n = 3.

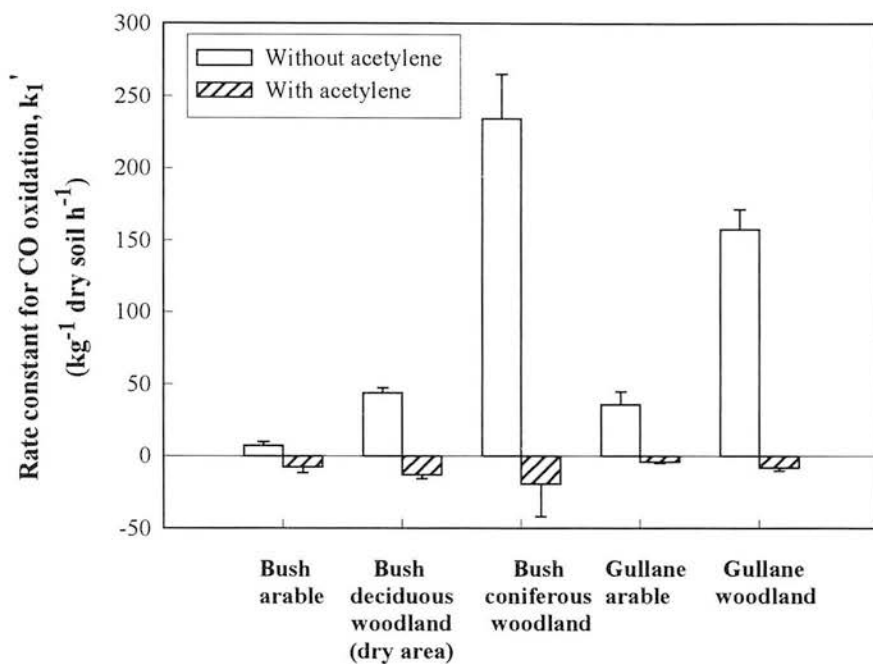


Figure 3.8 The effect of acetylene on CO oxidation
Error bars show 1 standard error. $n = 3$.

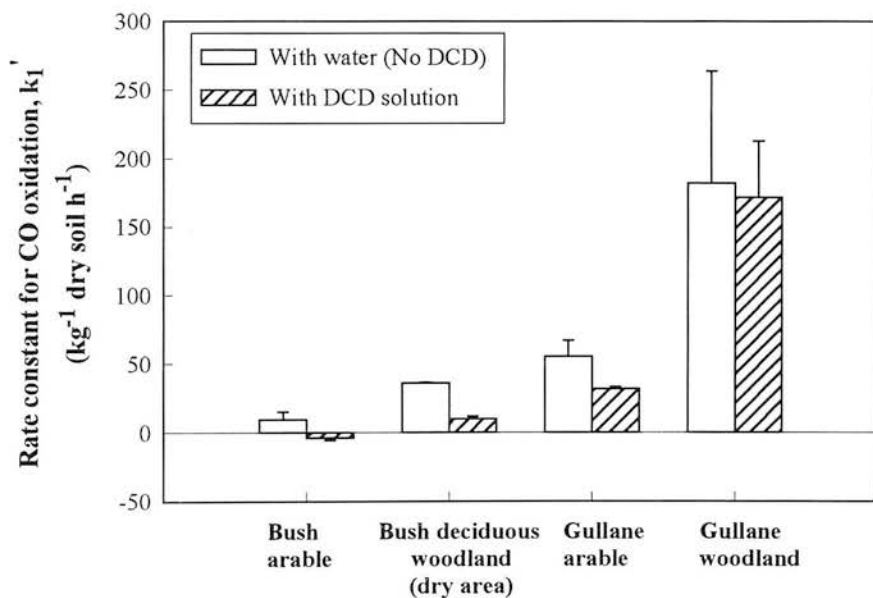


Figure 3.9 The effect of dicyandiamide (DCD) on CO oxidation.
Error bars show 1 standard error.
 $n = 3$ for soils from Gullane and 2 for soils from Bush.

3.3.2 Field Measurements

i) Bush

CO oxidation was measured in the field using closed chambers. The oxidation obeyed first order kinetics, although there was normally a detectable amount of CO left in the chambers at the end of the 20 min measurement period (Figure 3.10).

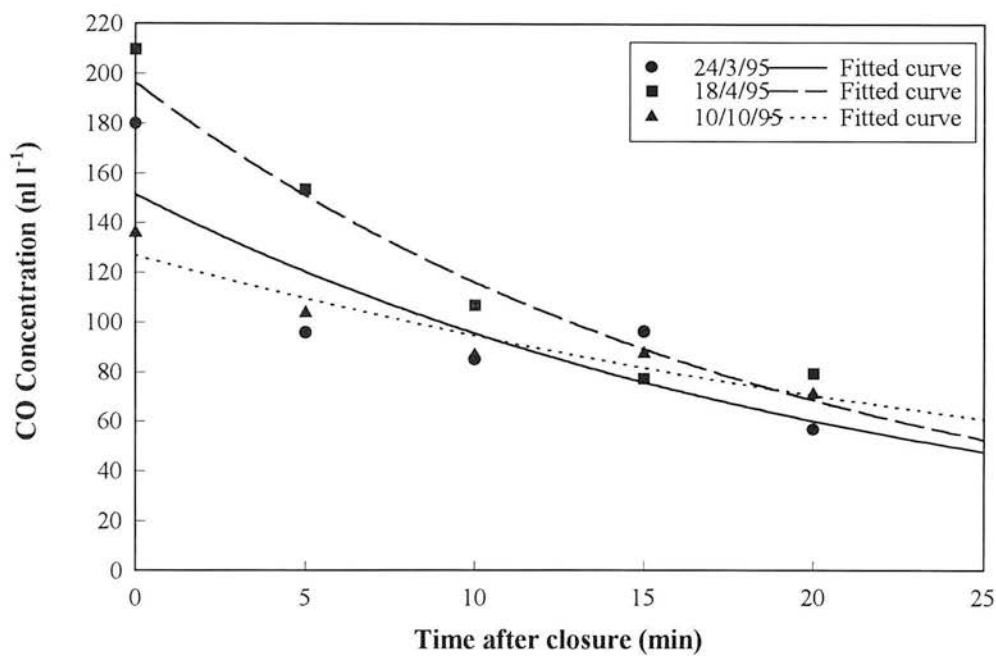


Figure 3.10 Decrease in CO concentration with time in the flux chamber on the coniferous woodland soil at Bush.

t-tests showed that there was a significant difference between mean CO deposition velocities in the arable soil and those in both of the deciduous woodland areas, but no significant differences between mean deposition velocities in the various woodland areas. Averaged over the period from January to November 1995, the deposition velocities for CO oxidation by the woodland soil were approximately twice those for the arable soil (Table 3.4).

Table 3.4 Mean CO deposition velocities from soils under different vegetation types determined in the field at Bush. 12/1/95 - 5/12/95.

Land use	Mean deposition velocity (cm s ⁻¹)	Standard error (cm s ⁻¹)
Arable	0.0084	0.0022
Coniferous woodland	0.0224	0.0026
Deciduous woodland (dry area)	0.0200	0.0016
Deciduous woodland (wet area)	0.0209	0.0020

The deposition velocities on the arable land appeared to reach maxima in the spring and autumn, and be lower in the summer and winter, although the spread of the results from the two chambers makes interpretation of the data somewhat difficult. During a very hot period in the summer, both the chambers on the arable soil became sources of CO (Figure 3.11). The coniferous woodland soil showed largest CO deposition velocity in the winter. Chamber 1 on the dry area of deciduous woodland appeared to show a similar pattern, although the magnitude of the apparent seasonal change was smaller than on the coniferous woodland. The data from chamber 2 were rather noisy, and no seasonal pattern was apparent. There was no obvious pattern to the CO deposition velocity determined with the chamber on the wet area of deciduous woodland.

The only apparent soil factor affecting CO deposition velocity was the temperature. However, clear differences were observed between the temperature dependence for the coniferous woodland and that of the arable land (Figure 3.12). The deposition velocities measured with both chambers on the arable soil showed temperature optima for CO oxidation at about 10 °C. Those measured with the single chamber on the coniferous woodland soil and one of the two chambers on the dry deciduous woodland soil showed a negative linear correlation between deposition velocity and temperature. For the other chamber on the dry area of deciduous woodland there was no relationship between deposition velocity and temperature or any other parameter.

Measurements of the deposition velocity made with five chambers on the coniferous woodland soil found that the mean standard deviation of the deposition velocity between the chambers was 0.0099 cm s⁻¹. A negative relationship was found between the soil temperature and the CO deposition velocity for four out of the five locations shown in Figure 3.1 (Chamber 1: $r^2 = 0.31$, $n = 43$; chamber 3: $r^2 = 0.30$, $n = 16$; chamber 4, $r^2 = 0.22$, $n = 16$ and chamber 5 $r^2 = 0.34$, $n = 16$). Chamber 2 did not show any significant correlation between temperature and CO deposition velocity.

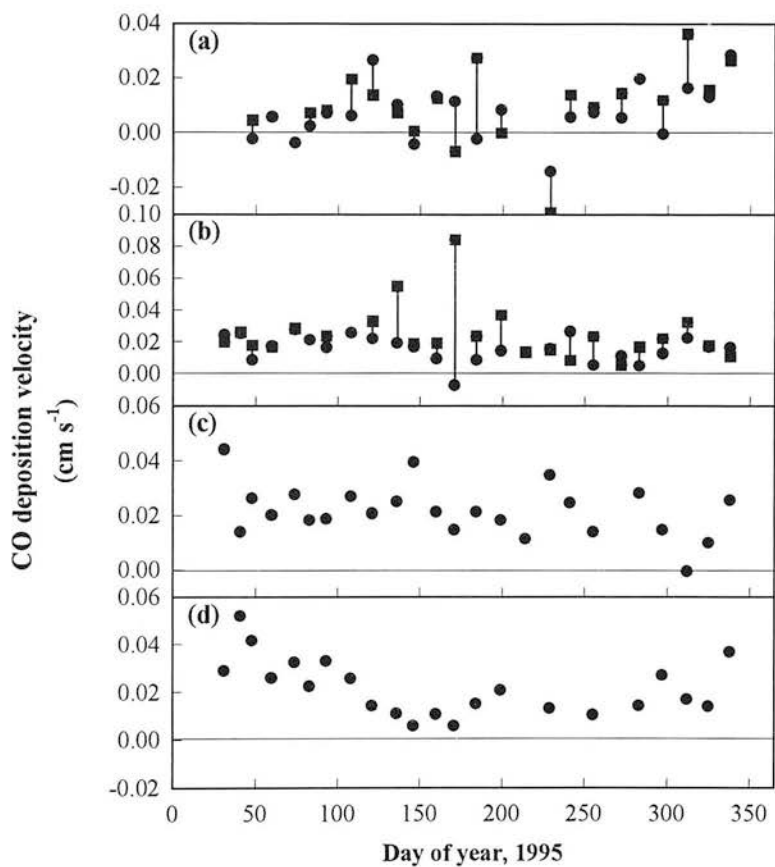


Figure 3.11 Seasonal variation in CO deposition velocity for soils at Bush a) arable b) dry deciduous woodland c) deciduous woodland (wet area) d) coniferous woodland.
 Bars show spread on sites with more than 1 chamber.
 ● Chamber 1 ■ Chamber 2

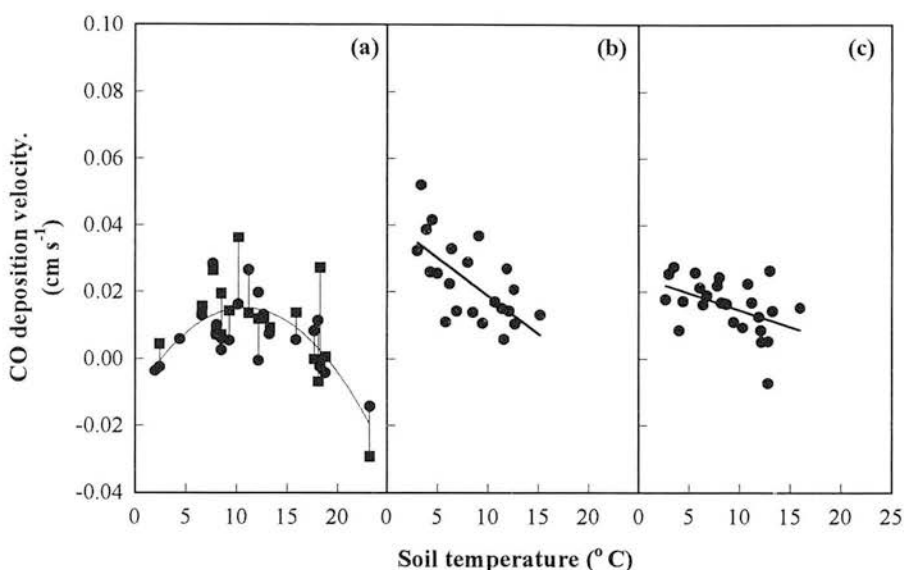


Figure 3.12 Relationships between CO deposition velocity and soil temperature at Bush a) Arable b) Coniferous woodland c) Dry deciduous woodland, chamber 1.

Bars show spread of data between chambers on arable soil.

• Chamber 1 ■ Chamber 2

ii) Gullane

The variation in CO deposition velocity with time at each site at Gullane is shown in Figure 3.13. Each vegetation type showed a similar pattern, with deposition velocities early in the year, a minimum around 6 March (day 65), followed by an increase, and another minimum around 20 May (day 140). The arable soil was fertilised with ammonium nitrate in February and April as in the previous year. The total amount of N applied was 226 kg ha⁻¹. The nitrate content of the woodland soil also increased in the spring due to mineralisation. In the set aside soil, the mineral nitrogen content remained low throughout the year (Figure 3.14)

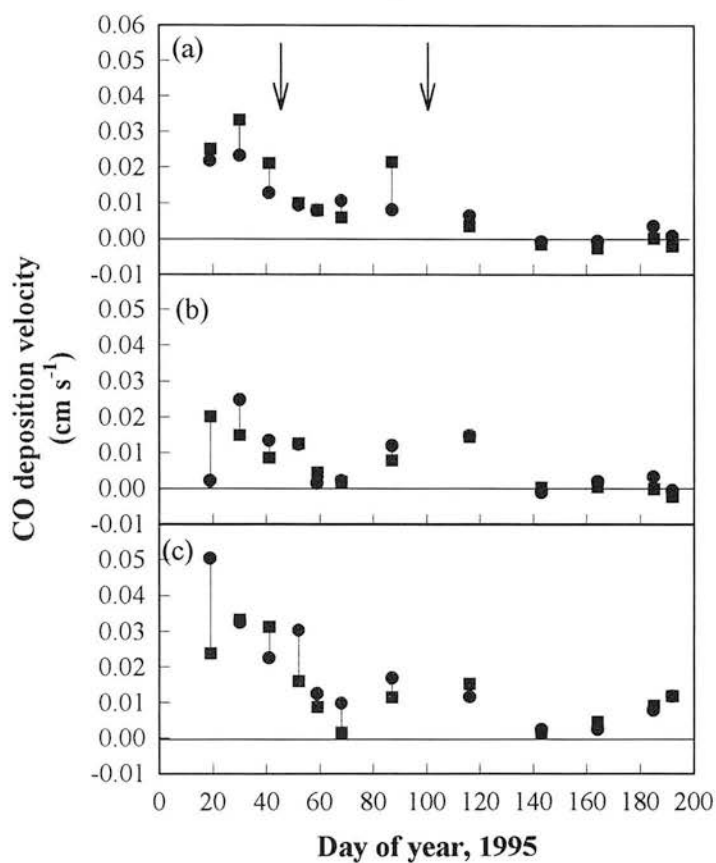


Figure 3.13 Seasonal variation in CO deposition velocity for soils at Gullane. a) arable b) set aside c) woodland. Arrows show dates of fertiliser application to arable site. Bars show spread of date between chambers
 • Chamber 1 ■ Chamber 2

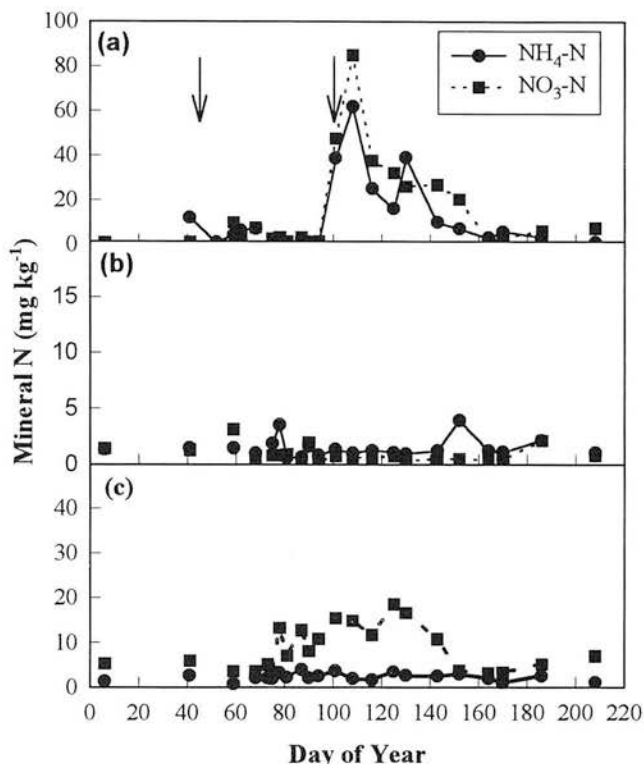


Figure 3.14 Nitrogen content of Gullane soils during 1995.
Means of two measurements.
Errors too small to be shown at this scale.
a) Arable b) Set aside c) Woodland.
Arrows show dates of fertiliser addition to arable site.

For each soil, stepwise multiple linear regression showed that the only variable which significantly affected CO deposition velocity was soil temperature. The relationships between the deposition velocity and temperature are shown in Figure 3.15. In all cases the deposition velocity decreased with increasing temperature. The temperature was strongly negatively correlated with water content for all of the soils ($r^2 = 0.73$, 0.77 and 0.51 for the set aside, arable and woodland soils respectively; $p < 0.01$ for the set aside and arable soils, and < 0.05 for the woodland soil). Therefore, although there was a significant negative correlation between CO deposition velocity and water content for these soils, the water content was not included in the stepwise multiple linear regression.

No significant correlations were found between methane and CO deposition velocities or between CO deposition velocity and nitrous oxide emission rate for any of the soils at Gullane.

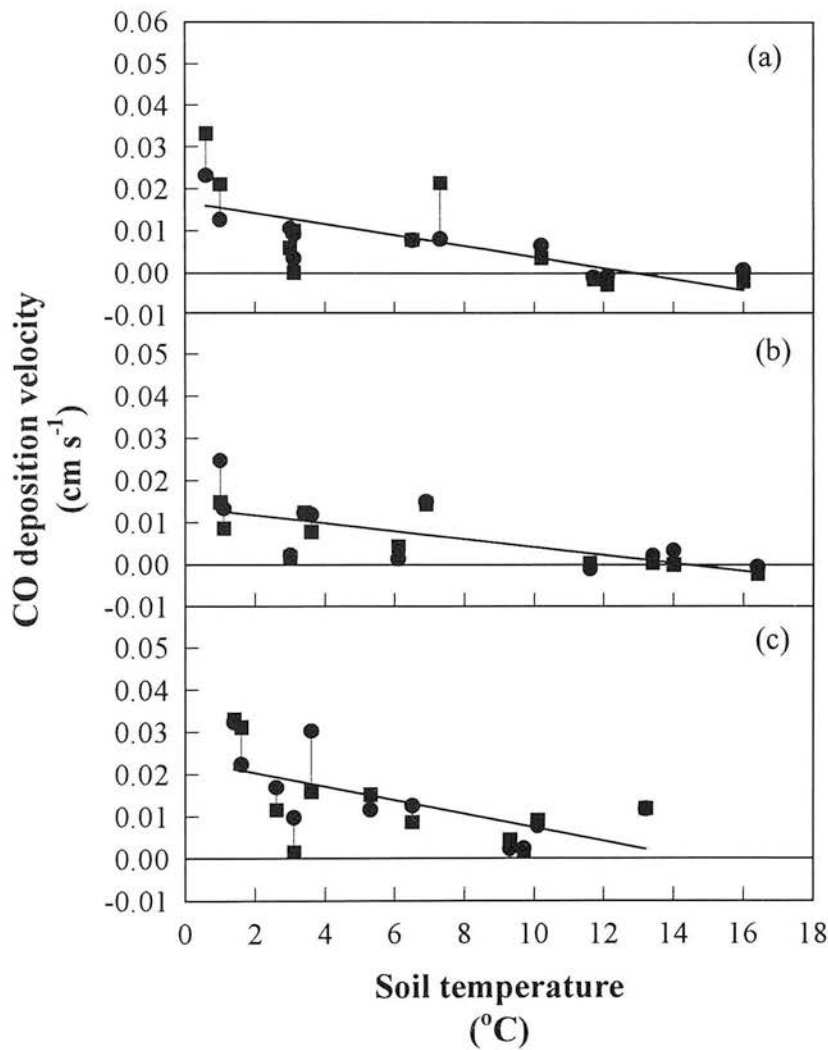


Figure 3.15 Relationships between CO deposition velocity and soil temperature at Gullane a) arable b) set aside c) woodland.
Bars show spread of data between chambers.
Regressions are through data from both chambers on each site.

3.4 Discussion

Soil TOC content and microbial biomass were closely correlated with the CO oxidation rate in the laboratory incubations. Both factors have been found to be important by other authors (Inman *et al*, 1971; Ingersoll *et al*, 1974; Hendrickson and Kubiseski, 1991). The amounts of microbial biomass carbon and TOC were themselves closely correlated. It is likely that soils with a higher TOC content are able to support a larger microbial population, including a larger population of CO oxidisers. Whilst the relationship between initial CO oxidation rate in the laboratory and TOC content was generally linear (Figure 3.2), the two soils with high organic matter contents appeared as outliers with much lower rates than predicted by the relationship for the other soils. The reason for this is not clear, but there are several possibilities, including CO production, under either aerobic (Conrad and Seiler, 1980, 1985c) or anaerobic (Funk *et al*, 1994) conditions, which reduces the net CO oxidation rate, or decreased oxidation potential in peaty soil.

Stepwise multiple linear regression (Chapter 2, Section 2.4.2) with the results for the peaty loam soils omitted suggested that water content may significantly influence the CO oxidation rate (Figure 3.3). Figure 3.3 shows that there was no obvious curvature in the relationship between the residuals of the regression of CO oxidation rate constant on TOC and the water content, although this may have been disguised by the spread of the data. However, Spratt and Hubbard (1981) found an optimum water content for CO oxidation rather than a linear relationship. A separate series of experiments, where noise was reduced by concentrating on a few soils, showed that there was an optimum, which depended on the soil but seemed to be related to the water holding capacity, occurring at higher water contents for woodland soils than for arable soils (Figure 3.4). This pattern could be explained by the likelihood that at very

low water contents microbial activity was reduced, while in very wet soils gaseous diffusion was hindered.

In the laboratory incubations, there was a marginal decrease in rate constant for CO oxidation by the Gullane arable soil after the application of fertiliser. However, the increase in the rate constant which might have been expected due to the increase in microbial biomass was not observed. It is possible that the fertiliser may have provided a substrate for a group of organisms which oxidise ammonium but not CO, at least when there are large amounts of ammonium present. The increase in microbial biomass could then be due at least in part to the increase in these organisms. If the increase in the microbial biomass was due to other changes, for example the soil becoming warmer, then it would be expected that the population of carboxydobacteria would also increase. However, there was no increase in the rate constant for CO oxidation, possibly because it was inhibited by ammonium from the fertiliser application. Bender and Conrad (1994) found that high levels of ammonium slightly inhibited CO oxidation.

The field data from Gullane showed no obvious relationship between soil nitrogen content and CO deposition velocity: similar trends were seen for the fertilised arable soil, the woodland soil with a moderate mineral nitrogen content, and the set aside soil which contained very little mineral nitrogen. In all cases, the CO oxidation rate declined during the late winter and early spring, then peaked in late spring before declining again. The incubations under an atmosphere containing acetylene showed that methanotrophs and nitrifiers were the chief organisms involved in CO oxidation as net CO production occurred when their activity was inhibited. When DCD was added, CO oxidation was inhibited in all cases, although the inhibition was not significant for the Gullane woodland soil. However, net CO production was only observed in one case. The way in which DCD inhibits nitrification is not clear, but it has been suggested that the $C\equiv N$ group might form complexes with metal ions in enzymes, possibly the copper ion thought to be associated with monooxygenases

(Amberger, 1989; Bédard and Knowles, 1989). There are no reported investigations for the effect of DCD on methanotrophs, but it has been reported that DCD does not effectively inhibit all nitrifiers (Jones and Morita, 1984). It is therefore not certain whether the reduced inhibition of CO oxidation produced by DCD can be attributed to it only inhibiting nitrifiers and not methanotrophs, to differences in the nitrifier species inhibited by DCD and acetylene, or simply to poor penetration of the DCD solution into the soil.

The evidence suggests that there is no simple relationship between CO oxidation and either the size of the methanotroph population, the size of the nitrifier population, or the ammonium concentration in the soil. CO production by soils is discussed in Chapter 4. A more detailed study is needed before the effect of ammonium on CO oxidation is fully understood.

In the field sites examined, temperature appeared to be the dominant controlling variable. On the arable land at Bush the form of the temperature dependence was similar to that observed elsewhere (i.e. a temperature optimum for CO oxidation). However, our results showed an optimum at a temperature rather lower than that observed by other workers (Heichel, 1973; Ingersoll *et al*, 1974, Liebl and Seiler, 1976). This may be because the soil used in this study was from a cooler region, and so supported microflora adapted to a cooler environment.

The temperature dependencies of the coniferous woodland soil at Bush, one of the two locations on the dry deciduous woodland soil at Bush, and all soils at Gullane were unusual for a biological process. Biological processes normally have an optimum temperature, with the rate increasing with temperature until the optimum is reached at about 30-40 °C, then decreasing. At the sites listed above, the CO deposition velocity decreased linearly with temperature throughout the temperature range. A possible reason is that production of CO may have occurred at these sites. Soils from arid areas, dried soil samples and dry vegetation are known to produce CO (Smith *et al*,

1973; Conrad and Seiler, 1982b, 1985b; Sanhueza *et al*, 1994a; Tarr *et al*, 1995). The mechanism is uncertain, but is thought to involve chemical or photochemical breakdown of the organic matter. If the plant litter at our sites (broad-leaf and coniferous litter and wheat stubble) was breaking down to produce CO, and the production rate increased sufficiently with temperature, this effect would have led to the observed decline in the net rate at which the CO concentration decreased during the experiment. Assuming that the temperature dependence of the CO oxidation rate constant was entirely due to increases in the CO production rate at increased temperature, activation energies can be calculated for CO production, as

$$k_p = Ae^{-\frac{E}{RT}} \tag{3.1}$$

where k_p is the rate constant for CO production, A is the Arrhenius constant, R is the gas constant, T is the temperature in K, and E is the activation energy. The assumption that the increase in CO production with temperature is much larger than the temperature dependence of CO oxidation is not unreasonable, given that Conrad and Seiler (1982b) found that the activation energy of CO production was approximately four times that of CO oxidation. The calculated activation energies are shown in Table 3.5, and are in good agreement with those obtained by other authors (Conrad and Seiler, (1982b, 1985a,c) found activation energies for CO production by soils of 57-110 kJ mol⁻¹).

Table 3.5 Activation energies for CO production by soils.

Soil	Activation energy for CO production kJ mol ⁻¹
Bush, coniferous woodland,	71
Bush, dry area deciduous woodland.	55
Chamber 1	
Gullane, arable	136
Gullane, set aside	107
Gullane, woodland	84

Material from the organic layer did produce CO, and the rate of production increased by $1.47 \mu\text{g CO m}^{-2} \text{ h}^{-1}$ surface area for each 1°C temperature increase (Figure 3.15), equivalent to an activation energy of 71 kJ mol^{-1} . In the field the apparent rate of CO oxidation decreased by $25.5 \mu\text{g CO m}^{-2} \text{ h}^{-1}$ surface area for each 1°C temperature increase. The larger changes in rate in the field could be due to increases in the effective depth of drying of the material from the organic layer with temperature, which would further enhance the rate of CO production per unit area. A similar mechanism, i.e. CO production from dry grass or decaying leaves, may have been responsible for the temperature dependence seen in one chamber on the dry deciduous woodland. Dry leaves collected from the deciduous woodland area, and dry pineapple mayweed stalks from the fallow land also produced CO when incubated in the laboratory.

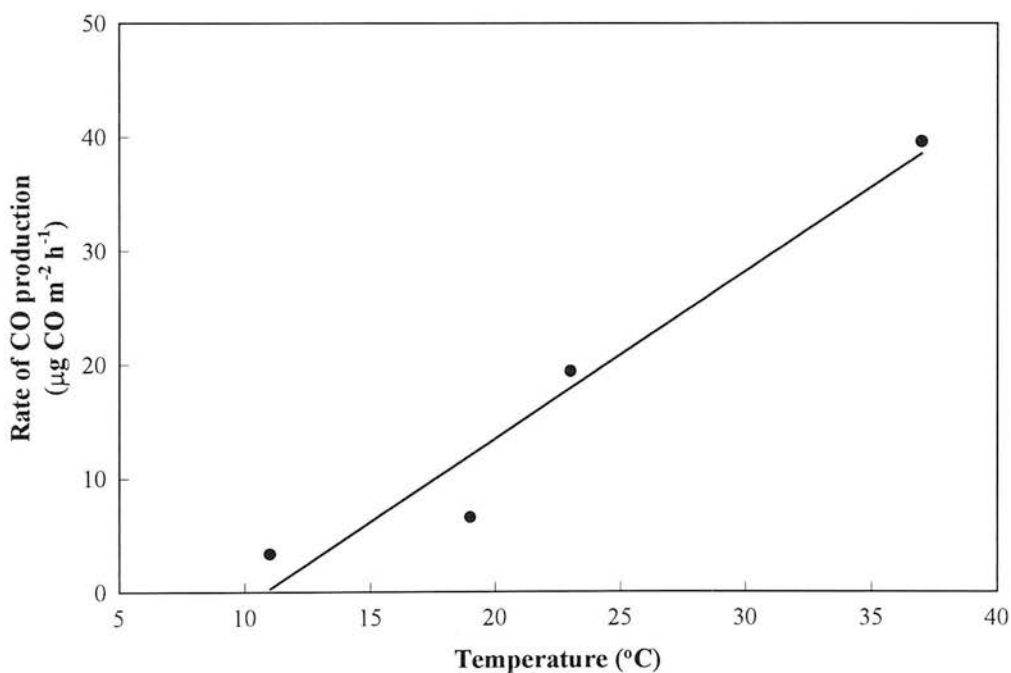


Figure 3.16 Temperature dependence of CO production by material from the organic layer coniferous woodland soil at Bush
 $r^2 = 0.95$, $p < 0.01$.

It is unlikely that temperatures were high enough to inhibit microbial activity, as those in the soils with negative correlations between CO oxidation rate constant and

temperature were only a few degrees higher than those which gave maximum oxidation rates in the arable soil at Bush. It is not clear why the rate constants in arable soils at Gullane and Bush showed different forms of temperature dependence. However, the arable land at Gullane, including the areas within the chambers, was sown with a wheat crop. By July there was a considerable amount of dry wheat stalks in the chambers. At Bush there was pineapple mayweed growing in the chambers, but the total amount of plant matter was less per chamber than at Gullane. The differences in the form of the temperature dependence seen between the arable sites could have been caused by the greater influence of CO production from dry plant matter at Gullane.

An alternative cause could be differences in soil pH, as Conrad and Seiler (1985c) suggest that the breakdown of phenolic substances to produce CO is enhanced by high pHs. This is in contrast with my results (Chapter 4 Section 4.3). In addition, the reaction proposed by Conrad and Seiler to be responsible for CO production from soils is unlikely to have occurred in the woodland soils from Bush, as it requires a much higher pH than the observed value of 4.2. As the chambers were in the dark while the CO fluxes were measured, photochemical processes are also unlikely to be involved. What the actual mechanism is remains unclear.

In most cases, no relationship was found in the field between CO oxidation and methane oxidation or N₂O emission. If a relationship exists it must be complex, for example organisms oxidise CO when their preferred substrate is not available.

3.5 Conclusions

The main factor affecting CO oxidation rates between soils was TOC content. Water content was also important. The relationship between CO oxidation rate constant and water content showed an optimum, which depended on the water holding capacity of the soil.

Within individual sites, temperature was the only factor which significantly affected CO oxidation rate constants. On the arable site at Bush there was an optimum temperature for CO oxidation of about 10 °C. Under the coniferous woodland at Bush, in one chamber on the deciduous woodland at Bush, and in all chambers at Gullane, the CO oxidation rate was negatively correlated with temperature. This seems to have been due to the effect of CO production from dry plant matter. The mechanism for this is investigated further in Chapter 4.

The effect of fertiliser-N on the CO oxidation rate constant is not clear, although there are suggestions that high ammonium concentrations may inhibit CO oxidation, possibly as it is preferentially oxidised by some organisms. However, the nitrifier population is also likely to be increased by the addition of ammonium, and it is possible that as the ammonium concentration declines some of this population switches to oxidising CO, thus giving an increase in the CO oxidation rate constant some time after the ammonium addition. Further work is needed in this area.

3.6 Acknowledgements

I would like to thank Dr. Karen Dobbie for allowing me to measure CO concentrations in air samples which she took at the Gullane site, for providing me data on methane oxidation rates and corresponding measurements of water content, soil temperature, NO₃⁻-N and NH₄⁺-N contents there; and Simona Castaldi for the nitrous oxide production data for the same site.

Chapter 4: Factors affecting CO production by soils under aerobic conditions: laboratory investigation

4.1 Introduction

It is suggested in the literature that CO may be produced by arid soils (see Chapter 1, Section 1.3.1), but little experimental work has been done to investigate this phenomenon.

CO production is thought to result from a chemical process, but it is uncertain what it is. The breakdown of phenolic compounds has been suggested by Conrad and Seiler (1985c), but the reaction they propose seems unlikely, as it requires an elevated pH. A photochemical breakdown of dry plant matter has also been suggested (Tarr *et al*, 1995), but CO production by soils is also known to occur in the dark (Sanhueza *et al*, 1994a). It is known that phenolic compounds break down in the presence of water and oxygen to yield a mixture of products including formic acid. The pathway for this reaction is complex (see Chapter 1, Figure 1.1), and is likely to depend on the exact conditions of the oxidation (Tseng and Huang, 1990; Joglekar, *et al*, 1991). Pure formic acid is known to decompose to CO and water (Drury, 1994). Dehydration of formic acid under acidic conditions is one of the standard methods of industrial CO production, but it is not known whether this dehydration occurs in soils. The effect of soil pH on CO production rates has not been investigated, nor has the effect of rewetting dried soil, despite an observation by Conrad and Seiler (1985a) that CO production by arid soils was promoted by heavy rainfall, and reports of very high CO concentrations over some soils which had been dried and rewetted in laboratory experiments (Smith *et al*, 1973). It is not clear whether increasing the amount of TOC *per se* influences CO production. In field experiments (Conrad and Seiler 1985a) there was a linear relationship between TOC and CO production rates, but this is in contrast

with laboratory results from the same authors (Conrad and Seiler 1985c). It is also not known whether CO production is restricted to soils from arid regions, or whether soils from temperate regions which normally act as a sink for CO can be converted to sources by drying.

CO production has also been observed from asphalt pavements (Tyler *et al.* 1990), which also contain aromatic compounds. CO production was enhanced by heating and exposure to sunlight. The rate of production decreased with the age of the asphalt which develops an inert crust over a period of years, but peak emission rates were $2.6 \text{ mg m}^{-2} \text{ h}^{-1}$, equivalent to about 0.2 Tg y^{-1} world wide. It is possible that the mechanism which operates here is the same as that responsible for CO emissions from soils.

This investigation used the incubation techniques described in Chapter 2, Section 2.2 to investigate factors affecting rates of CO production.

4.2 Materials and Methods

4.2.1. Incubations

Incubations were carried out following the method in Chapter 2, Section 2.2, using 20 g soil per 1.5 l jar, and the ambient CO concentration as the starting concentration. All determinations of CO production rates were carried out in triplicate except where otherwise stated.

Soils were air dried either at room temperature ($\sim 25 \text{ }^{\circ}\text{C}$) or in an oven at $103 \text{ }^{\circ}\text{C}$ to constant weight except where otherwise stated. Rewetted soils were wetted with deionised water to maximum water holding capacity unless otherwise stated. When sterilised soils were used, the soils used were either autoclaved for 30 min or gamma

irradiated by exposure to a dose of > 25 kGy in a cobalt 60 unit (Ethicon Ltd, Edinburgh, UK).

To check that CO evolution was not due to the release of molecules held on the surface on soil particles by a physical adsorption processes (i.e no chemical bonding), samples of soil which had been air dried at room temperature, but not sterilised, were stored at 200 mbar for 48 h at room temperature in a vacuum oven. This should be enough to remove any CO attached to the surface by van der Waals forces, as the maximum observed enthalpy for the physical adsorption of CO on a surface is 25 kJ mol^{-1} (Atkins, 1982).

To investigate further the effects of sterilisation, drying and wetting of soils, and the interactions between them, and to try to determine which components of soil organic matter were responsible for the production, a series of 2^4 factorial experiments were carried out. The experiments were repeated for each of 4 soils (woodland and arable soils from Gullane, dry deciduous woodland and arable soils from Bush), and with 6 different organic materials. The materials used, chosen to represent different classes of soil compounds, were cellulose, glucose, humic acid, sodium acetate, starch, and sucrose. All of the chemicals were supplied by Fluka AG, Buchs, Switzerland and all were Biochemika grade except for the humic acid. The design matrix for the factorial experiments is shown in Table 4.1. "+" shows that a treatment was applied, "-" indicates that it was not. Drying was carried out at room temperature to constant weight; sterilisation was by gamma irradiation; organic material additions were of $0.025 \text{ g organic material g}^{-1} \text{ soil}$, and wetting was with $0.25 \text{ ml deionised water g}^{-1} \text{ soil}$. Treatments were carried out in the order drying, sterilisation, addition of organic material, wetting. The experiment was repeated using each of the six organic materials with each of four different soils (arable soil and soil from the dry area of deciduous woodland at Bush, and arable and woodland soil from Gullane).

Table 4.1 Design matrix for factorial experiments to investigate CO production by soils.

Drying A	Sterilisation B	Organic material C	Wetting D
+	+	+	+
+	+	+	-
+	+	-	+
+	+	-	-
+	-	+	+
+	-	+	-
+	-	-	+
+	-	-	-
-	+	+	+
-	+	+	-
-	+	-	+
-	+	-	-
-	-	+	+
-	-	+	-
-	-	-	+
-	-	-	-

To see whether the rate of CO production varied with pH, as suggested by Conrad and Seiler, (1985c), 5 g samples of humic acid were rewetted with 0.25 ml g⁻¹ of either deionised water, or 0.25 N NaOH, KOH, HCl or H₂SO₄.

4.2.2. Analytical methods

CO concentrations were measured using an RGA 3 Reduction Gas Analyser (Trace Analytical, Menlo Park, California, USA), which had been calibrated with a standard containing 1000 nl l⁻¹ CO (BOC Speciality Gases, Guildford, UK). In some cases the concentrations of CO measured were greater than this. It is not possible to be absolutely certain of the CO concentration in these cases, as the RGA3 is known to be non-linear at high CO concentrations (reported CO concentration is lower than actual). However, relative measurements, showing whether one concentration is

higher or lower than another, are still possible. Soils were analysed using the methods in Chapter 2, Section 2.1.2.

4.3 Results

All soils which were normally sinks for CO were converted into sources by drying. Full details of their properties before drying are included in Table 3.1. Table 4.2 and Figure 4.1 show the rates of CO production from soils which had been air dried at either room temperature or 103 °C, and which had then either been left dry or rewetted to maximum water holding capacity. ANOVA showed that both increasing the drying temperature and rewetting the soil significantly increased the rate of CO production ($p < 0.05$ for both factors). Rewetting after drying at the higher temperature had a dramatic effect on CO production, compared with the effect at 25 °C. The average increase in production when dry soil was rewetted was twelve fold after drying at 103 °C, but was only up to two fold after drying at 25 °C.

Table 4.2 CO production rates from dried soils

Soil	TOC (%)	CO production rate ($\mu\text{g CO kg}^{-1}$ dry soil h^{-1})			
		Dried at 25 °C		Dried at 103 °C	
		Dry	Rewetted	Dry	Rewetted
Cowpark, grassland	3.3	4.2	4.2	6.5	74.8
Cowpark, woodland	6.0	6.6	14.0	11.9	151.0
Gullane, arable	1.1	1.8	2.8	2.7	17.8
Gullane, woodland	3.1	2.4	5.0	3.9	63.3

Figure 4.2 shows that there was a linear relationship ($r^2= 0.72$, $p < 0.01$) between TOC content and CO production rate.

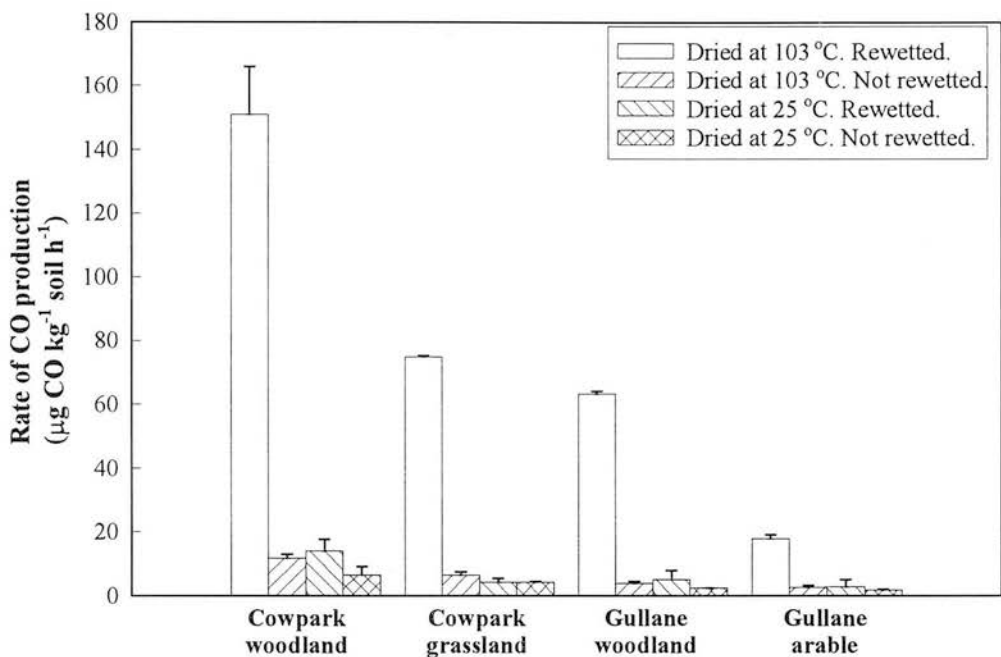


Figure 4.1 Effect of drying and rewetting on soils from 4 sites.
Error bars show 1 standard error. n = 3.

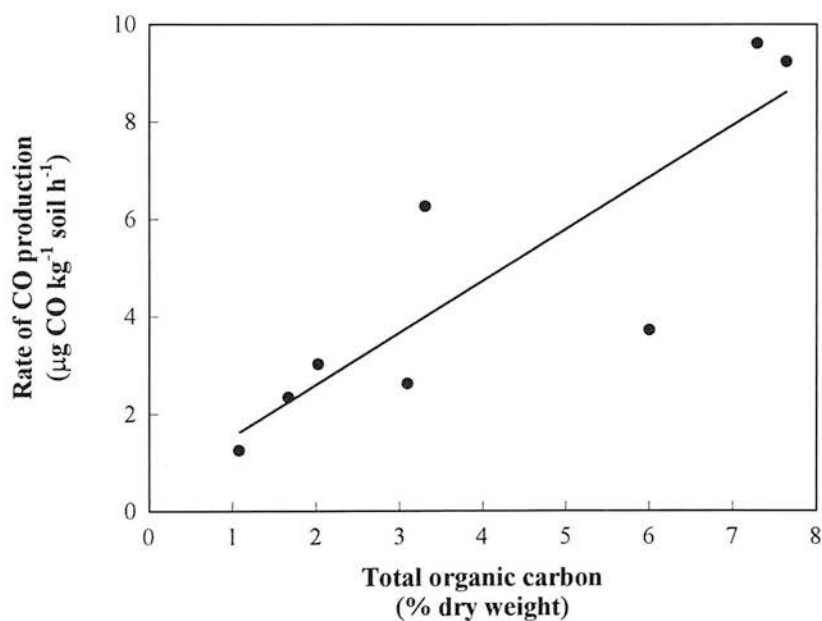


Figure 4.2 Relationship between TOC content and rate of CO production by soils air dried at room temperature and not rewetted.

Figure 4.1 and the data in Table 4.1 suggest that the rate of CO production increases for soil with a higher TOC content. This was investigated further using soils from the woodland and arable sites at Bush (See Chapter 3) which were dried at room temperature and not rewetted. There was a linear increase in CO production rate with TOC content (Figure 4.2).

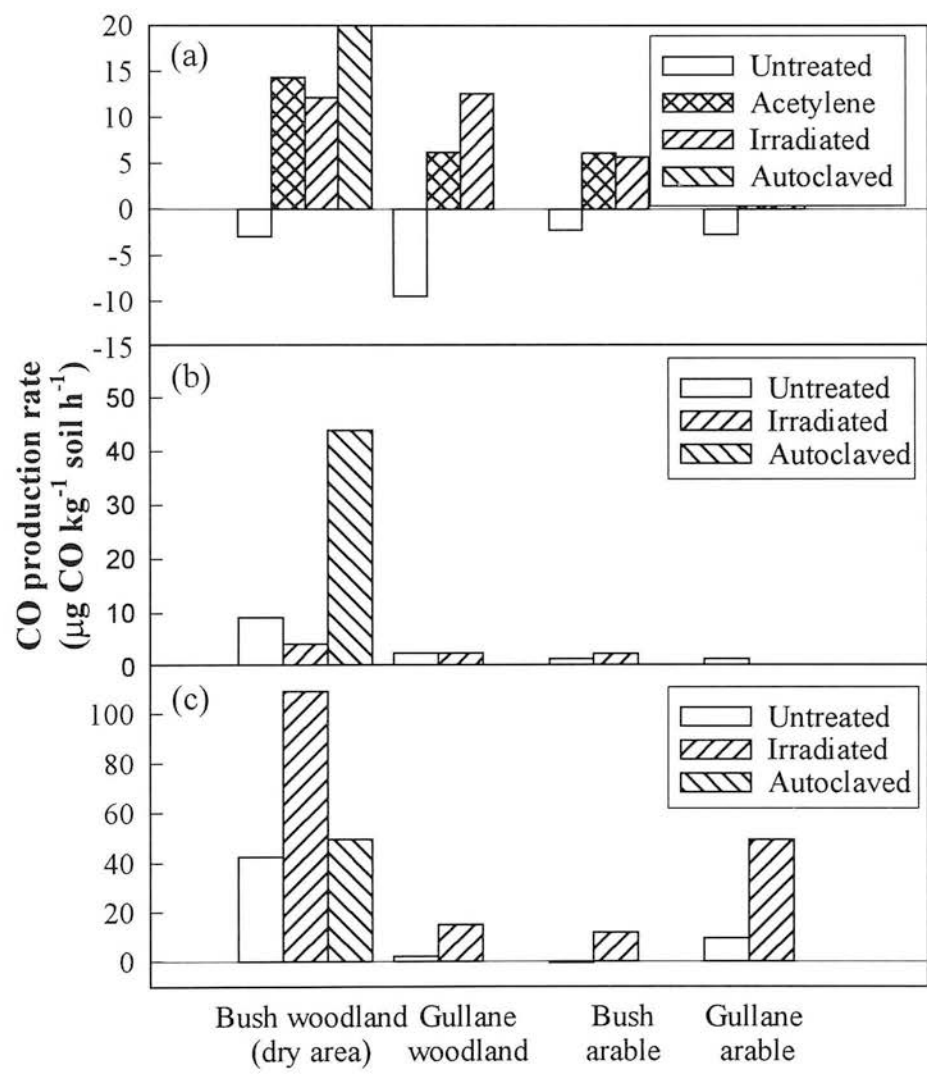


Figure 4.3 Effect of sterilising soils on CO production
a) fresh soil b) soil air dried at ~ 25 °C
c) As b, but rewetted with 0.25 ml H₂O g⁻¹ soil

Both autoclaving and gamma irradiation actually enhanced CO production in fresh, air dried (~25 °C), and rewetted soils (Figure 4.4), so CO production cannot be a biological process. In many cases, sterilisation by either method noticeably changed the smell of the soil to a more vinegary one, typical of organic acids. This suggests that sterilisation affected the soil chemistry.

Net CO production also occurred when CO oxidation by methanotrophs and nitrifiers was inhibited by 1 ml l⁻¹ acetylene in the headspace above the soil (Figure 4.3a) (See also Chapter 3, Section 3.3 and Figure 3.8).

Following storage under vacuum, CO production was halted, and net CO oxidation occurred. A t-test found that these changes were significant at the 95 % confidence level. After the first run, it was noted that the soils had become significantly moister after storage in the vacuum oven, possibly due to rewetting with water which had condensed in the vacuum oven tubing during previous use. To ensure that this did not occur in subsequent runs approximately 300 g dry silica gel was placed in trays in the vacuum oven to remove water. When the experiment was repeated with the silica gel in place, there was no significant change in the water content, and a t-test showed that there was no significant difference in CO production rates between soils which had been stored under vacuum, and controls which had been stored in the laboratory. The silica gel was not mixed with the soil, but kept in separate containers. It was not in the jars when measurement of CO fluxes were made, and therefore could not have affected them. The experiment was repeated, with the soil being rewetted with 0.25 ml water per g soil after storage under vacuum. Again there was no significant difference in CO production rates between soils which had been stored under vacuum, and soils which had been stored in the laboratory at atmospheric pressure.

As the addition of water to the soil had an influence on CO production, further work was undertaken to see whether the process had an optimum water content. Soils from

Bush and Gullane were dried to constant weight at room temperature, then rewetted with deionised water to give a range of water contents for each soil. There were contrasting results between soils from the Bush site and those from Gullane. For all the Bush soils except the arable one, there was an optimum water content for CO production at about 20 % (Figure 4.4). For the Gullane soils and for the arable soil from Bush, there was a minimum in CO production at about the same water content (Figures 4.4 and 4.5).

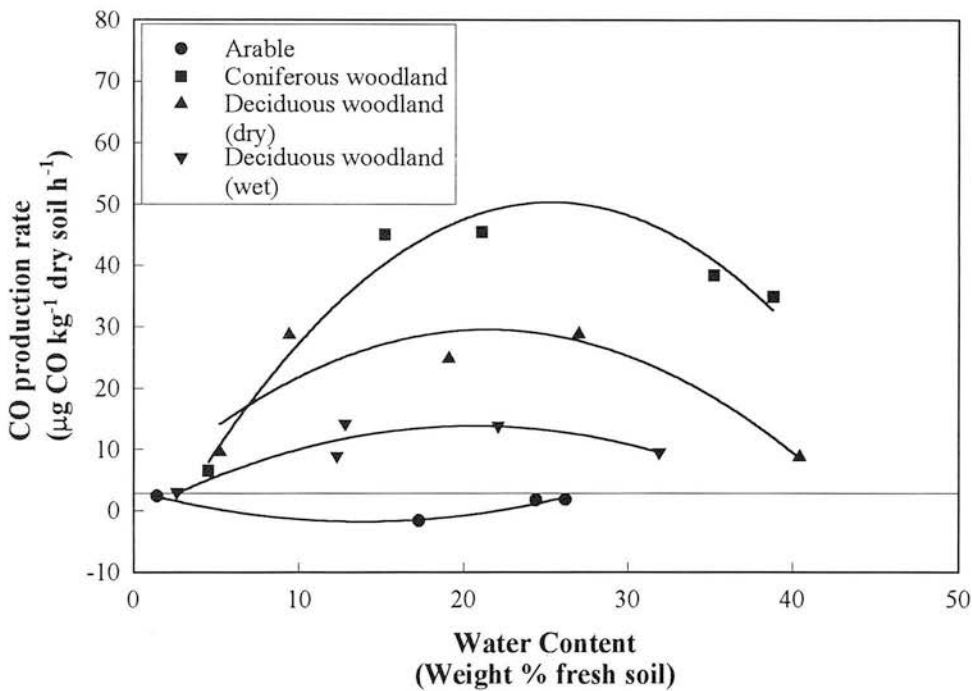


Figure 4.4 Relationship between water content and CO production rate for soils from Bush air dried at $\sim 25^{\circ}\text{C}$ and rewetted.

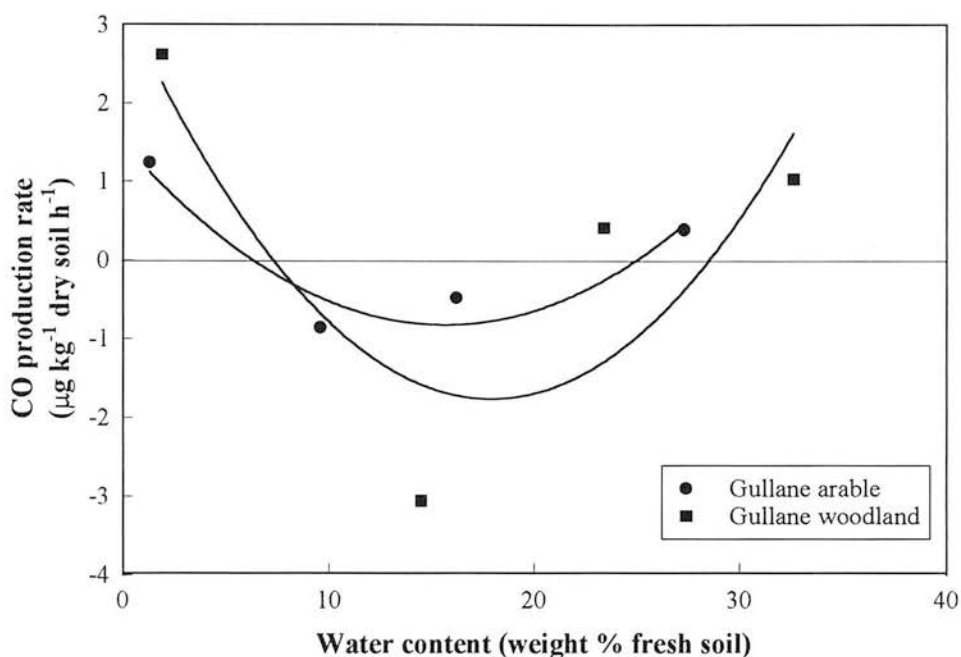


Figure 4.5 Relationship between water content and CO production rate for soils from Gullane air dried at ~ 25 °C and rewetted.

It was only possible to complete the factorial experiments for some of the organic additives (humic acid, glucose and sodium acetate) with the soil from the dry deciduous woodland at Bush; this was because in some cases a peak appeared during the gas chromatographic analysis between the H₂ and CO peaks, preventing a quantitative measurement of CO. It is not known which gas caused these peaks, except that it was not methane, formaldehyde or acetylene. The results of the factorial experiments are shown graphically in Appendix 2, and are summarised in Table 4.3

In all cases but two, sterilisation of the soil significantly increased CO production. For all soils except the one from the dry deciduous woodland area at Bush it had the most significant effect. Drying and wetting of soils also had a significant effect in most cases, as did their interaction. The only organic substrate which consistently increased CO production was humic acid, although glucose, sodium acetate and sucrose also increased CO production from the Bush arable soil, but their effects were much

smaller than that of humic acid. Sodium acetate significantly increased CO production by the soil from deciduous woodland area at Bush. The interaction between drying, sterilisation and wetting was significant for all additives with most soils, except for the Gullane arable one where it was only significant when humic acid was added. To see whether any of the organic additives produced or removed CO in the dry or wet states, 5 g samples of each material were incubated when dry, and wetted with 0.25 ml deionised water g⁻¹. None of the dry organic materials produced changes in CO concentration of more than 30 nl l⁻¹ in a 1.5 l jar over a six hour period i.e. 1.8 µg CO kg⁻¹ additive h⁻¹: far lower than rates of CO production for dried soils. However, when the organic materials were stored at 103 °C prior to incubation, the humic acid produced CO at a rate of 13 µg CO kg⁻¹ additive h⁻¹. When wetted, all of the organic materials produced CO. In most cases the rate of production was less than 10 µg CO kg⁻¹ organic material h⁻¹, but in the case of humic acid, the rate of CO production was 165 µg CO kg⁻¹ h⁻¹. When the organic materials stored at 103 °C were rewetted rates were 173 µg CO kg⁻¹ h⁻¹, 40 µg CO kg⁻¹ h⁻¹, 12 µg CO kg⁻¹ h⁻¹ for humic acid, starch and cellulose respectively. The other materials produced CO at less than 10 µg CO kg⁻¹ h⁻¹. To check that CO was not simply absorbed onto clay minerals, and released by displacement with water, CO evolution from molecular sieves was investigated. 4Å and 5Å Union Carbide molecular sieves were used. CO fluxes over molecular sieves which had been stored at room temperature and at 104 °C were measured, before and after they were wetted with 0.25 ml deionised water g⁻¹. Very little CO (< 10 µg CO kg⁻¹ h⁻¹) was evolved over either of the unwetted molecular sieves whether they had been stored at room temperature or 104 °C. When water was added a little CO was evolved, but the rate of evolution was far slower than over humic acid (maximum rate for molecular sieve 4Å: 26 µg CO kg⁻¹ h⁻¹ and for molecular sieve 5Å: 28 µg CO kg⁻¹ h⁻¹), and there was no clear trend in CO production rate with the storage temperature of the molecular sieve.

t tests showed that differences in pH did not cause significant differences in CO production rate.

Table 4.3 Summary of results of factorial experiments to investigate CO production by dry soils.

Soil	Drying A	Sterilisation B	Organic material C	Wetting D	Interaction AD	Other interactions
Gullane arable	None	All except sodium acetate and glucose	Humic acid	Humic acid only	Humic acid only	ABD: humic acid only.
Gullane woodland	✓	✓	Humic acid	✓	✓	BD: all except glucose and starch. ABD: all.
Bush arable	✓	✓	Glucose Humic acid Sodium acetate Sucrose	✓	✓	AB: glucose and starch BD: all except cellulose and humic acid. ABD: all. ABCD: sodium acetate.
Bush deciduous woodland (dry area) ⁽¹⁾	✓	✓	Humic acid and sodium acetate	✓	✓	AB: humic acid. BD: all ABD: all

A ✓ shows that the variable or interaction had a significant positive effect. Capitals show variables, and groups of capitals show interactions e.g. ABD is the interaction between variables A, B and D i.e. between drying, sterilising and wetting.

(1) Results for trials with glucose, humic acid and sodium acetate only.

Rates of CO production did not change significantly for soils which were stored for periods of up to 6 months in the dry state, although during incubations, the CO concentration reached a plateau after about a week (Figure 4.6). Once rewetted, soils eventually regained their ability to oxidise CO (Figure 4.7). This recovery was faster for unsterilised soils than for sterilised soils.

4.4 Discussion

It is clear from this investigation that CO production by soils is not restricted to soils from arid regions, but can occur in any soil which becomes dry enough (Smith *et al*, 1973). Even drying at ambient temperatures induced CO production, although rates were increased by drying at higher temperatures. It is possible that drying, especially at higher temperatures, breaks down some components of the soil organic matter, which are partially oxidised to CO. CO production rates were enhanced by the addition of water, and were proportional to the TOC content. This may simply be because when the TOC content is low, the rate of CO production per unit mass of soil is slower. Alternatively, it is may be that in the soils with low TOC contents, it is possible that most of the organic matter is associated with clay minerals, and thus is stabilised with respect to breakdown.

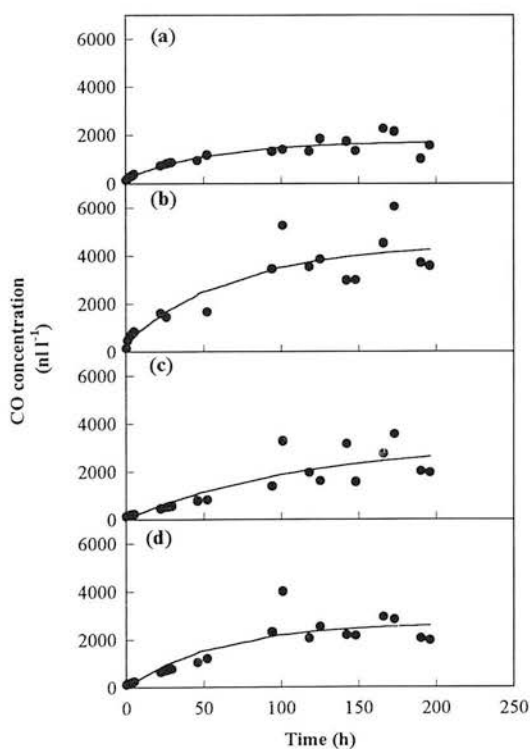


Figure 4.6 CO concentration over air dried soils without rewetting.
a) Cowpark grassland b) Cowpark woodland
c) Gullane arable d) Gullane woodland.

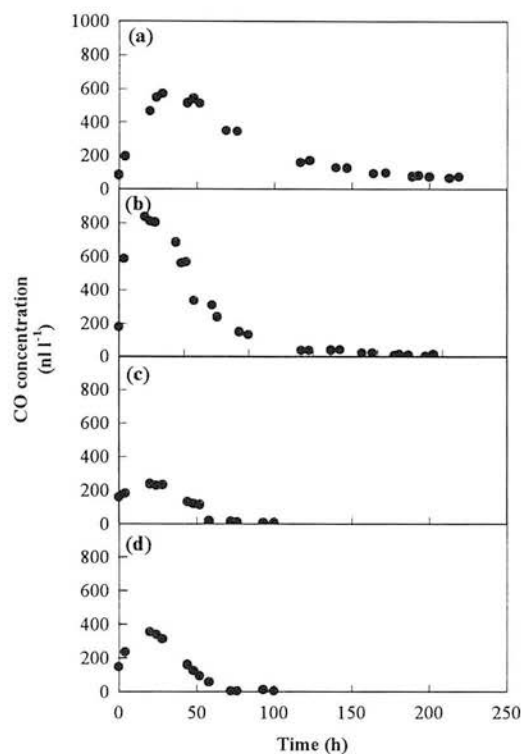


Figure 4.7 CO concentration over air dried soils after rewetting.
a) Cowpark grassland b) Cowpark woodland
c) Gullane arable d) Gullane woodland.

CO production cannot be caused by biological activity, as it was not reduced by sterilisation. In fact it was enhanced by sterilisation in most cases. This may be because the conditions required to kill microorganisms also broke down soil organic matter or because CO is normally formed by soils, but this effect is masked by microbial oxidation, leading to net CO oxidation. Net CO production was also observed when CO oxidation was halted by acetylene. As acetylene is unlikely to affect the chemical composition of the soil, this suggests that the CO production may be a process which normally occurs in soils, but is often masked by CO oxidation leading to net CO oxidation. The rate of CO production following treatment with acetylene was similar to that after sterilising the soil by gamma irradiation, which suggests that while autoclaving enhances CO production, possibly by accelerating the

breakdown of organic matter, gamma irradiation prevents biological activity, while not greatly affecting soil composition. CO evolution was not caused by the release of CO held on the surface of soil particles by a physical (i.e. van der Waals) adsorption process, as it was not halted by storage under vacuum in dry conditions. Whilst it is still possible that CO was retained at the surface by the formation of a chemical bond, it is not clear what this would be. While a little CO was released from zeolite molecular sieves when they were wetted, the rate of CO evolution was far less than from humic acid. Therefore it is unlikely that the evolution of CO observed over soils is simply due to the release of CO adsorbed onto clay minerals. CO is known to form complexes with transition metals including iron and nickel, but it is unlikely that the CO would be released from these by the addition of water, as the metal-CO bond in the carbonyl complexes is stronger than a single bond due to σ - π back bonding, although CO might be released on heating (Cotton and Wilkinson, 1980). In any case this would not explain the evolution of CO from pure humic acid on heating or after the addition of water. There is no evidence in the literature to suggest that CO adsorbs chemically onto the surface of any organic material.

The soil water content influenced CO production rates, although the relationship was not simple. In unsterilised soils with high organic matter, which had high CO production rates when dried, production rate increased with water content up to a maximum, and then decreased. The increase may have been caused by increasing dissolution of organic matter, while the decrease in production rate with increasing water content beyond the maximum may have been caused by hindered gaseous diffusion as the soil became waterlogged. In unsterilised soils with lower organic matter contents, there was a decrease in CO production with increasing water content to a minimum, followed by an increase. It is possible that in these soils, increases in the biological oxidation of CO with water content outweigh any increases in CO production, leading to a net decrease in production with water content. However,

once the soil becomes waterlogged, and gaseous diffusion is reduced, the CO oxidation rate decreases. (See Chapter 3, Figure 3.4).

The factorial experiments showed that sterilisation was the factor that caused the most significant increase in CO oxidation. The effects of drying the soil and wetting it, as well as the interaction between these two factors, were also significant. The significance of the interaction suggests that CO production is caused by a breakdown of soil organic matter into smaller molecules which oxidise to CO. The oxidation is increased if water is present. This agrees with the finding that the interactions between sterilisation (which also breaks down soil organic matter), and wetting the soil, and between sterilisation, drying and wetting are significant. Humic acid was the only organic material which significantly enhanced CO production in most cases. Sugars, other polysaccharides, and the salts of organic acids did not significantly affect CO production. These observations agree with the results of Conrad and Seiler (1985c). Humic acid itself was not a source of CO when dry if stored at room temperature, but was after storage at 103 °C, and when wetted. The conditions which induced CO production from humic acid were similar to those which induced it in soils (i.e. drying at high temperatures and rewetting). Exposure to high temperatures, followed by rewetting, also induced CO production by starch and cellulose, but to a lesser extent than humic acid.

In contrast to Conrad and Seiler's results the pH did not affect the rate of CO production from moist humic acid. This suggests that the reaction which they suggest is responsible for CO production may not be the one which occurs in soils, and a different one may be involved, for example that proposed by Joglekar *et al*, (1991) for oxidation of phenolic compounds, followed by dehydration of formic acid. The activation energy for the decomposition of phenolic materials to formic acid is in the range 12-201 kJ mol⁻¹, which includes the range of estimates of the activation energy

of CO production by soils of 55-137 kJ mol⁻¹ (Conrad and Seiler, 1985c; this work, Chapter 3).

Dry soils retained their ability to produce CO for considerable periods of time, but once rewetted gradually regained their capacity to oxidise it, as active microbial populations became reestablished, and sterile soils were recolonised.

CO production by soils could be important if climate change leads to increased aridity in regions which currently have a temperate climate, especially as many soils in temperate regions have high carbon contents, and so are potentially large sources of CO when dried. Even if soils are not net sources of CO, the effect of CO production can affect net oxidation rates (see Chapter 3, Sections 3.3.2 and 3.4).

4.5 Conclusions

CO production can be induced in soils which normally oxidise it when the soils are dried. It can also occur if CO oxidation is inhibited by the addition of acetylene, autoclaving or gamma irradiation, which suggests that it is a process which normally occurs in soils, but is masked by oxidation. CO production is caused by a chemical rather than a biological or physical process and is enhanced by autoclaving the soil and the addition of water to dried or sterilised soils. CO production increases with the amount of soil organic matter, and is probably caused by the breakdown of organic materials, in particular humic acid. The mechanism for this is not certain.

4.6 Acknowledgement

I would like to thank John Walker and Derek Dickson of Ethicon Ltd, Sighthill, Edinburgh for their assistance with gamma sterilisation of soils.

Chapter 5: CO production by waterlogged soils.

5.1 Introduction

There are several suggestions in the literature that waterlogged soils could be a source of CO, but the evidence is sparse (Chapter 1, Section 1.3.2). The clearest evidence comes from the incubation of waterlogged taiga bog cores (Funk *et al.* 1994), which produced CO at a mean rate of $37 \mu\text{g CO m}^{-2} \text{ h}^{-1}$. There is also evidence from airborne measurements that there are sources of CO close to the ground in the Amazon basin (Harriss *et al.* 1990a; Kirchoff and Marinho, 1990; Ritter *et al.* 1990) and the north American tundra (Gosink and Kelley, 1979; Ritter *et al.*, 1992,1994), although it is not clear whether the CO is emitted from the soil, or by some other source such as direct emission from vegetation. The north American tundra source had a strength of up to $30 \mu\text{g CO m}^{-2} \text{ h}^{-1}$ (Ritter *et al.*, 1994). Conrad *et al.* (1988) and Khalil *et al.* (1990) found CO emissions from rice paddies in the range $12\text{-}110 \mu\text{g CO m}^{-2} \text{ h}^{-1}$.

This investigation used closed chamber techniques (Chapter 2, Section 2.3.1) to investigate fluxes at a peatland site in Midlothian, and also attempted to measure fluxes from cores incubated under anaerobic conditions.

5.2 Materials and Methods

5.2.1 Laboratory studies

To make a preliminary investigation of CO fluxes from waterlogged soils in the laboratory, four 30 cm long cores, 6.5 cm in diameter were taken from the peatland field site at Leadburn (see Section 5.2.2 below), two from a drier area and two from a wetter area. Averaged throughout the year, the water table at the wetter area was 4.7

cm higher than at the drier site. During the winter puddles formed at the wetter area, but this did not happen at the drier site. The cores were taken by pushing rigid plastic drainage pipe into the ground. The peat around the outside of the pipe was cleared, and the pipe and its contents removed. The lower end of the core was capped to try to maintain anaerobic conditions. The cores were pushed out of the pipes and cut into 5 cm long sections under a nitrogen atmosphere in a glove-box within three days of extraction. Each section was placed in a Kilner jar (Chapter 2, Section 2.2), and incubated under nitrogen at room temperature. A piece of anaerobic indicator paper (Becton Dickinson Microbiology Systems, Cockeysville USA) was placed in each jar to show whether anaerobic conditions were maintained.

Gas samples for CO analysis were withdrawn from each jar every few hours. The CO concentration was measured using an RGA 3 reduction gas analyser (Chapter 2, Section 2.1.1). At the end of each incubation, oxygen and methane concentrations were measured. Oxygen concentrations were measured using a gas chromatograph with a thermal conductivity detector. Gases were separated using a 1.2 m stainless steel column 6 mm in diameter packed with Poropak Q, followed by a 1.5 m by 3 mm stainless steel column filled with 5Å molecular sieve. The columns were at 65 °C, and the detector at 80 °C. Helium at a flow rate of 40 ml min⁻¹ was used as the carrier gas. The sample loop held 0.5 ml. Methane concentrations were measured using a gas chromatograph fitted with a flame ionisation detector, maintained at 120 °C. The column used was 1.5 m long, and 6 mm in diameter, packed with alumina and maintained at 36 °C. Nitrogen at a flow rate of 40 ml min⁻¹ was used as the carrier. The sample loop held 1 ml, and to ensure that it was completely filled 5 ml of each sample was flushed through it.

5.2.2. Field measurements

Field measurements were made approximately once a fortnight using the closed chamber method (Chapter 2, Section 2.3.1) at a peatland site a Springfield Farm, Leadburn, Midlothian, Scotland, UK (55 ° 47 ' N, 3 ° 14 ' W, Ordnance Survey grid reference NT 221562) from February 1995-February 1996 (Plate 5.1). The peat layer at the site was 30 cm deep on a base of Upper Old Red Sandstone (Ordnance Survey, Soil Survey of Scotland). The vegetation consisted mainly of mosses and grasses. Mosses such as *Sphagnum* and *Polytrichum*, and sedges (*Carex ovalis* and *Carex nigra*) dominated the wetter areas, while the drier areas were dominated by grasses, especially *Deschampsia flexuosa*, *Molinia caerulea*, *Eriophorum vaginatum*, *E. angustifolium*, *Festuca ovina* and *F. rubra*. There were also scattered patches of heathers (*Erica tetralix*, and *Calluna vulgaris*) and bilberry (*Vaccinium myrtillus*). Three chambers were used, one on a relatively dry area, one on an area of wetter ground, and one on an intermediate area. Only three chambers were used, as this allowed spatial variability to be estimated, while keeping the number of samples to be collected and analysed to a practicable level, bearing in mind that soil atmosphere samples were to be collected on each occasion, in addition to the chamber samples (see below). As no other measurements of CO fluxes at waterlogged sites exist, it was not possible to use such measurements to estimate the variability between chambers, and so calculate the number of chamber necessary to achieve a given uncertainty in the estimation of the population mean (Chapter 2, Section 2.4.1).

The temperature at 10 cm and soil water content was measured each time the flux was measured. From June 1995 to February 1996, air samples were taken from 30 cm long brass tubes, 0.4 cm in diameter, capped by rubber septa. Triplicate sets of tubes were inserted to 3, 6, 9, 12, 15, 18, 21, 24, and 27 cm depths close to the wettest and driest chambers, to determine profiles of CO concentration. The water table depth

was also recorded, by making dip-stick measurements in a 2 cm diameter well lined with plastic pipe.

No measurements of meteorological parameters were made at this site to accompany the measurements of CO fluxes, but the soil temperature at 10 cm and soil moisture content were measured whenever CO fluxes were measured to allow the possible effect of changes in temperature and hydrology to be assessed. (See Chapter 2, Section 2.3.1 for details.)



Plate 5.1 The Field Site at Leadburn, Midlothian, Scotland.

5.3 Results

5.3.1 Laboratory experiments

The water content of cores from the drier area ranged from 52 % to 84 % by weight, while those from the wetter area had water contents of between 76 and 90 %. The water content of the cores increased with depth.

The laboratory investigation of CO production by waterlogged peaty soils did not give clear results. In all cases, the Kilner jars contained at least 2 % oxygen after a few days of incubation, and enough oxygen for the anaerobic indicator paper to show its presence a few minutes after the Kilner jars were removed from the anaerobic glove box. This may seem surprising when as little leakage of CO from jars was found (Chapter 2, Section 2.2) however, the CO concentration in the jars was only a few hundred nl l^{-1} greater than the ambient concentration, whereas the oxygen concentration was several percent lower in the jars than outside. Assuming that the diffusion coefficients of oxygen and CO are similar the rate of diffusion of oxygen into jars which were originally anaerobic would have been very much faster than the rate of diffusion of CO as the concentration gradient between inside and outside the jars is much larger.

In most cases little or no CO was evolved, even when the incubation was allowed to continue for several days. Although some sections of some of the cores produced CO, there was no trend in CO production with the depth from which the core section came (Figure 5.1). Only one core (core 1 from the wetter area) showed a significant correlation between CO and methane production rates. There was no relationship between the final oxygen concentration in the jars and the CO production rate.

The gravimetric water content remained nearly constant in the core to a depth of about 20 cm, then decreased sharply, presumably because at this depth the peat

became compacted, leaving less pore space. There was a significant correlation between water content and CO production rate in most cases, but these correlations relied heavily on one point per core from deeper down the profile with a lower water content (Figure 5.2).

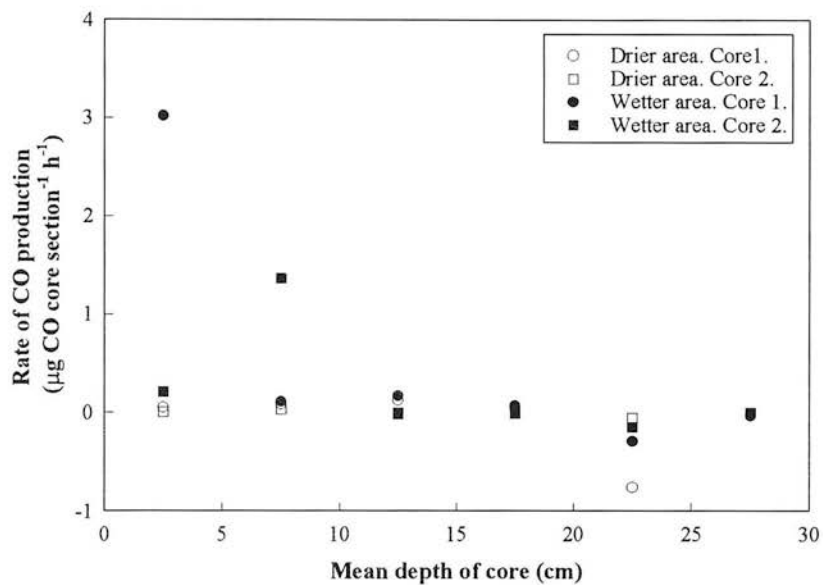


Figure 5.1 Variation in CO production rate with depth for peat cores from Springfield Farm, Leadburn, Midlothian, Scotland.

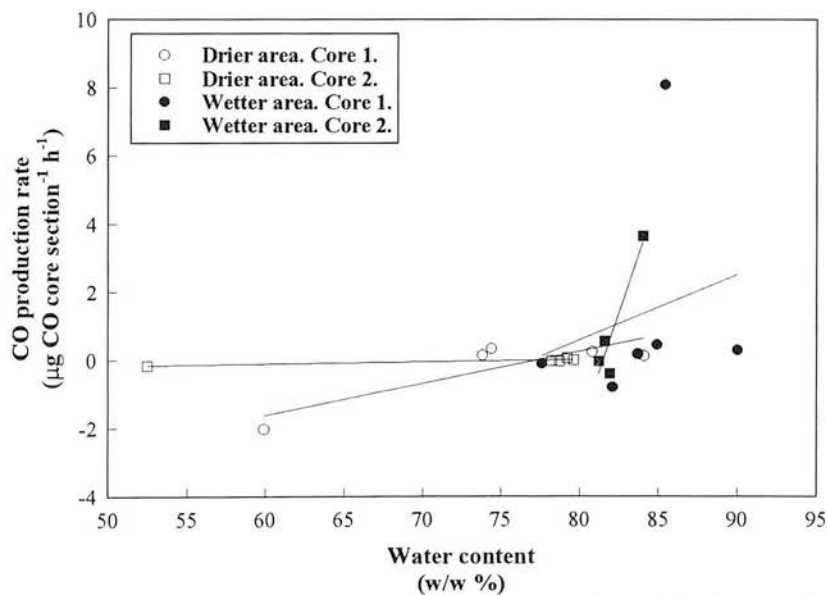


Figure 5.2 Relationship between water content and CO production rate for peat cores from Springfield Farm, Leadburn, Midlothian, Scotland.

5.3.2 Field measurements

The measurements of CO fluxes in the field showed that, at the drier chamber, CO was oxidised most of the time, while at the wetter chamber it was produced most of the time. At the chamber with the intermediate water content, there was a mixture of oxidation and production. Oxidation of CO occurred in all chambers during a period of warm, dry weather in the summer, and CO production tended to occur during cooler, wetter weather in the winter (Figure 5.3). Over a one year period, the wettest chamber was a net source of CO, with a mean production rate of $7.6 \mu\text{g CO m}^{-2} \text{ h}^{-1}$, while the other two chambers were net sinks. The only significant correlation between CO production rate and soil water content or soil temperature was in the driest chamber, where there was a significant positive correlation between soil water content and CO production rate.

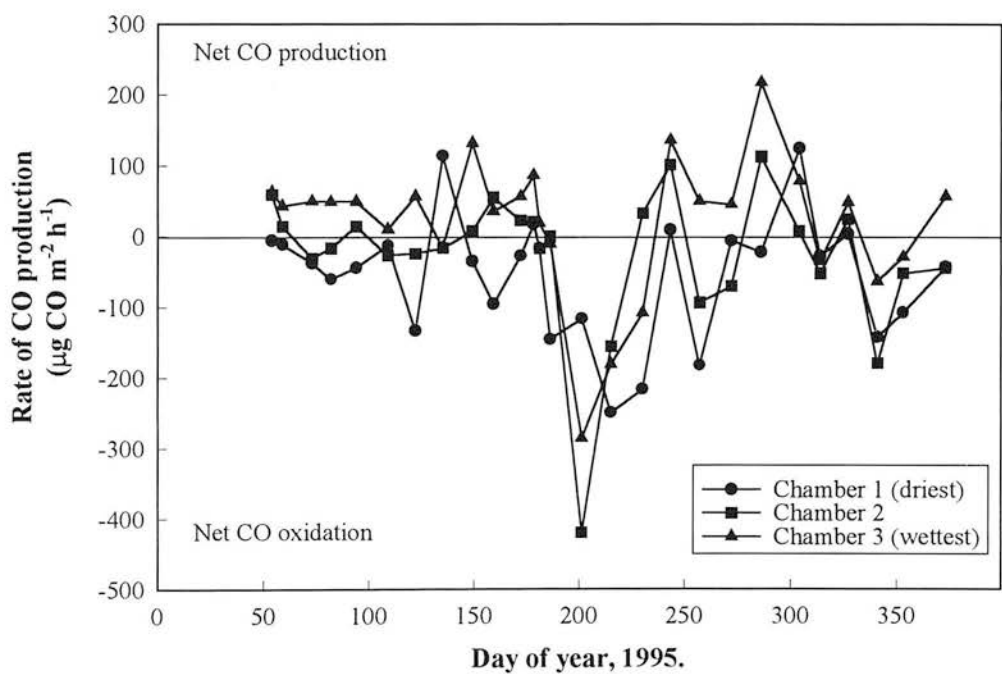


Figure 5.3 Seasonal variation in CO production rate on peat land at Springfield Farm, Leadburn, Midlothian, Scotland.

The profiles of CO concentration with depth generally showed a sharp increase in concentration some distance beneath the surface (Figure 5.4). There were significant correlations between the depth of the increase in CO concentration and the water table depth ($r^2 = 0.38$ for the driest chamber and 0.27 for the wettest, $p < 0.05$ for both chambers). There were also significant correlations between net CO production rates and the position of the water table ($r^2 = 0.47$ for the driest chamber, $p < 0.01$ and 0.27 for the wettest, $p < 0.05$).

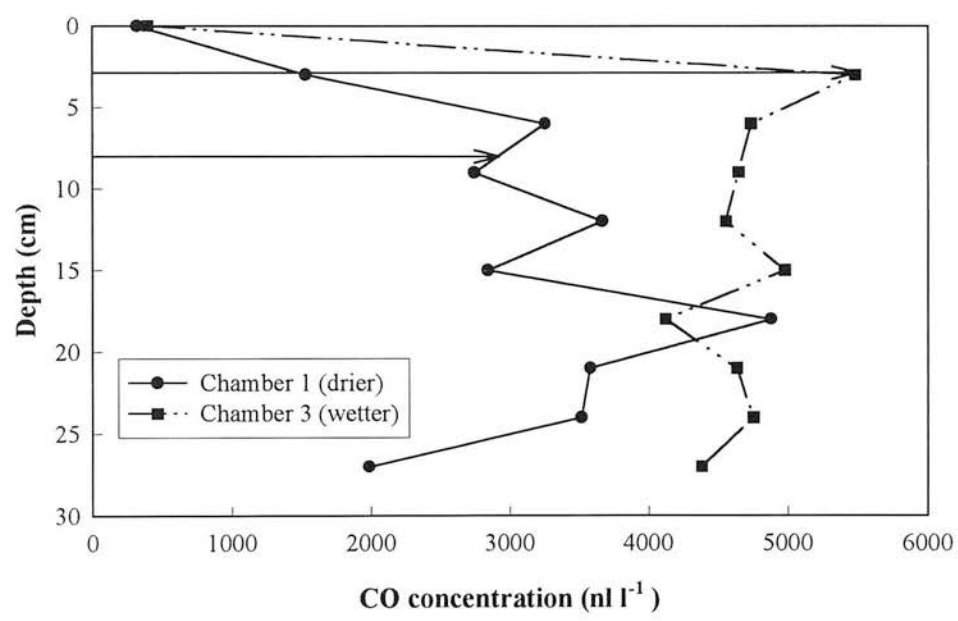


Figure 5.4 Change in CO concentration with depth at Leadburn 13/10/95. Arrows show the position of the water table at each chamber. Chamber 1 oxidised $22.1 \mu\text{g CO m}^{-2} \text{ h}^{-1}$; chamber 3 produced $218 \mu\text{g CO m}^{-2} \text{ h}^{-1}$.

5.4 Discussion

The results from the field experiments clearly show that wet peat can produce CO. There was considerable variability in the size of the fluxes at different chambers. To get a clearer picture of whether peatlands are net sources or sinks for CO, larger scale methods such as micrometeorology should be used. However, taking the area of

northern hemisphere wetlands to be $2.89 \times 10^{12} \text{ m}^2$ (Matthews and Fung, 1987: total for forested and nonforested bog), northern wetlands could only emit $0.2 \text{ Tg y}^{-1} \text{ CO}$ based on the mean flux from the wettest chamber in this study. This agrees well with emissions based on other published fluxes (Chapter 1, Section 1.3.2). Although not globally important sources of CO, emissions from northern wetlands could be locally important in regions where there are few anthropogenic sources of CO.

The net rate of CO production appears to be related to the position of the water table rather than to the gravimetric water content. The pattern of CO concentration in sampling tubes below the water table was very variable, but this may be a reflection of the difficulty in obtaining a large enough gas sample (at least 2 ml from a tube with a volume of 3.8 ml). It is possible that CO is produced in anaerobic zones at or just above the water table, and that some or all of the CO is oxidised in aerobic zones above the water table before reaching the atmosphere. This would explain why CO production displayed no straightforward temperature dependence, as changes in temperature would affect both production and oxidation processes.

It is not clear whether CO production is the result of biological activity or of chemical breakdown of organic materials in the peat. If microbial activity is responsible for the CO production, methanogenesis and acetogenesis are possible sources, as both are known to produce CO as a by-product (Chapter 1, Section 1.3.2). Alternatively, the source of the CO may be a chemical decomposition similar to the breakdown of phenolic compounds such as humic acid which produces CO under aerobic conditions (Chapter 4), possibly via breakdown to formic acid, which decomposes to give CO and water. However, this is not thought to occur under anaerobic conditions. Cellobiose, a disaccharide formed by cellulose decomposition (Streitwieser and Heathcock, 1981) can be broken down by soil microorganisms under anaerobic conditions to give formic acid (Küsel and Drake, 1995). This could then decompose

to give CO as described above. (In the laboratory, formic acid produced CO even when diluted with twice its own volume of water).

Attempts to investigate CO production from peat in the laboratory failed, as in most cases no CO evolution was observed. As methanogenesis (another process requiring anaerobic conditions) was also inhibited, it is likely that the cores were affected by oxygen during sampling or incubation. For further work in this area to have any chance of success, the incubations must be carried out in anaerobic jars, rather than Kilner jars, which allowed oxygen to leak into them.

5.5 Conclusions

Peatland can be a source of CO which while not important on a global scale could be significant locally. CO production appeared to occur in anaerobic regions at or just above the water table. Some of the CO produced was then oxidised as it passed through aerobic regions prior to escaping to the atmosphere. It was not clear whether CO production was a biological or chemical process, or how the rate depended on temperature. Further laboratory work is needed in anaerobic conditions to resolve these questions.

5.6 Acknowledgement

I would like to thank the Microbiology Department and Mr. John Kinross at Napier University for allowing me to use their anaerobic glove box.

Chapter 6: Depletion of carbon monoxide from the nocturnal boundary layer¹

6.1 Introduction

To date, measurements of the strength of the soil sink for CO have relied on laboratory incubations of small amounts of soil (Bender and Conrad, 1994; Conrad and Seiler 1982a), or field measurements based on closed chambers (Conrad and Seiler 1985a; Sanhueza *et al*, 1994a,b). It is not known how well these mimic the behaviour of the real atmosphere/soil interaction. Many early experiments were carried out at CO concentrations which were much higher than ambient, and so did not give rates of CO oxidation which are representative of those at ambient levels (Duggin and Cataldo, 1985; Ingersoll *et al*, 1974). CO deposition velocities for various soils are summarised in Table 6.1. Chambers have been used to measure rates of CO oxidation by soil over periods of a few days to examine the diurnal cycle of the sink. This work has been done predominantly in arid regions where CO is produced by a chemical process in the soil as it warms up during the day, and is removed by microbial oxidation as it cools at night (Conrad and Seiler, 1985b; Sanhueza *et al*, 1994a,b). Few measurements have been made in the temperate regions. Furthermore, the extent of leakages from chamber systems which would affect the results of this work is unknown.

This chapter describes an attempt to measure CO fluxes on a larger scale by measuring the decrease in CO concentration in the nocturnal boundary layer. This method has been used to measure the rates of destruction at the ground of other trace

¹Based on Moxley, J.M and Cape, J.N. Depletion of carbon monoxide from the nocturnal boundary layer. *Atmospheric Environment*, **31**, 1147-1155, 1997.

gases, such as ozone (Garland and Derwent, 1979). It has the advantage of averaging fluxes over a large area, so removing variation due to changes in soil properties on a small scale. It also allows turbulent flow of air over the soil, which may enhance transport of gases between the soil and the atmosphere.

Table 6.1 Literature values of the deposition velocity of carbon monoxide into soil

Deposition velocity ($\times 10^{-4} \text{ m s}^{-1}$)	CO concentration (nl l^{-1})	Measurement system	Reference
0.89-1.11	20 $\mu\text{l l}^{-1}$	Flow-through laboratory chamber	Heichel (1973)
0.4-6.7	Ambient	Chambers in the field	Liebl and Seiler (1976)
0.7-1.1	Ambient	Chambers in the field	Conrad and Seiler (1985a)
3.98	Ambient	Chambers in the field	Scharffe <i>et al.</i> (1990)
0.5-7.6	Not stated	^{14}C oxidation by cores	Förstel and Jansen (1991)
0.56 ⁽¹⁾	Ambient	Chambers in the field	Sanhueza <i>et al.</i> (1994a)
1.89 ⁽¹⁾	Ambient	Chambers in the field	Sanhueza <i>et al.</i> (1994b)

⁽¹⁾ For soils which acted as sinks for CO.

The only sink for CO at night is oxidation by the soil. As long as there are no anthropogenic inputs of CO into the air mass, there will be no sources, as production from methane and NMHCs requires the presence of hydroxyl radicals, which form photochemically. It is important that the daytime concentration of the gas concerned is typical of the background, and declines below this value at night. If there are local daytime sources, such as traffic, which raise the concentration of the gas being measured above ambient during the daytime, results can be misleading because the concentration then declines when the sources are inactive. An example of this is an

attempt to use this method to determine fluxes of nitrous oxide, N_2O , for which the concentration increased during the day, and declined at night. This was interpreted as being due to loss of N_2O to the soil (Brice *et al*, 1977). In fact, soil is now known to be a net source of N_2O (Watson, R.T. *et al*, 1990) and the diurnal pattern seen may have been caused by local emissions, which brought the concentration above ambient during the day. At night these local emissions would have been reduced, and the N_2O concentration may have declined because of advection of clean air.

CO is removed from the troposphere mainly by reaction with the hydroxyl radical (Chapter 1, Section 1.1.3). The mean atmospheric lifetime of CO is approximately 2-3 months (Cicerone, 1988), but the actual lifetime at any time and place will depend on the local concentrations and sink strengths, with shorter lifetimes in places with low concentrations relative to the sink strength, according to the relationship:

$$\tau = \frac{M}{S} \quad (6.1)$$

where τ is the lifetime, M is the mass of CO, and S the sink strength. The lifetime will be reduced further for CO trapped close to the ground in the nocturnal boundary layer because of oxidation at the earth's surface, making it possible to observe changes in the CO concentration in the nocturnal boundary layer over periods of a few hours.

6.2 Measurement Procedures

Measurements of ambient CO concentration, along with measurements of other atmospheric trace gases, temperature, solar radiation, and wind speed and direction were made over a 17 day period during May and June 1994 (Julian days 150-167) on the Bush Estate, Midlothian, Scotland, UK ($55^\circ 51' \text{ N}$, $3^\circ 12' \text{ W}$, Ordnance Survey grid reference NT 243637). The site is at 200 m above sea level, 5 km south of Edinburgh and 2 km to the north of the small town of Penicuik. The nearest main

road is 1 km away to the west. Beyond this to the west and north west are the Pentland Hills. The sea is approximately 100 km from the site in the direction of the prevailing winds during the campaign (west). Measurements of CO losses from the nocturnal boundary layer were also made at Springfield Farm, Leadburn, Midlothian (See Chapter 5 Section 5.2.2 for site description) in August and September 1996.

Measurements of CO concentration were made using an RGA3 reduction gas analyser (Trace Analytical, Menlo Park, CA, USA) (Chapter 2, Section 2.1.1). During this campaign the instrument was run in the continuous sampling mode described in Chapter 2, Section 2.3.2. During the work at Bush, the CO concentration recorded by the integrator on the RGA3 was converted to an analogue signal by an 8 bit D/A converter, and logged by a data-logger. With the range set to 2000 nl l^{-1} to cover the likely range of CO concentrations, this gave a resolution of only 8 nl l^{-1} . To compensate for the "stepping" caused by the resolution of the D/A converter, data were smoothed by taking 15 min running means. The range of the D/A converter was reduced to 1000 nl l^{-1} during the experiment at Leadburn, and no "stepping" was observed, so the data were not smoothed. The measurements at Leadburn were made during an attempt to measure CO fluxes using flux gradient micrometeorology (Chapter 7), so CO concentrations were measured at 3 heights (2.82 m, 1.21 m and 0.49 m). This allowed the deposition velocity to be calculated for each height.

At both sites, measurements of windspeed and direction, air temperature and solar irradiance were made using instruments and dataloggers operated by ITE, Bush Estate. Measurement of windspeed at Bush was made by a cup anemometer, and wind direction was measured by a weather vane. Data from both of these instruments was logged at 1 min intervals. At Leadburn, windspeed and direction were measured using a sonic anemometer, averaging over 30 min. Temperatures were measured using thermocouples. At Bush the measurement height was 5 m, while at Leadburn the temperatures were measured at 0.57 m and 2.42 m, then averaged.

If there is a nocturnal decline in CO concentrations, caused by deposition and oxidation at the ground, the deposition velocity can be calculated if the height of the boundary layer is known. The technique has already been used to measure the rate of removal of ozone at the ground by Garland and Derwent (1979), who used a modification of a model of the boundary layer proposed by Wyngaard (1975). This uses measurements of windspeed and cooling rate to calculate the height of the boundary layer.

Under clear skies and in moderate to high windspeeds over horizontally homogeneous terrain, the boundary layer height, h (m) is given by:

$$h = \sqrt[3]{\frac{\gamma^2 T u_*^4}{f k g \left(\frac{-dT}{dt} \right)}} \quad (6.2)$$

where γ is the Zilitinkevich profile constant, which is taken to be 0.4 (Garland and Brost, 1981); T is the mean temperature (K); u_* is the friction velocity in m s^{-1} which can be calculated from the windspeed (see below); f is the Coriolis parameter, which is $1.207 \times 10^{-4} \text{ s}^{-1}$ at $55^\circ 51' \text{ N}$; k is the von Karman constant (0.4); g is the acceleration due to gravity (9.81 m s^{-2}); and $\frac{-dT}{dt}$ is the mean cooling rate (K s^{-1}).

u_* is calculated by numerically solving the following equation:

$$u_{(z)} = \left(\frac{u_*}{k} \right) \ln \left(\frac{z}{z_0} \right) + \alpha z \sqrt[3]{\frac{\gamma^2 g^2 \left(\frac{-dT}{dt} \right)^2}{k f T^2 u_*^2}} \quad (6.3)$$

where $u_{(z)}$ is the windspeed (m s^{-1}) at height z : 4 m in this case; z_0 is the roughness length (a value of 0.01 m was used as this is typical for agricultural land (Galbally and

Roy, 1980; Wyngaard, 1975); and α is a constant. A value of 5 was used for α , as Garland and Derwent (1979) suggest this is typical for stable conditions.

Once the boundary layer height has been calculated, it is possible to calculate the deposition velocity, v_d (m s^{-1}), as

$$v_d = k_{ox}h \quad (6.4)$$

where k_{ox} is the first order decay constant for the decrease in CO concentration (s^{-1}) and h is the boundary layer height (m). See Appendix 3 for explanations of meteorological parameters.

6.3 Results

During the measurement campaign at Bush the wind was from a west to south-westerly direction, except for a period between 22:00 GMT on day 152 and 10:00 GMT on Julian day 153, when the wind was very light and variable, and a short period between 15:30 and 16:00 GMT on day 162. The wind speed ranged from near zero to 7.3 m s^{-1} . The days were sunny with a few scattered clouds, except for day 152, and parts of days 153 and 161 which had complete cloud cover. Sunrise was around 03:40 GMT, and sunset at 22:00 GMT.

CO concentrations were very low: the mean was 90 nl l^{-1} ; and the minimum was only 15 nl l^{-1} .

The diurnal pattern of CO concentration (Figure 6.1) generally showed an increase from sunrise until about 09:00 GMT. Overall, the CO concentration was not correlated with total solar irradiance. However after sunrise, between 04:00 and 09:00 GMT, there was a strong correlation on most mornings. The concentration then remained fairly stable until sunset. The CO concentration was not correlated with total solar irradiance during the middle of the day or the sunset period. From sunset until

sunrise, there was a gradual decrease in CO concentration. On nine nights out of twelve for which a full night's data were available, a decrease in CO concentration was recorded between sunset and sunrise. The decrease in concentration followed first order kinetics (Figure 6.2)

$$\text{i.e.} \quad -\frac{d[CO]}{dt} = k_{ox}[CO] \tag{6.5}$$

or
$$[CO]_t = [CO]_0 e^{-k_{ox} t} \tag{6.6}$$

where $[CO]_0$ is the CO concentration at sunset, $[CO]_t$ is the CO concentration at time t after sunset, and k_{ox} is the first order decay constant, with units time^{-1} . The expression assumes that the CO concentration would be zero after an infinite time. The rate constants for the decay, k_{ox} ranged from $5.75 \times 10^{-6} \text{ s}^{-1}$ to $3.72 \times 10^{-5} \text{ s}^{-1}$ (Table 6.2).

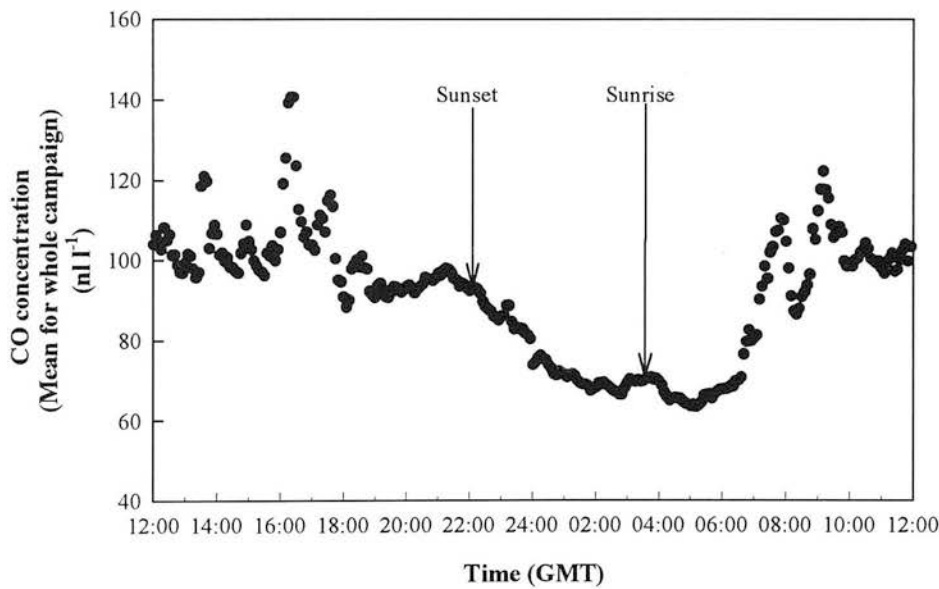
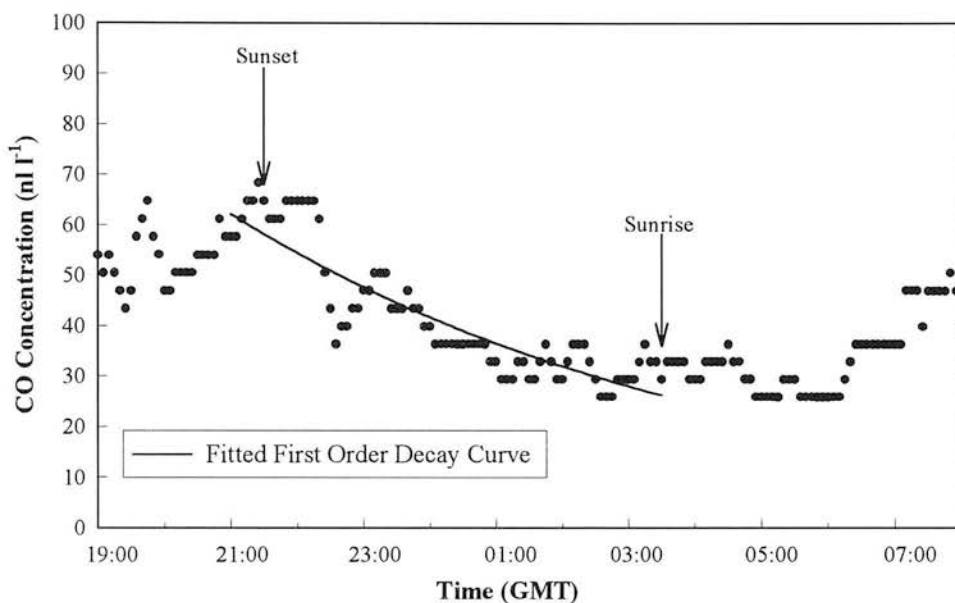


Figure 6.1 Diurnal variation in CO concentration at Bush, May-June 1994. Average data for whole campaign.



**Figure 6.2 CO concentration in boundary layer air overnight at Bush.
Julian days 165-166 (14 - 15 June), 1994.**

The values of u^* , h and v_d are available for the 10 nights where there was a full night's data, and for which it was possible to solve the equation for u^* , and are shown in Table 6.2. First order decay in the CO concentration was seen on nine of these ten nights. Two of the three nights when no correlation was seen were those when the boundary layer was unstable, and the equations for u^* could not be solved. These were also two of the three nights when CO concentration was not significantly correlated with solar irradiation in the morning, which again suggests that no boundary layer formed, and so was not destroyed in the morning when heating of the ground led to turbulence. The calculated boundary layer heights were relatively insensitive to uncertainties in temperature: an increase from 280 to 295 K gave an increase in boundary layer height of only 0.5 m, calculated using average values of u^* and cooling rate. However, the calculated heights were sensitive to changes in cooling rate (especially at low cooling rates) and in windspeed (and hence u^*) (Figures 6.3 and 6.4).

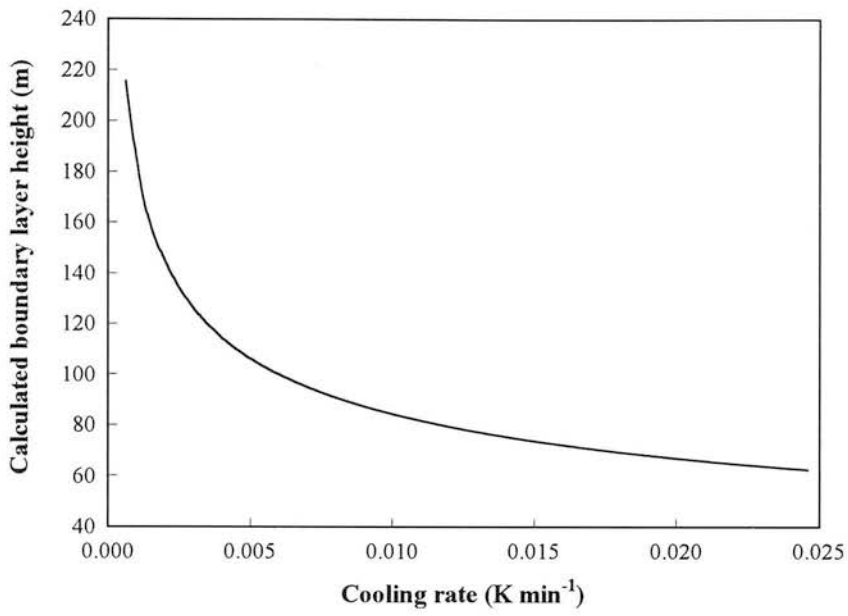


Figure 6.3 The relationship between cooling rate and boundary layer height calculated using mean values for windspeed and temperature.

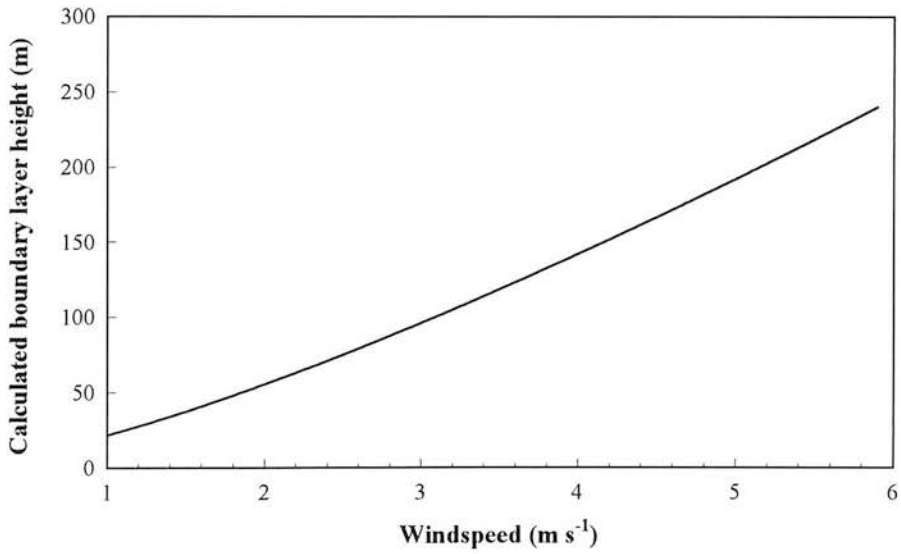


Figure 6.4 The relationship between windspeed and boundary layer height calculated using mean values for cooling rate and temperature

Table 6.2 Nocturnal boundary layer parameters and CO deposition velocities at Bush Estate, Midlothian, Scotland during May and June 1994.

Nights without full CO data between 19:00 and 04:00 are not included.

Julian day	First order decay constant for CO removal, k_{ox} ($\times 10^{-6} \text{ s}^{-1}$)	Correlation with first order behaviour, r	Mean windspeed (m s^{-1})	Mean rate of change of temperature (K min^{-1})	Calculated CO depletion(1) %	Calculated boundary layer height (m)	Deposition velocity ($\times 10^{-4} \text{ m s}^{-1}$)	Comments
150-151	10.5	-0.932	5.55	-0.0087	17	222	23	Cannot solve for friction velocity, u^*
151-152	-0.71	0.137	3.61	0.0012				
152-153	-3.60	0.399	0.93	-0.0192				
156-157	5.75	-0.648	3.00	-0.0113	17	80	4.6	
158-159	58.2	-0.841	2.91	-0.0126	18	72	4.2	
159-160	98.3	-0.843	2.30	-0.0108	35	52	5.1	
160-161	-10.0	0.164	2.16	-0.0111	5 % increase	45	-0.5	
161-162	11.9	-0.704	2.25	-0.0162	41	38	4.5	
162-163	66.8	-0.669	1.93	-0.0097	29	38	2.6	
163-164	34.7	-0.780	3.13	-0.0243	67	59	20	
165-166	24.7	-0.842	2.34	-0.0109	65	53	13	
166-167	37.2	-0.924	2.38	-0.0038	79	89	33	

(1) Based on 100 km fetch over land, and $e^{-k_{\text{ox}} t} = \frac{[\text{CO}]_t}{[\text{CO}]_0}$.

During the experiment at Leadburn, the wind was predominantly from the west. Windspeeds ranged from 0.2 to just over 7 m s⁻¹. The presence of thick cloud on some nights meant that a stable boundary layer did not form every night. The mean CO concentration was 107 nl l⁻¹, which is close to the northern hemisphere background concentration.

There were 13 nights with a full night's data, and for which it was possible to calculate the height of the boundary layer. On 9 of these nights, there was a first order decay in the CO concentration ($p < 0.05$). The deposition velocities and the boundary layer heights for each night are shown in Table 6.3. There was a significant negative correlation between wind direction and deposition velocity, i.e deposition velocities were generally larger when the wind was from the sector 0-60° than from 170-360° (data from the sector between 60° and 170° was excluded, as the fetch was unsuitable).

6.4 Discussion

The mean CO concentration measured at Bush was slightly lower than recent estimates of the Northern Hemisphere background concentration (Khalil and Rasmussen, 1994), with concentrations considerably below background being recorded at night. The wind direction meant that the air arriving at the site had not passed over any major sources of CO in its recent history. The most likely local source would be commuter traffic in the morning and evening. However, the diurnal pattern of CO concentration does not show peaks corresponding to the morning and evening rush hours, as would be expected in this case (Wang and Shaw, 1969). Neither is there any systematic variation in the pattern with day of the week. A similar pattern was observed at Leadburn, which is also an inland, remote site.

Table 6.3 Nocturnal boundary layer parameters and CO deposition velocities at Springfield Farm, Leadburn, Midlothian, Scotland during August and September 1996.

Nights without full CO data, or where it was not possible to calculate the boundary layer height are not included.

Julian day	First order decay constant for CO removal, k_{ox} ($\times 10^{-6} \text{ s}^{-1}$)			Mean rate of change of temperature (K min^{-1})	Calculated boundary layer height (m)	Deposition velocity, V_d ($\times 10^{-4} \text{ m s}^{-1}$)		
	Top	Middle	Bottom ⁽¹⁾			Top	Middle	Bottom ⁽¹⁾
232-233	6.28	64.5	66.7	-0.0030	29	1.82	1.87	1.93
239-240	16.5	1.52	2.22	-0.0005	366	60.3	55.5	81.3
240-241	8.41	85.4	94.5	-0.0012	88	7.36	7.48	8.27
242-243	8.91	86.3	90.3	-0.0081	59	5.26	5.10	5.33
244-245	5.71	54.7	54.4	-0.0018	146	8.35	8.00	7.96
246-247	19.3	2.02	2.28	-0.0070	109	21.1	22.1	24.9
247-248	37.7	3.70	5.26	-0.0070	109	41.2	40.5	57.4
248-249	10.6	9.45	95.0	-0.0035	102	10.8	9.61	9.66
249-230	18.0	18.0	8.00	-0.0034	66	11.8	11.8	52.6
Mean						18.0	18.7	27.7

(1) Data from the lowest sampling point may be subject to an interference from a substance other than CO, and hence overestimate fluxes. See Chapter 7, Section 7.4 for discussion.

The diurnal cycles in CO concentration are similar to those observed at other remote sites receiving air which has passed over land prior to arriving at the site (Marenco and Delaunay, 1980). During the night, the only known non-anthropogenic process occurring which can affect CO concentrations is deposition to soil. When the sun sets, photochemical processes are halted, and the nocturnal boundary layer starts to form. The CO concentration falls slowly, as it is removed at the ground. At sunrise, convection starts to occur, leading to mixing of higher concentrations of CO into the boundary layer from the free troposphere. In addition, photochemical-driven production of CO starts to occur. These two factors lead to an increase in the CO concentration until an equilibrium is reached in the afternoon. Because the removal rate is slow, and the boundary layer is higher during the daytime, CO concentration is not correlated with solar radiation during the sunset period, nor does it respond to short-term changes in solar irradiation caused by clouds.

The nocturnal decline in CO concentrations may be attributable to depletion of a well-mixed boundary layer at the Earth's surface. With a night-time mean windspeed of 3 m s⁻¹, and a nocturnal depletion rate constant, k_{OX} , of $1.45 \times 10^{-5} \text{ s}^{-1}$ (the mean values during the Bush campaign), this would lead to a reduction of 50 % in the CO concentration over a 100 km fetch, as

$$e^{-k_{\text{OX}}t} = \frac{[\text{CO}]_t}{[\text{CO}]_0} \quad (6.7)$$

where $[\text{CO}]_0$ is the CO concentration at the coast, and $[\text{CO}]_t$ is the CO concentration after travelling over land for t seconds. On some nights the depletion was calculated to have been up to 80 % (Table 6.2).

The mean CO concentration at Bush was slightly lower than that recorded in June 1990-1992 by Derwent *et al.* (1994) at a remote site (Mace Head, Ireland) which receives predominantly maritime air from the Atlantic. They found mean concentrations in June of 106-122 nl l⁻¹ CO for 1990-1992, with no diurnal pattern (Doddridge *et al.*, 1994). During the measurement campaign at Bush 1994, the air flow at Mace Head was predominantly from the west (R.G. Derwent, *pers. comm.*) bringing clean air, except for a pollution episode on days 152-53, and a short period on day 164. The CO concentration was in the range 90-150 nl l⁻¹, and showed no diurnal pattern (P.G. Simmonds *pers. comm.*; R.G. Derwent, *pers. comm.*). At Bush CO concentrations fell to approximately half these values at night, in agreement with the rate of depletion calculated above. If it is assumed that CO concentrations in air reaching the west coast of Scotland were similar to those at Mace Head over the same period and that there was a 100 km fetch over land before reaching Bush, the minimum CO concentration can be calculated using the percentage depletions shown in Table 6.2. The calculated and measured minima are shown in Table 6.4. There was good agreement on most nights, especially as the 100 km fetch over land is only an estimate.

The mean deposition velocity measured at Bush was $1.1 \times 10^{-3} \text{ m s}^{-1}$ ($s = 1.1 \times 10^{-3} \text{ m s}^{-1}$). This compares well with values measured using other methods (Table 6.1), although the mean value is approximately 50 % higher than the highest values obtained using chambers. This may be due to lack of turbulence in the closed chambers to assist gas exchange between soils and the atmosphere, leakage into or out of the chambers or to uncertainties in the model used to calculate the boundary layer height.

Table 6.4 Calculated and actual overnight CO concentration minima at Bush during May and June 1994 and corresponding concentrations at Mace Head, Ireland.

Julian day	CO concentration at Mace Head ⁽¹⁾ (nl l ⁻¹)	Calculated CO depletion ⁽²⁾ (%)	Overnight minimum CO concentration at Bush (nl l ⁻¹)	
			Calculated	Actual
156-157	111	17	92	68
158-159	107	18	87	79
159-160	146	35	95	38
161-162	139	41	82	79
162-163	137	29	97	88
163-164	139	67	46	15
165-166	135	65	47	26
166-167	138	79	29	33

(1) Based on mean of daily CO concentration for the two days preceding and following the night in question (R.G. Derwent, *pers. comm.*).

(2) Based on 100 km fetch over land and the windspeeds and deposition velocities shown in Table 6.2.

At Leadburn slightly higher deposition velocities were obtained, with a mean of $2.15 \times 10^{-3} \text{ m s}^{-1}$ (standard deviation = $2.11 \times 10^{-3} \text{ m s}^{-1}$). The highest two sampling points showed good agreement, but the lower point gave a faster deposition velocity. In theory the deposition velocity should be the same throughout the constant flux layer. Possible reasons for the anomalous behaviour of the lowest sampling point are discussed in Chapter 7, Section 7.4, but it seems possible that the CO measurements were affected by an interference from another gas, which the RGA3 measured as CO. The discrepancy was largest on nights 239-240, 247-248 and 249-250. Night 239-240 was after a day of heavy rain, nights 247-248 and 249-250 were both characterised by mist which did not clear until mid-morning. This may suggest that the interference was associated with wet conditions, but further investigation is needed. Night 248-249 was also misty, but the deposition velocity obtained from the measurements at the lowest height was in good agreement with those obtained at the other two heights. If the results from the lowest sampling point are ignored the mean deposition velocity at

Leadburn was $1.83 \times 10^{-3} \text{ m s}^{-1}$ (standard deviation = $1.74 \times 10^{-3} \text{ m s}^{-1}$), which is in good agreement with that measured at Bush. The fact that similar effects were observed at two different sites confirms the view that the depletion of CO from the nocturnal boundary layer is caused by removal at the ground, and not by a local CO source with a diurnal pattern of emissions.

The global land surface is $13 \times 10^{12} \text{ m}^2$ (World Resources Institute, 1992). At a mean global CO concentration of 100 nl l^{-1} , a deposition velocity of $1.1 \times 10^{-3} \text{ m s}^{-1}$ would be equivalent to a rate of CO oxidation by soils of 560 Tg y^{-1} . This is slightly higher than previous estimates of $240\text{--}530 \text{ Tg y}^{-1}$ (Conrad, 1988; Khalil and Rasmussen, 1990a), but there is reasonable agreement, especially when allowance is made for the possible differences between measurement methods described above, and as the value of the calculated sink strength assumes that the CO deposition velocity is the same for all land surfaces. In areas where the ground is covered by buildings there will be no sink, and there is evidence that arid soils can act as net sources of CO (Conrad and Seiler, 1985a,b; Sanhueza *et al*, 1994a,b). The estimated deposition velocity assumes a roughness length, z_0 , of 0.01 m , which is equivalent to a canopy height, h_c , of approximately 8 cm , if $z_0 = 0.13 h_c$ (Monteith and Unsworth, 1990). For shorter canopies, the deposition velocity increases; for taller ones it decreases. The magnitude of the change in deposition velocity with canopy height depends on windspeed, but based on Monteith's calculations, for a windspeed of 3 m s^{-1} at 4 m , the friction velocity, u^* decreases by a factor of 3 as the canopy height increases from 1 cm to 1.5 m . As the boundary layer height, and hence the deposition velocity, is proportional to $u^{*4/3}$, this means that the deposition velocity decreases by a factor of 4.5. However, in practice the change in deposition velocity is likely to be less than this, as z_0 is inversely proportional to the canopy density and woodland canopies are generally less dense than arable crops. The estimate of deposition velocity also neglects spatial variation in CO concentration, which may lead to

underestimation of the sink strength as the CO concentration is above background over appreciable areas.

6.5 Conclusions

The air was generally very clean during the measurement campaigns, with CO concentrations at or below current estimates of the Northern Hemisphere marine background. Low overnight values may have been caused by depletion of CO in the boundary layer by removal at the ground upwind of the measurement site.

Measurements of CO concentrations in the nocturnal boundary layer showed that the CO concentration decreased during the night. This is thought to be due to oxidation at the ground by soil microorganisms. Calculations using the Bush data showed that on some nights up to 80 % of the CO was removed during the passage of air over approximately 100 km of land. It has been possible to calculate deposition velocities, and these are in reasonable agreement with those obtained by other methods, although the mean value is larger. This suggests that closed chamber methods may underestimate the strength of the soil sink for CO. The strength of the soil sink for CO predicted by this deposition velocity is close to that predicted in other studies.

6.6 Acknowledgements

I would like to thank Dr Peter Simmonds, INSCOM, Ringwood, Hants and Dr Richard Derwent, The Meteorological Office, Bracknell for providing data for the Mace Head site.

I would also like to thank ITE, Edinburgh Research Station, Bush Estate for allowing me to use their data on windspeed and direction, air temperature and solar irradiance at both Bush and Leadburn.

Chapter 7: Attempted measurement of CO fluxes using flux gradient micrometeorology

7.1 Introduction

Flux gradient micrometeorology relies on the measurement of profiles of the concentration of a component with height. If a component is deposited at the ground, its concentration increases with height, whereas if it is emitted concentration decreases with height. The size of the change in concentration with height depends on the extent of turbulent mixing, and on the strength of the source or sink. Stable atmospheric conditions and large source or sink strengths lead to larger concentration gradients. The flux gradient method has the advantage that it measures fluxes over larger areas than chambers, although the "footprint" is not a linear function of the upwind fetch: the influence of ground very close to the sampling point is small, as the area of ground enclosed by a circle with a small radius is small. Points a few tens of metres from the sampling point have most influence on the measured fluxes, and the importance of fluxes from points beyond this decreases with distance (Fan *et al*, 1992; Smith *et al*, 1994b). The method requires a flat upwind fetch of a few hundred metres, and assumes that the fluxes are uniform throughout the fetch (i.e. there is no horizontal diffusion). In addition to measurements of the concentration of the component of interest, at at least three heights, the temperature and windspeed gradients, and latent heat flux must be known.

Early work using the flux gradient technique focused on fluxes of water and carbon dioxide, both of which are large over plant canopies (Stewart and Thom, 1973; Biscoe *et al*, 1975), but more recent work with sensitive detectors has allowed the measurement of trace gas fluxes (Hargreaves, *et al*, 1992, 1994; Christensen *et al*, 1996). However, the technique has not previously been used to measure CO fluxes.

7.2 Measurement procedures

Measurements were made at Springfield Farm, Midlothian, Scotland (see Chapter 5, Section 5.2.2 for site description) during August and September 1996. Air was sampled at 0.49, 1.21 and 2.82 m during a 10 min cycle. The air flowed from a sample manifold through the RGA3 sample loop at the rate of 3 ml min⁻¹. The air was allowed to flow through the sample loop for 85 s before being injected into the chromatography system of the RGA3. The volume of tubing between the manifold and the RGA3 was 2.5 ml. Temperatures at 0.57 m and 2.42 m were measured using thermocouples and data loggers belonging to ITE, and averaged over 30 min periods. Measurements of the windspeed profile were not made directly, but calculated from the friction velocity, u_* , as

$$\frac{du}{d \ln(z - d)} = \frac{u_*}{k} \quad (7.1)$$

where z is the measurement height (m), d is the zero plane displacement, and k the von Karman constant (0.4) (Monteith and Unsworth, 1990). The friction velocity was obtained from windspeed measurements made by a sonic anemometer belong to ITE calculated according to $u_* = \sqrt{(u')^2}$.

The flux of CO could then be calculated as

$$F = -k^2 \frac{du}{d \ln(z - d)} \frac{d[CO]}{d \ln(z - d)} (\phi_m \phi_h)^{-1} \quad (7.2)$$

where F is the flux of CO (g m⁻² s⁻¹), $[CO]$ is the CO concentration in g m⁻³, and $(\phi_m \phi_h)^{-1}$ is a correction for atmospheric stability (Hargreaves *et al*, 1994). $(\phi_m \phi_h)^{-1}$ is given by

$$(\phi_m \phi_h)^{-1} = (1 - 16Ri)^{0.75} \text{ for } Ri < -0.1 \quad (7.3)$$

and $(\phi_m \phi_h)^{-1} = (1 - 5Ri)^2$ for $-0.1 < Ri < 1$ (7.4)

where Ri , the Richardson number is given by

$$Ri = \frac{g dT / d \ln(z - d)}{T (du / d \ln(z - d))^2} \quad (7.5)$$

where g is acceleration due to gravity (9.81 m s^{-2}), and T is the temperature (K) (Monteith and Unsworth, 1990).

As the measurement of the CO concentration was made at constant temperature in the RGA3, no correction was necessary for the sensible heat flux, but it was still necessary to correct for the latent heat flux.

$$\delta F = 0.65 \times 10^{-9} \frac{\rho_c \lambda E}{\rho_a} \quad (7.6)$$

where δF is the correction to the flux ($\text{g m}^{-2} \text{ s}^{-1}$), ρ_c is the mass concentration of CO (g m^{-3}), ρ_a is the density of air (g m^{-3}), and λE is the latent heat flux (W m^{-2}) (λ is the latent heat of evaporation of water, and E the evaporation rate). This correction allows for the water vapour in the air. The latent heat of evaporation of the water is released as the air rises and expands, and water condenses out. This decreases the density of the air compared to that of dry air, and so increases transport away from the ground. Although not very important under conditions where there is little moisture in the air, this term becomes important under humid conditions.

To measure a flux, F , the instrument resolution required, Δc is given by Equation 7.7 (Businger and Delany, 1990)

$$|\Delta c| = |F| \frac{G}{ku_*} \quad (7.7)$$

where G is a function of stability with values ranging from 0.2 for an atmospheric stability factor, ζ of -1 (unstable conditions) to 5.69 when ζ is +1 (stable conditions) for a system where $z_2 = 2z_1$. Chamber measurements at the site (Chapter 5) showed that CO fluxes varied from consumption of up to $400 \mu\text{g m}^{-2} \text{h}^{-1}$ to production of up to $200 \mu\text{g m}^{-2} \text{h}^{-1}$. Under stable conditions ($\zeta = +1$), a flux of $200 \mu\text{g m}^{-2} \text{h}^{-1}$ would need an instrument resolution of 3 nl l^{-1} to be detectable. However, as the sampling mast used was arranged so that z_2 was larger than $2z_1$, the actual resolution needed would be slightly less than this. The resolution of the RGA3 was 6 nl l^{-1} , and it was hoped that it would be possible to detect fluxes, at least under stable conditions e.g. at night, especially as the time chosen for the micrometeorological campaign, mid - late summer, was the time of year when chambers showed large fluxes for CO oxidation the previous year (Chapter 5).

For comparison with the micrometeorological data, the CO flux was measured approximately every 3 days using static chambers (Chapter 2, Section 2.3.1) in the same positions as those used to measure fluxes as described in Chapter 5.

See Appendix 3 for explanations of meteorological parameters.

7.3 Results

An Excel programme developed by John Moncrieff of IERM, University of Edinburgh was used to assess the footprint at the site. This was based on an equation given by Schuepp *et al.* (1990). With a maximum sampling height of 3 m, a windspeed of 7 m s^{-1} (the maximum measured during the campaign), latent heat flux of 34 W m^{-2} (the mean for the campaign) and a zero plane displacement of 0.25 m, 90 % of the contribution to the flux measurement came from within 200 m of the sampling point. The area with the strongest influence on the measurements was approximately 40-60 m upwind. The requirement for an upwind fetch of 200 m was not met when the wind

direction was between 60° and 170°, and measurements when the wind was from this direction have been excluded.

The fluxes were such that CO concentration gradients were only detectable under stable atmospheric conditions. These conditions tended to occur at night, when convective mixing was suppressed by the formation of the nocturnal boundary layer, hence most of the profiles recorded were measured at night. However, on some days it was possible to detect CO profiles during the daytime as well. The fluxes measured are shown in Figure 7.1.

An example showing how the fluxes were calculated is included below, using the data for the profile obtained at between 23:12 and 23:19 on 23/8/96.

$u^* = 0.100$ m/s, therefore $du/d\ln(z-d) = 0.250$ m/s.

The CO concentrations at 2.82, 1.21 and 0.49 m were 168.8, 162.27 and 159.58 nl l⁻¹ respectively and $d = 0.16$ m, and so $d[CO]/d\ln(z-d) = 5.26 \times 10^{-6}$ g m⁻³.

The mean temperature, T , was 281.6 K.

The temperatures at 2.42 and 0.57 m were 282.1 and 281.1 K respectively, giving a value of $dT/d\ln(z-d)$ of 0.601, therefore $Ri = 0.355$, and $(\phi_m\phi_h)^{-1} = 0.456$.

$$\begin{aligned}\text{Therefore the CO flux} &= -(0.41^2 \times 0.250 \times 5.26 \times 10^{-6} \times 0.456) \text{ g CO m}^{-2} \text{ s}^{-1} \\ &= -1.01 \times 10^{-7} \text{ g CO m}^{-2} \text{ s}^{-1} \\ &= -363 \text{ } \mu\text{g CO m}^{-2} \text{ h}^{-1}.\end{aligned}$$

The correction for latent heat flux is negligible, as $\lambda E = -9.928$ W m⁻² and the mass concentration of CO, ρ_c is only 1.03×10^{-7} kg m⁻³, for a CO concentration of 85 nl l⁻¹ at 285 K, while the density of air, ρ_a is 1.24 kg m⁻³, therefore $\delta F = 5.40 \times 10^{-14} \lambda E \text{ kg m}^{-2} \text{ s}^{-1} = -1.93 \text{ } \mu\text{g m}^{-2} \text{ h}^{-1}$.

Some of the fluxes recorded were considerably larger than those recorded at the same site over the same period using static chambers, which averaged $55 \mu\text{g CO m}^{-2} \text{ h}^{-1}$ (maximum $200 \mu\text{g CO m}^{-2} \text{ h}^{-1}$) or nocturnal boundary layer measurements (Chapter 6), which were a few hundred $\mu\text{g CO m}^{-2} \text{ h}^{-1}$.

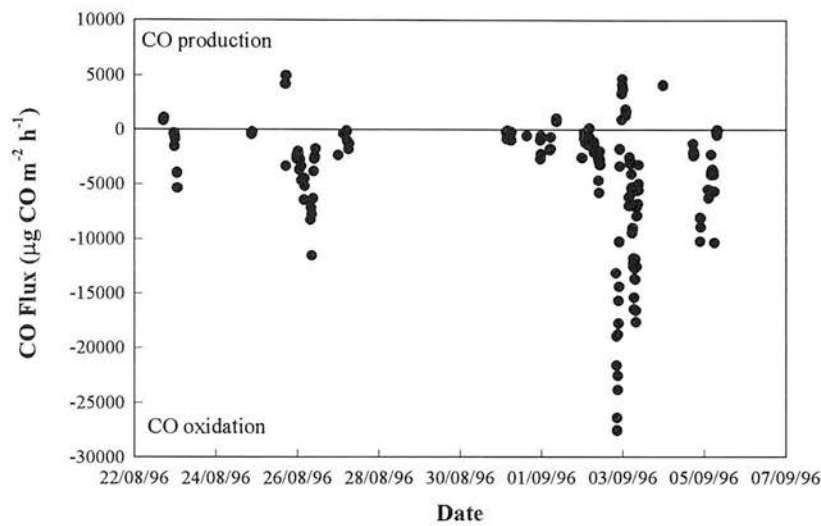


Figure 7.1 CO fluxes measured by flux gradient micrometeorology at Springfield Farm, Leadburn, Midlothian, Scotland. Aug-Sept 1996.

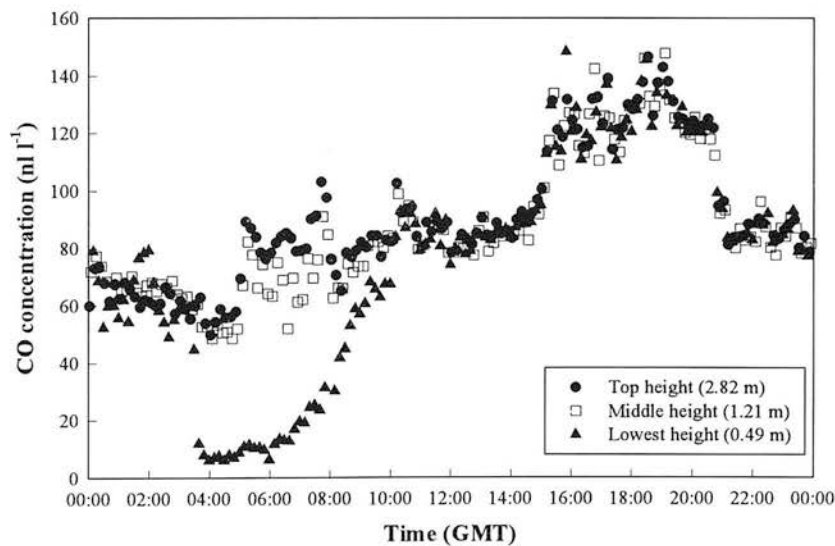


Figure 7.2 CO concentrations at Springfield Farm, Leadburn, Midlothian, Scotland, 4/9/96 showing very low values recorded for lowest sampling height between 03:30 and 09:30.

7.4 Discussion

While some of the smaller fluxes measured fell into the same range as those measured by other methods, some (e.g. those measured between 20:22 and 22:29 on 3/9/96 and 03:32 and 09:39 on 4/9/96) were so large as to arouse the suspicion that they were artefacts, possibly caused by the RGA3 measuring a gas other than CO. The samples from the lowest points of the profiles in the times mentioned showed extremely low CO concentrations (less than 10 nl l^{-1} in some cases) (Figure 7.2) and it is possible that they were not caused by CO at all, but by another interfering gas. A similar effect has been noticed in laboratory experiments where a peak was detected between the H_2 and CO peaks which the RGA3 measured as CO (Chapter 4 Section 4.3). (The integrator on the RGA3 was set so that the second peak detected would always be measured as CO.) However, in the laboratory, the peak between the hydrogen and CO peaks was always very small - generally less than 1 nl l^{-1} , and never more than 5 nl l^{-1} . Unfortunately, only the integrated peak areas, and not the full chromatograms were saved, and so it is not possible to determine whether a peak between CO and hydrogen was responsible for the very low CO concentrations measured.

Attempts to identify what causes the peak between the hydrogen and CO peaks have not been successful. The instrument manufacturers do not know of any substance which have retention times between those of H_2 and CO (Terry Jones, Anatrol, *pers. comm.*). However, other users have also occasionally recorded unexpectedly low CO concentrations recorded, especially at night (Laura Cárdenas, UEA, *pers. comm.*). Laboratory tests were carried using methane, acetylene and formaldehyde, all materials of similar molecular weight to CO none had the necessary retention time. Another possible contender would be HCN, which is iso-electronic with CO, structurally similar and slightly lighter, but this compound has not been investigated for safety reasons.

Figure 7.3 shows sample profiles for a period when fluxes were comparable with those obtained by other methods. The lowest sample height also gave anomalous values of deposition velocity calculated using the nocturnal boundary layer method (Chapter 6). If an interfering substance is not responsible for the apparent low CO concentrations, it may be that they were real, and that such low concentrations occurred because the lowest sampling point at 0.59 m was below the constant flux layer. However, even with the lowest point in each profile removed, fluxes of several thousand $\mu\text{g CO m}^{-2} \text{ h}^{-1}$ were recorded in the periods mentioned above.

In any future work, it may be possible to ascertain whether or not such very low CO concentrations are real. Changing the carrier gas flow rate and column temperature to achieve better separation between CO and other peaks would be desirable. Raising the height of the lowest sampling point would reduce the concentration of any interference to a level where it is not detected by the RGA3, and would also ensure that this sampling point is in the constant flux layer.

In view of the possible interferences it would be unwise to comment on possible diurnal patterns in the CO fluxes, or links between CO fluxes and other variables such as temperature, rainfall or windspeed and direction

7.5 Conclusions

Although there are signs that it may be possible to use flux gradient micrometeorology to measure CO fluxes, this attempt did not obtain values which are in agreement with those measured by other methods (static chambers and nocturnal boundary layer measurements). This may have been due to an interfering chromatographic peak between the H_2 and CO peaks which the RGA3 integrator measured as CO.

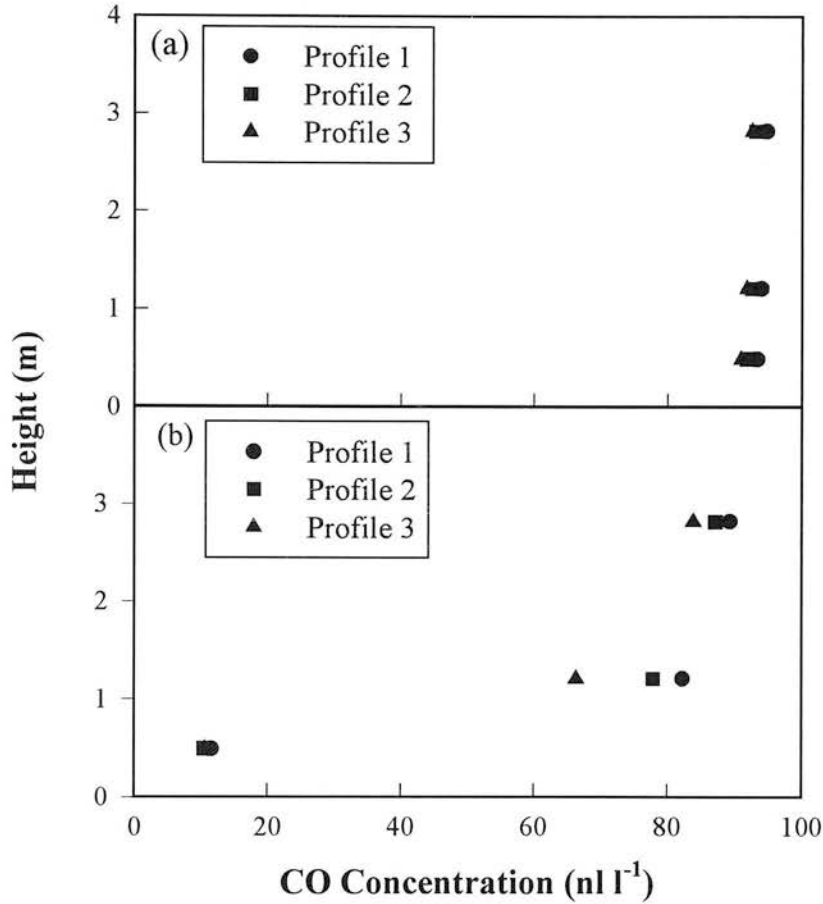


Figure 7.3 CO concentration profiles a) Profiles giving reasonable fluxes (03:02-03:29, 1/9/96). Mean flux = $-232 \mu\text{g CO m}^{-2} \text{ h}^{-1}$. b) Profiles giving very large fluxes (05:12-05:39, 4/9/96). Mean Flux = $-6710 \mu\text{g CO m}^{-2} \text{ h}^{-1}$

7.6 Acknowledgements

I would like to thank Chris Fletchard and Robert Storeton-West of ITE, Bush for their assistance in transporting equipment to the field site, and for providing the meteorological data, and John Moncrieff of IERM, University of Edinburgh for allowing me to use his Excel Programmes for the footprint models.

Chapter 8: Discussion and Conclusions

The project which forms the subject of this thesis had the objectives of identifying the key factors affecting the fluxes of CO to and from soils and obtaining a better estimate of the strength of the soil sink for CO. Better information on these issues will improve the capacity to predict possible changes in the sink in response to changes in soil and environmental factors.

Previous work by other authors reviewed in Chapter 1, and the results of this project, show that there are three principal processes occurring in soils which lead to exchanges of CO between soils and the atmosphere: 1) oxidation of atmospheric CO by soil microorganisms; 2) a chemical breakdown of soil organic matter to produce CO, which may then be oxidised in the soil by process 1, or emitted to the atmosphere; 3) production of CO under anaerobic conditions which may also be oxidised or give rise to emissions. It is likely that all three processes occur to some extent at different locations and/or times within any soil.

Although it is difficult to prove directly, there is evidence that the observed relationships between CO oxidation rates and environmental variables are the net result of concurrent oxidation and production processes. For example, the decrease in CO deposition velocity with temperature seen for many soils in the field (Chapter 3) is unusual for a biological process, which would normally be expected to have an optimum temperature and this is interpreted as being due to CO production from organic matter increasing more rapidly with temperature than the oxidation process. Increases in temperature can thus result in soils changing from being net sinks for CO to becoming net sources. This project has shown that this effect is particularly marked for aerobic soils with high organic carbon contents.

In almost all of the soils examined in this study, oxidation of CO by soil microorganisms was the dominant process, resulting in the soil acting as a net sink for CO. The only exceptions were an area of peatland which was sometimes waterlogged, which produced CO during wetter periods, where anaerobic CO production appeared to dominate (Chapter 5); and soils which had been dried or irradiated in the laboratory, in which the chemical breakdown of organic matter was the main process involving CO (Chapter 4). The rate at which the breakdown occurred increased with increasing organic matter content, and with increasing temperature. CO production from dry soil has been observed in the field in arid regions (e.g. Marengo and Delaunay, 1980; Conrad and Seiler, 1982b, 1985 a,b), but is not important in temperate regions except for its influence on the temperature dependence of the net CO oxidation rate. CO appears to be produced mainly from the oxidation of phenolic compounds, such as humic acid, in the soil, possibly with formic acid as an intermediate. In this project it was shown that the rate of CO production increased with increasing temperature, and was promoted by sterilisation, drying and rewetting of soils, all of which are processes which might be expected to break up large organic molecules.

Another example of different processes occurring concurrently in the same soil profile is in wet peat, where it has been demonstrated that CO is produced just above the watertable, but oxidised in aerobic regions nearer the surface before it can be released to the atmosphere. This phenomenon is closely analogous to that widely reported for methane (Smith *et al* 1994a; Nedwell and Watson, A. 1995). CO production was observed on some occasions from parts of a wet peat moorland, but the fluxes were small. The mechanism for this is not clear, but may involve release of CO generated anaerobically during methanogenesis or acetogenesis, or decomposition of formic acid produced by the breakdown of larger organic molecules. As formic acid may be involved in CO production under both aerobic and anaerobic conditions, the link

between the formic acid concentration in soils and the rate at which they produce CO should be investigated further.

On the basis of the results of this work (Chapter 5), and data from other workers (Chapter 1, Section 1.3.2), CO production from northern wetlands with high carbon contents (defined as bogs by Matthews and Fung, 1987) could only account for a tiny proportion of global CO production (about 0.2 Tg y^{-1}), but could be locally important in regions with little anthropogenic CO emission. CO fluxes from tropical wetland areas, which tend to have low carbon contents (defined as swamps by Matthews and Fung, 1987) have not been measured. Few measurements of methane fluxes have been made in these areas, which suggest that they have much lower methane emissions rates than northern carbon-rich wetlands (Harriss and Sebach, 1981; Matthews and Fung 1987). If this is repeated for CO, the rate of CO from swamps is likely to be small, and even if emission rates equal those from bogs they are unlikely to give an emission of more than 0.1 Tg y^{-1} . However other work suggests that methane fluxes from tropical wetlands may be large (Prather *et al*, 1995), which may suggest that these regions are significant source of CO. The magnitude of CO emissions from tropical wetlands needs to be investigated. In addition to direct emission from wetland areas, CO is also produced from the oxidation of methane emitted from them. Approximately one quarter of CO in the atmosphere ($\sim 600 \text{ Tg y}^{-1}$) is derived from the oxidation of methane, and approximately one quarter of methane is produced by wetlands (Watson, R.T. *et al*. 1990) therefore about 40 Tg y^{-1} is produced from the photooxidation of methane from wetlands, which far exceeds that likely to be produced by these areas by direct emission. Other possible sources of CO from anaerobic microbial activity, such as landfill sites, which are known to produce substantial amounts of methane (Shine *et al*, 1990; Bogner 1992) have not been investigated. Large CO production fluxes have been reported from soils following the application of cheese whey (Bullock *et al*, 1995), but the fluxes after the

application of other slurries with high oxygen demands, such as manure, have not been investigated.

The net rate constant for CO oxidation by soils increased with increasing soil organic matter content, and showed an optimum water content. The effect of the increase in soil mineral N content following the application of fertiliser is not clear, but there are some suggestions that high ammonium concentrations may reduce the CO oxidation rate in the short term, as some organisms switch from oxidising CO to oxidising ammonium. In the longer term, adding ammonium increases the population of nitrifiers, which are the main group of organisms responsible for CO oxidation in soil, and hence increases the CO oxidation rate (Bender and Conrad, 1994). The work in this thesis demonstrated that CO oxidation is halted by acetylene, which suggests that methanotrophs and nitrifiers are the main organisms involved in oxidising CO in soils (Chapter 3).

More work is needed to investigate the factors affecting CO production in anaerobic soils. To date, measurements of CO production under anaerobic conditions have only been made in the field in this project (Chapter 5), or elsewhere by using cores in the laboratory (Funk *et al*, 1994). In both of these cases net fluxes, resulting from a combination of CO oxidation in aerobic regions within the soil and CO production in anaerobic regions, were measured. To examine factors which affect anaerobic CO production, laboratory work is needed under anaerobic conditions. To measure net CO fluxes from peatlands, which appear to display considerable spatial variability, and to assess their overall importance it will be necessary either to use a large number of chambers, or to use methods which measure fluxes over larger scales, for example micrometeorology (if the problems mentioned in Chapter 7 can be overcome), or nocturnal boundary layer techniques.

The scale at which all flux measurements are made is important. If chambers (which usually have an area of less than 1 m²) are used, many are required to estimate the mean flux over larger areas, because of the potential for the flux to be heavily influenced by a few "hotspots" of activity. This issue has been discussed in detail for N₂O fluxes (Smith *et al.* 1994b; Christensen *et al.* 1996), where comparisons have been made between chamber and micrometeorological measurements. Measurements of CO depletion from the nocturnal boundary layer in this project gave CO deposition velocities approximately 50 % higher than those obtained using chambers. This may be because chambers do not allow for turbulent exchange of gases between soils and the atmosphere, whereas this is included in measurements using boundary layer techniques. Data from chamber systems, therefore, while useful for comparing fluxes in different locations and with different treatments applied should be interpreted with caution when scaling up the data to give global fluxes.

The nocturnal boundary layer measurements made in this study showed that at night, with no photoproduction of CO and a fetch with no significant sources of anthropogenic inputs, up to 80 % of the CO in the nocturnal boundary layer could be removed when an air mass passed over land for about 100 km. The nocturnal boundary layer occupies about 10 % of the free troposphere; therefore this loss is equivalent to the removal of about 8 % of the total CO in the troposphere. However, in many cases, air masses pass over considerably more than 100 km of land free from anthropogenic CO sources, and in such circumstances a larger proportion of the CO in the troposphere may be removed. Some models of the oxidising capacity of the troposphere contain the simplifying assumption that CO removal by soils is negligible (Mak *et al.*, 1992; Isaksen and Hov, 1987). The evidence of this project is that this assumption is often invalid. At least part of the "missing" sink for CO postulated by Mak *et al.* (1992) may simply be soil oxidation which was not included in their model.

Appendix 1: Standard RGA3 Reduction Gas Analyser settings

The RGA3 separates CO from other gases by passing the sample through 2 chromatographic columns in series. After separation, the CO is passed over a mercuric oxide bed where the CO reduces mercuric oxide to mercury. The mercury vapour produced is detected by its absorption in the UV (See Chapter 2, Section 2.1.1). A control panel on the right hand side of the instrument (Plate A1.1) allows the set and actual temperatures of the chromatography columns and of the mercuric oxide bed detector to be displayed. The set temperatures can be adjusted using a screw. The instrument's integrator electronics, which are set via on control panel on the left of the instrument compare the size of the absorbance peak with that of calibration standards, and display the concentration.

The standard settings on both control panels are given below.

Right Hand (Chromatography) Control Panel:

Range x1
Column Temp (°C) 105
Detector Temp (°C) 265

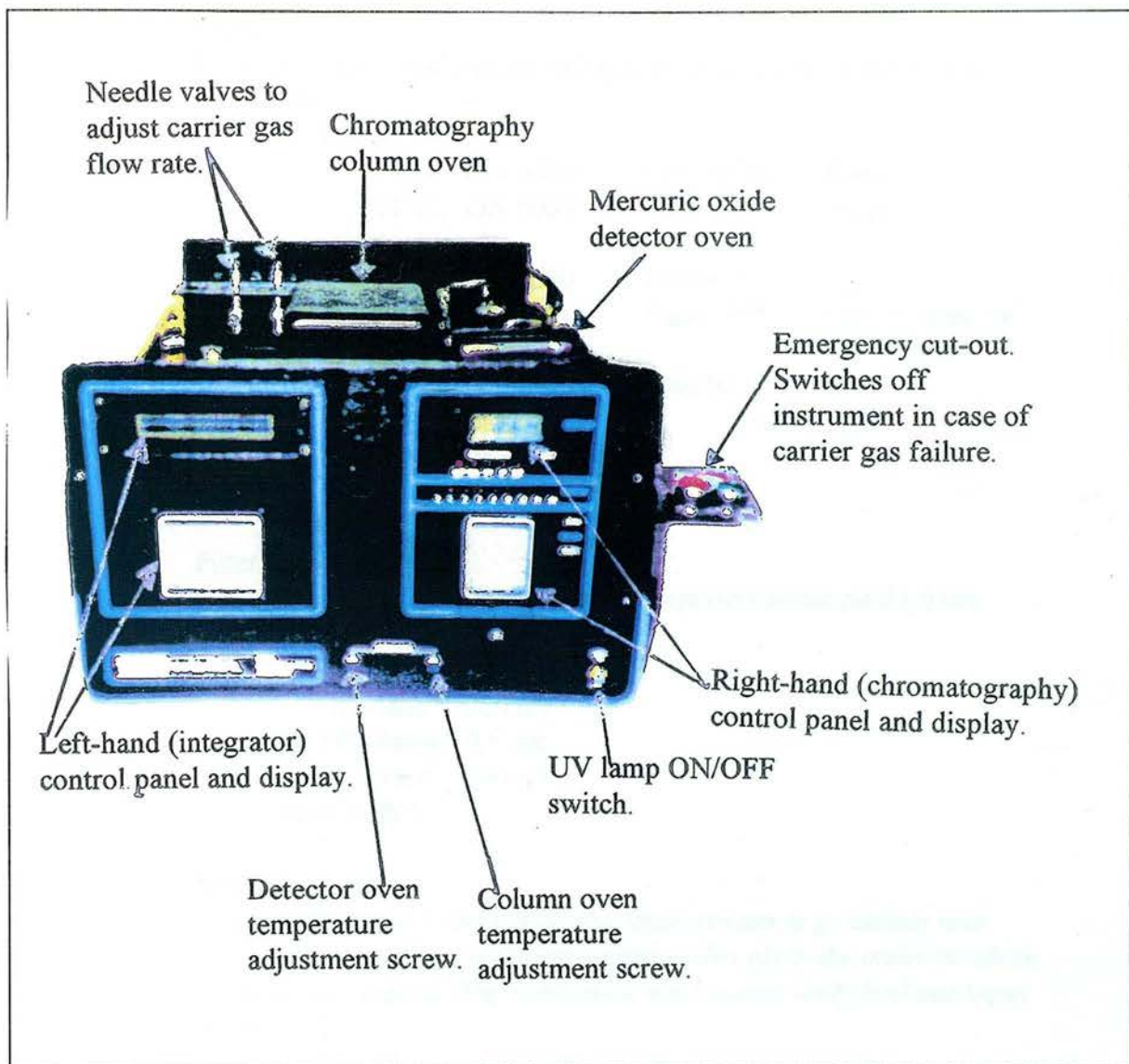


Plate A1.1 The RGA3 Reduction Gas Analyser

Left Hand (Integrator) Control Panel:

Table

Valve

Controls the times at which the valve on the chromatograph injection system switches from the load to inject positions.

(A) = switch from inject to load

(B) = switch from load to inject

1) Autotable

(A) = 0035 9999 9999

(B) = 0006 9999 9999

Peaks

Gives the names and timings of expected peaks, and concentration of standards.

1) Gates

Pk 01	ON 0010	OFF 0028	Forced
Pk 02	ON 0035	OFF 00100	Slope

2) Standards

Pk 01	Std 0000	Caltol 000	
Pk 02	Std xxxx	Caltol 10%	xxxx = conc. of std.

3) Alarms

000000	000000	00
--------	--------	----

4) Units

Std:	Ext Std	Units: ppb
------	---------	------------

5) Names

Pk 01	H2
-------	----

Pk 02	CO
-------	----

Filter

Settings which allow integrator to distinguish sample peaks from noise.

1) F01 Sense

0.12500 sec

Slice 200 μ V

2) F02 Sense

0.5 sec

Slice 500 μ V

Rest as F02

Streams

On instruments with more than one input stream (e.g. sample and calibration, or several different samples) this gives the order in which streams are sampled. The instrument used in this study had one input stream only.

Seq 01	01	00	00	00
	00	00	00	00

Seq 02	00	00	00	00
	00	00	00	00

Fault

External Start

Allows measurement cycle to be started by an external signal.

Normally:

Active - No State - Hi

During continuous measurement campaigns with external start from datalogger:

Active - Yes State - Lo

Trends

Allows maximum expected concentrations to be set to define the range of the D/A converter.

STM	CMP	Zero	Span	
TR01	01	02	0000	1000
TR02	00	00	0000	0000

Plotter

Allows running parameters of external plotter to be set.

Attn	Speed	Print Rt
x256	0.5cm/min	Yes

Event

Autotable

Sets the times within measurement cycle at which specified activities occur.

Cycle time	0075	
Stream step	0002	
Process data	0074	
Integ 1 On	0009	
Integ 1 Off	0029	
Integ 2 On	0035	
Integ 2 Off	0100	
Integ 3 On	9999	
Integ 3 Off	9999	
Auto Zero 1 On		0001
Auto Zero 2 On		9999
Auto Zero 3 On		9999
Filter 1 On	0003	
Filter 2 On	9999	
Filter 3 On	9999	
Filter 4 On	9999	
Filter 5 On	9999	
Plotter On	9999	

Appendix 2: Results of factorial experiments, to investigate CO production

The results of the factorial experiments to investigate CO production by soils carried out in Chapter 4 are shown graphically on the following pages.

See Chapter 2, Section 2.4.5 for details of the factorially designed experiment methodology.

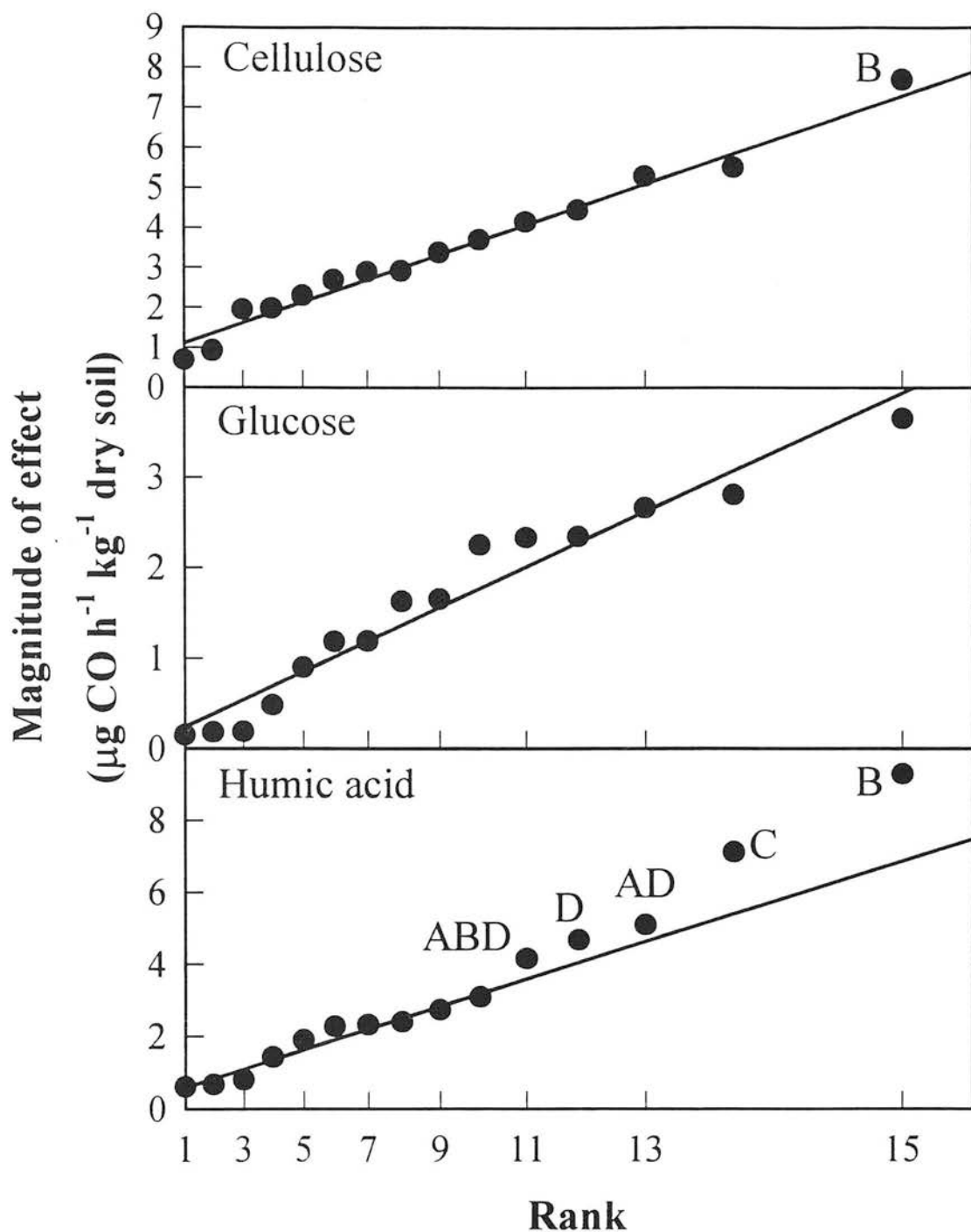


Figure A2.1 Results of factorial experiments on CO production by Gullane arable soil. Lines show regressions through non-significant points.

Capital letters show significant effects (see Chapter 4, Table 4.3).

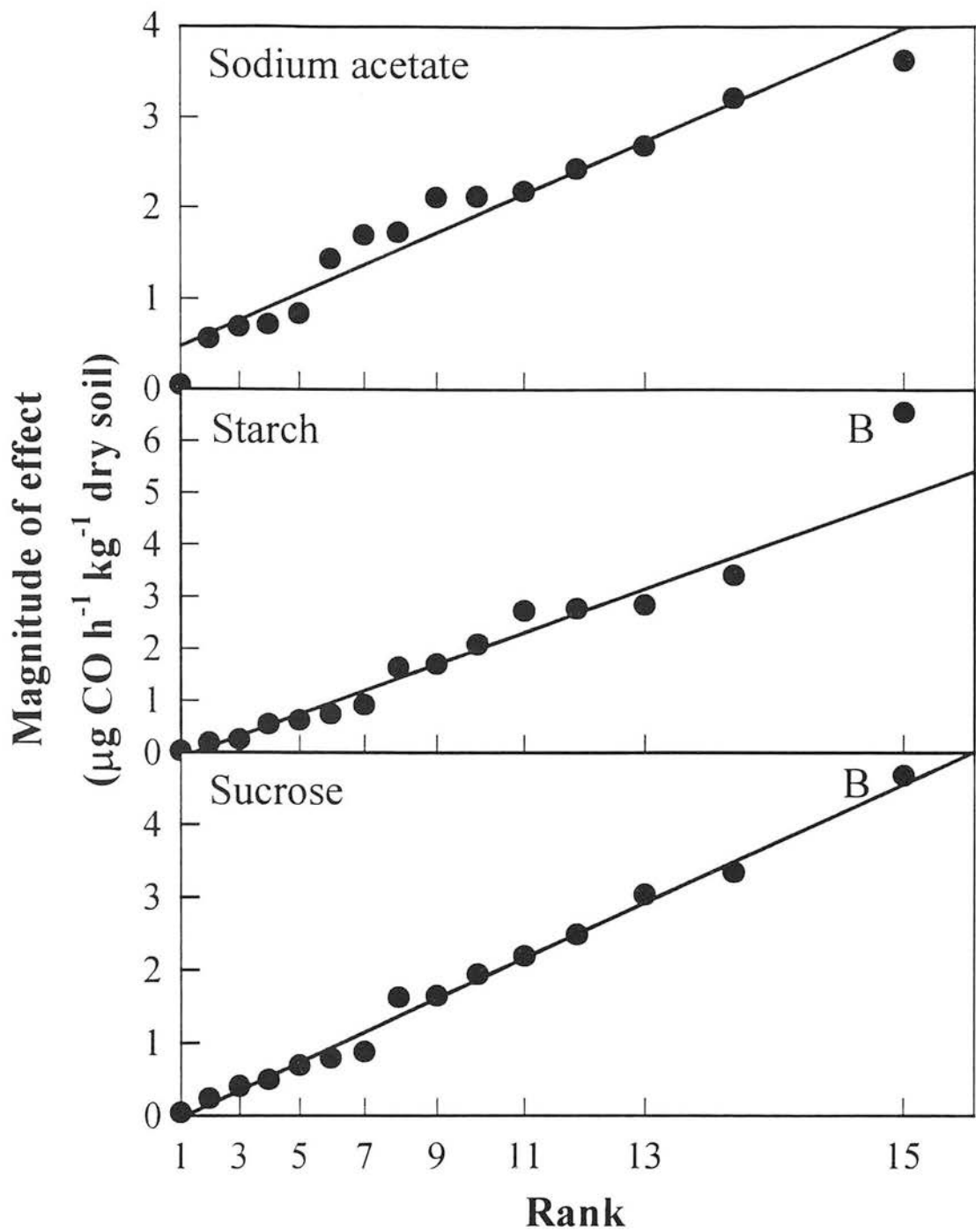


Figure A2.1 (cont). Results of factorial experiments on CO production by Gullane arable soil.
Lines show regressions through non-significant points.
Capital letters show significant effects (see Chapter4, Table 4.3).

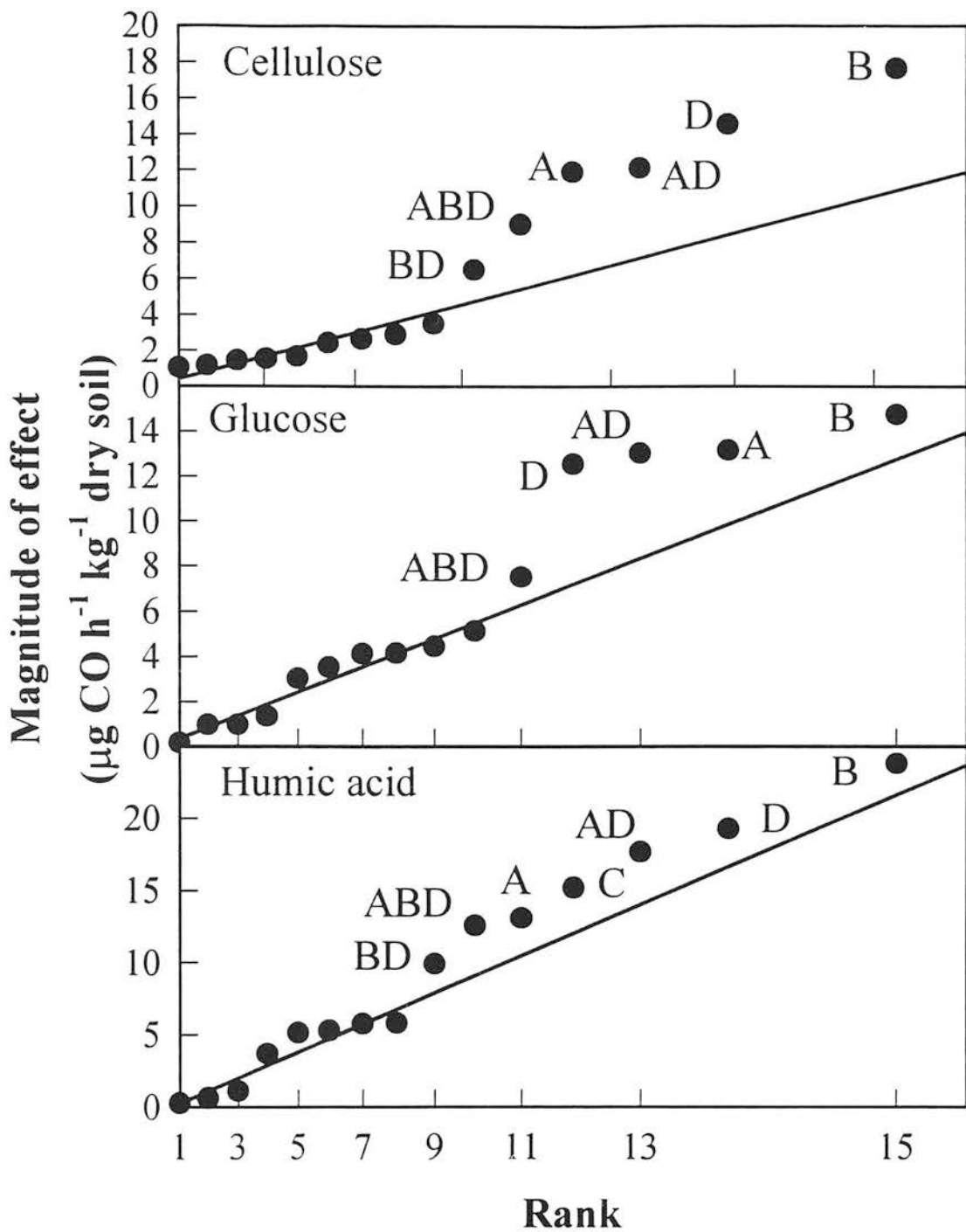


Figure A2.2 Results of factorial experiments on CO production by Gullane woodland soil. Lines show regressions through non-significant points.

Capital letters show significant effects (see Chapter 4, Table 4.3)

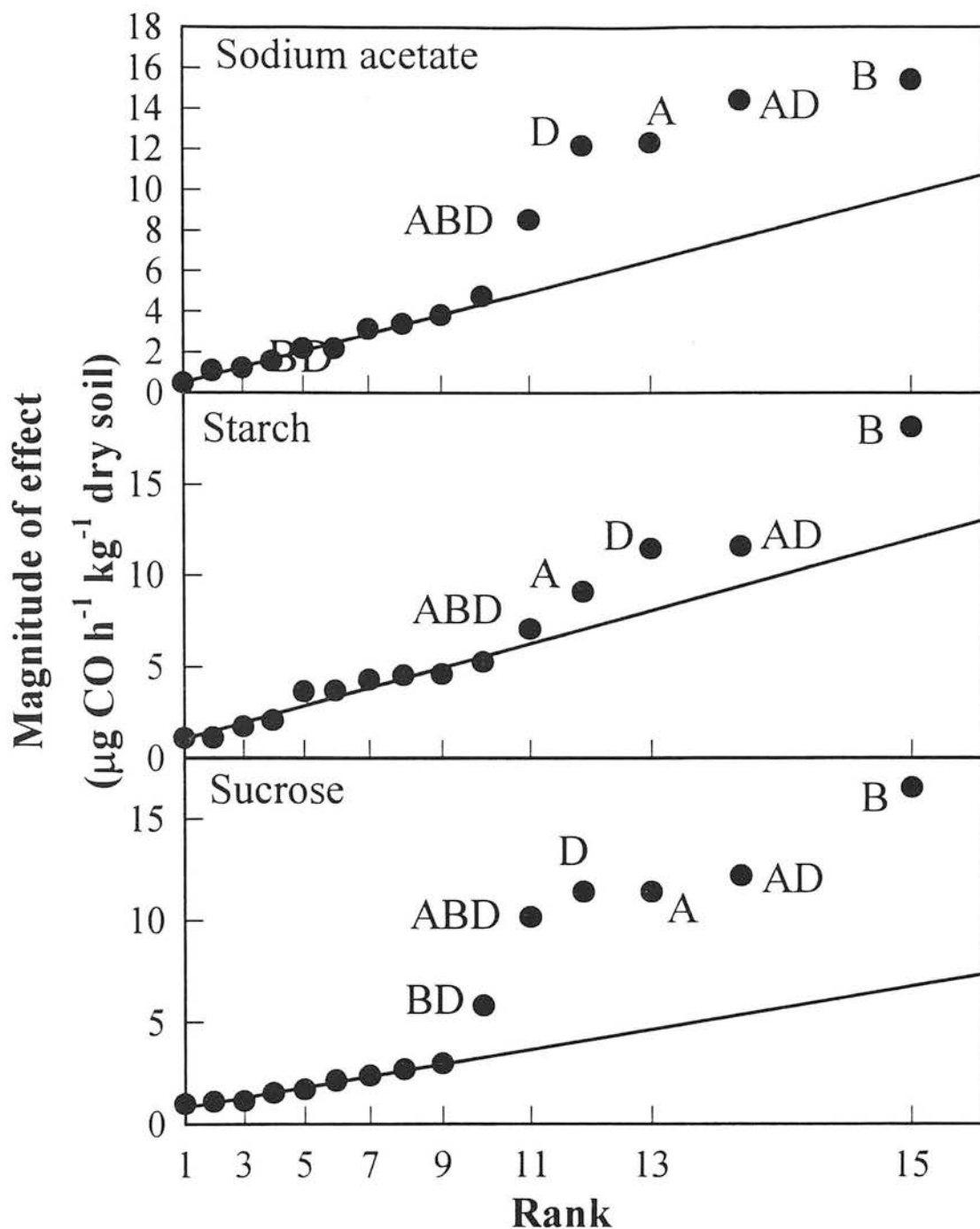


Figure A2.2 (cont). Results of factorial experiments on CO production by Gullane woodland soil.
 Lines show regressions through non-significant points.
 Capital letters show significant effects (see Chapter 4, Table 4.3).

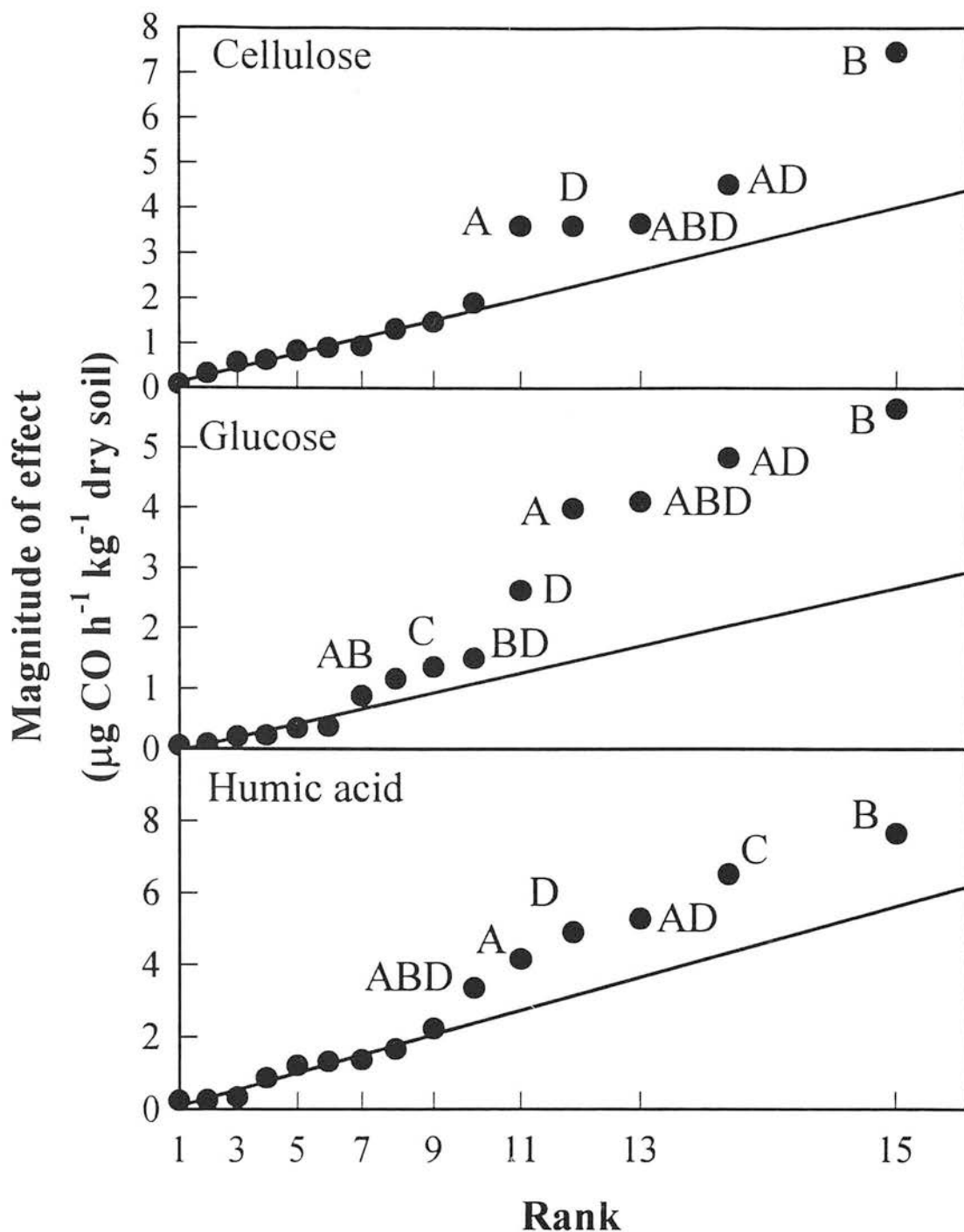


Figure A2.3 Results of factorial experiments on CO production by Bush arable soil. Lines show regressions through non-significant points.

Capital letters show significant effects (see Chapter 4, Table 4.3).

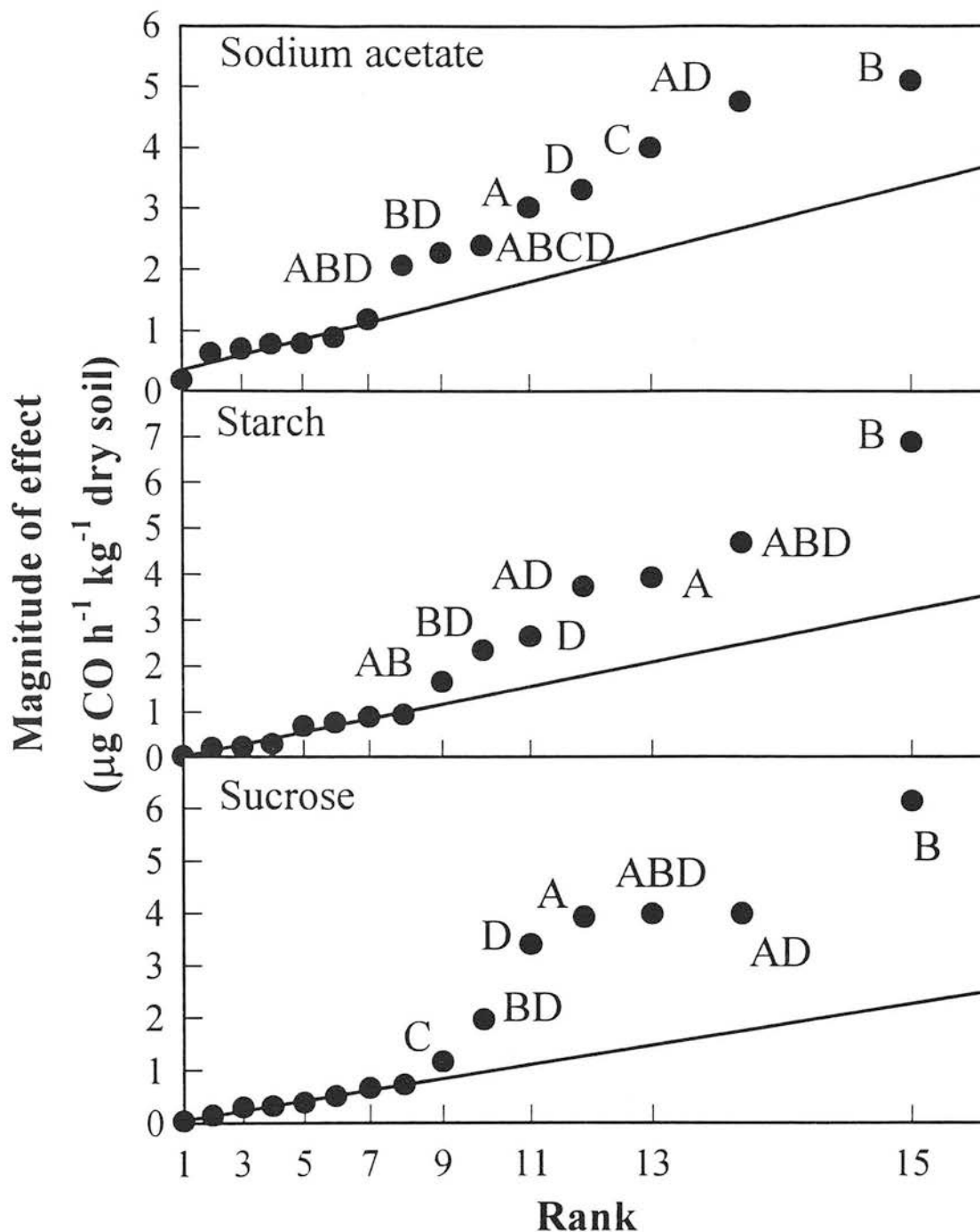


Figure A2.3 (cont) Results of factorial experiments on CO production by Bush arable soil.

Lines show regressions through non-significant points.

Capital letters show significant effects (see Chapter 4, Table 4.3).

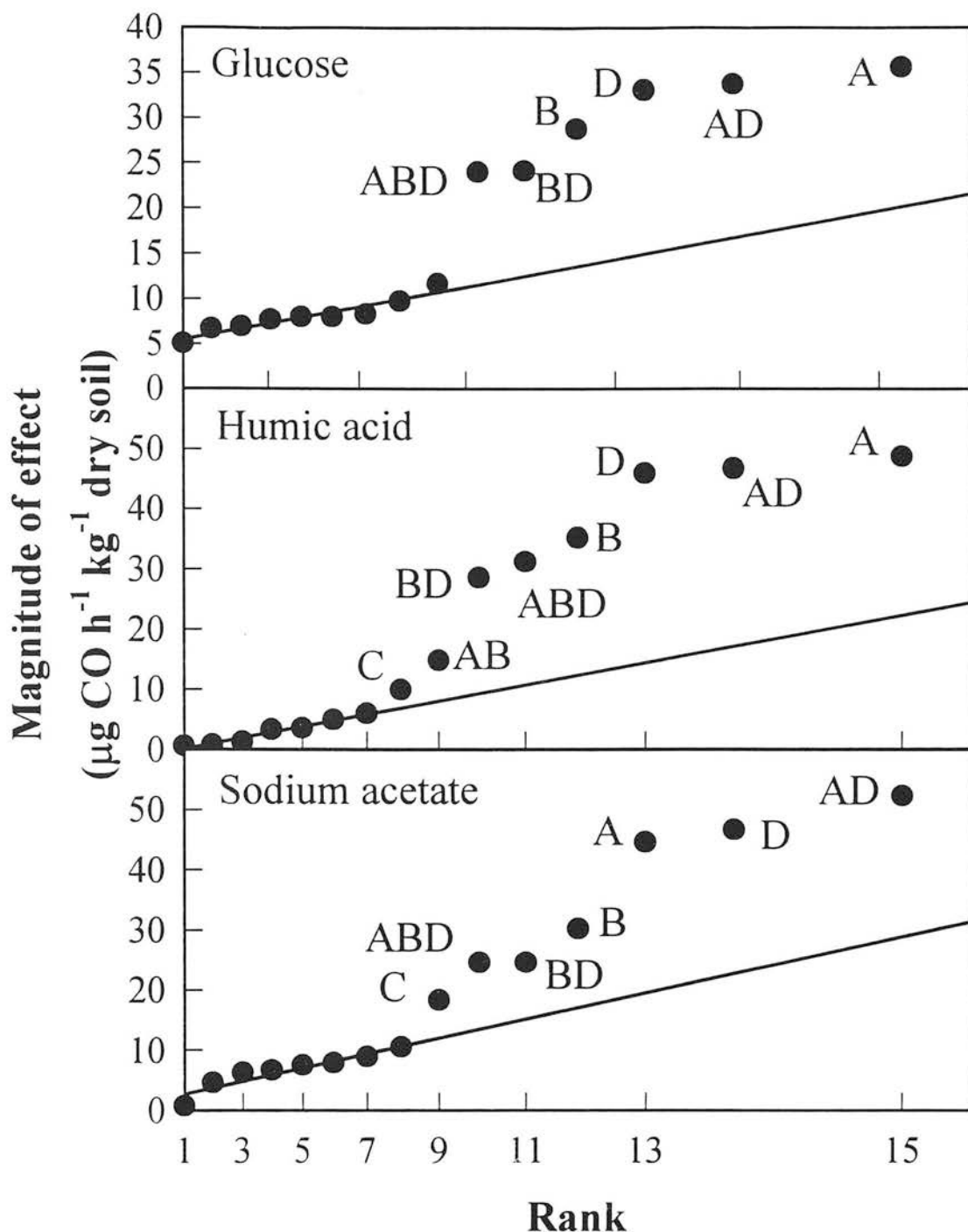


Figure A2.4 Results of factorial experiments on CO production by Bush deciduous woodland soil (dry area). Lines show regressions through non-significant points.

Capital letters show significant effects (see Chapter 4, Table 4.3).

Appendix 3: Explanation of meteorological parameters

The table below defines the meteorological parameters mentioned in Chapters 6 and 7, and other parameters used in their definitions.

Table A3.1 Meteorological parameters

Symbol	Name	Explanation	Reference
c _p	Specific heat of air.		Campbell, 1977.
d	The zero plane displacement	The height from zero (ground level) to the mean height of heat, vapour, gas or momentum exchange.	Campbell, 1977.
E	The evaporation rate		
f	Coriolis parameter	A correction factor which allows for the influence of the Earth's angular momentum on the atmosphere. The value varies with latitude.	Wyngaard, 1975.
g	Acceleration due to gravity, (9.81 m s ⁻²).		
H	Sensible heat flux		Campbell, 1977.
k	The von Karman constant	A constant which relates u* to the windspeed profile.	Monteith and Unsworth, 1990.
		$u_* = k \frac{du}{d \ln(z - d)}$	

Table A3.1 (cont.)

Symbol	Name	Explanation	Reference
L	The Monin-Obukhov length	<p>A parameter proportional to the height above a surface at which buoyancy factors dominate over mechanical (shear) factors in the production of turbulence</p> $L = \frac{\rho \ c_p \ T u_*^3}{kgC}$ <p>where ρ is the density of air, c_p is the specific heat capacity of air, and C the heat flux.</p>	Stull, 1993.
Ri	The gradient Richardson number	<p>A thermal stability parameter. $Ri = 0$ for neutral conditions and forced convection, is large and negative under unstable conditions, and large and positive under stable conditions</p>	Garratt, 1992
u	Horizontal windspeed		
u*	The friction velocity	<p>The square root of the shear stress, τ divided by the density of air.</p> $u_* = \sqrt{\frac{\tau}{\rho_a}}$ <p>(Can also be expressed as the root mean square deviation in the horizontal windspeed.</p> $u_* = \sqrt{(u')^2}$	Monteith and Unsworth, 1990.
u'		<p>Deviation of a measured horizontal windspeed from the mean.</p>	Stull, 1993.
v	Vertical windspeed		
v'		<p>Deviation of vertical windspeed from the mean</p>	Stull, 1993.

Table A3.1 Meteorological parameters

Symbol	Name	Explanation	Reference
v_d	Deposition velocity	The mass of a substance deposited per unit area divided by the mass per unit volume above the surface	Monteith and Unsworth, 1990.
z	Height above surface		
z_0	The roughness length	A constant for a given landcover such that $u = 0$ when $z = z_0$. Calculated from the equation $u = \frac{u_*}{k} \left(\ln \frac{z}{z_0} \right)$ A measure of the surface roughness based on observed windshear in the surface layer.	Monteith and Unsworth, 1990.
γ	The Ziltinkevich profile constant	The constant in the equation $\frac{hf}{u_*} = \gamma \sqrt{\frac{u_*}{fL}}$	Wyngaard, 1975.
λ	The latent heat of evaporation of water		
λE	The latent heat flux		
ρ_a	The density of air		
ρ_c	The mass concentration of CO		
τ	Shear stress	$\tau = -\rho_a v \frac{du}{dz}$	Monteith and Unsworth, 1990.
ζ	Atmospheric stability factor	The ratio of convective to mechanical production of turbulence. $\zeta = \frac{-kzgH}{\rho c_p T u_*}$	

References

- Amberger, A. Research on dicyandiamide as a nitrification inhibitor and future outlook. *Commun. in Soil Sci. Plant. Anal.* **20**, 1933-1955, (1989).
- Arah, J.R.M, Crichton, I.J, Smith, K.A, Clayton, H. and Skiba, U. Automated gas chromatographic system for micrometeorological measurements of trace gas fluxes *J. Geophys. Res.* **99**, 16593-16598, (1992).
- Atkins, P.W. *Physical Chemistry (2nd Edition)*. Oxford University Press, Oxford, (1982).
- Bae, J. and McCarty, P.L. Variation of carbon monoxide production during methane fermentation of glucose. *Water Environ. Res.* **65**, 890-899, (1993).
- Bakwin, P.S, Tans, P.P. and Novelli, P.C. Carbon monoxide budget in the northern hemisphere. *Geophys. Res. Lett.* **21**, 433-436, (1994).
- Bartholomew, G.W. and Alexander M. Microbial metabolism of carbon monoxide in culture and in soil. *Appl. Environ. Microbiol.* **37**, 932-937, (1979).
- Bartholomew, G.W. and Alexander, M. Soil as a sink for atmospheric carbon monoxide. *Science.* **212**, 1389-1391, (1981).
- Bartholomew, G.W. and Alexander M. Microorganisms responsible for the oxidation of carbon monoxide in soil. *Environ. Sci. Technol.* **16**, 300-301, (1982).
- Bates, D.R. and Witherspoon, A.E. The photochemistry of some minor constituents of the Earth's atmosphere. (CO₂, CO, CH₄, N₂O) *Monthly. Proc. Roy. Astron. Soc.* **112**, 101-124, (1952).
- Bédard, C. and Knowles, R. Physiology, biochemistry and specific inhibitors of CH₄, NH₄⁺ and CO oxidation by methanotrophs and nitrifiers. *Microbiol. Rev.* **53**, 68-84, (1989).
- Bender, M. and Conrad, R. Microbial oxidation of methane, ammonium and carbon monoxide, and turnover of nitrous oxide and nitric oxide in soils. *Biogeochem.* **27**, 97-112, (1994).
- Best, E.K. An automated method for determining nitrate-N in soil extracts. *Queensland J. Agric. Ani. Sci.* **33**, 161-165, (1976).

Biscoe, P.V, Scott, R.K. and Monteith, J.L. Barley and its environment. III. Carbon budget of the stand. *J. Appl. Ecol.* **12**, 269-293, (1975).

Bogner, J.E. Anaerobic burial of refuse in landfills: Increased atmospheric methane and implications for increased carbon storage. In *Trace Gas Exchange in a Global Perspective*. Ojima, D.S and Svensson, B.H. (Eds.) Ecol. Bull. (Copenhagen). **42**, 98-108, (1992).

Bower, J.S, Broughton, G.F.J, Willis, P.G. and Clark, H. *Air Pollution in the UK 1993/94*. AEA Technology, Abingdon, UK (1995).

Box, G.E.P, Hunter, W.G. and Hunter, J.S. *Statistics for Experimenters*. John Wiley and Sons, New York, (1978).

Brice, K.A, Eggleton, A.E.J. and Penkett, S.A. An important ground surface sink for atmospheric nitrous oxide. *Nature*. **268**, 127-129, (1977).

Brunke, E-G, Scheel, H.E. and Seiler, W. Trends in tropospheric CO, N₂O and CH₄ as observed at Cape Point, South Africa. *Atmos. Environ.* **24A**, 585-595, (1990).

Bullock, D.K, Hansen, C.L. and Poe, S.E. Carbon monoxide production from land applied cheese whey. *Bioresource Technol.* **54**, 231-233, (1995).

Businger, J.A. and Delaney, A.C. Chemical sensor resolution required for measuring surface fluxes by three common micrometeorological techniques. *J. Atmos. Chem.* **10** 399-410, 1990.

Campbell, G.S. *An Introductiton to Environmental Biophysics*. Springer-Verlag. New York. (1977).

Christensen, S, Ambus, P, Arah, J.R.M, Clayton, H, Galle, B, Griffith, D.W.T, Hargreaves, K. J, Klemetsson, L, Lind, A-M, Maag, M, Scott, A, Skiba, U, Smith, K.A, Welling, M, and Wienhold, F.G. Nitrous oxide emission from an agricultural field: Comparison between measurements by flux chamber and micrometeorological techniques. *Atmos. Environ.* In press, (1996).

Cicerone, R.J. How has the atmospheric concentration of CO changed? In *The Changing Atmosphere*. Rowland, F.S. and Isaksen, I.S.A (Eds), 49-61, John Wiley and Sons Ltd, New York, (1988).

Clayton, H, Arah, J.R.M. and Smith, K.A. Measurement of nitrous oxide emissions from fertilized grassland using closed chambers. *J. Geophys. Res.* **99**, 16599-16607, (1994).

Conrad, R. Capacity of aerobic microorganisms to utilize and grow on atmospheric trace gases (H_2 , CO and CH_4). In *Current Perspectives in Microbial Ecology*. Klug, M.S. and Reddy, C.A. (Eds). Am. Soc. for Microbiology. Washington. 461-467, (1984).

Conrad, R. Biogeochemistry and ecophysiology of atmospheric CO and H_2 . In *Advances in Microbial Ecology. Vol 10* Marshall, K.C. (Ed.) Plenum Press, New York. 231-283, (1988).

Conrad, R. and Seiler, W. Role of microorganisms in the consumption and production of atmospheric CO by soil. *Appl. Environ Microbiol.* **40**, 437-445, (1980).

Conrad, R. and Seiler, W. Utilization of traces of carbon monoxide by aerobic oligotrophic microorganisms in ocean, lake and soil. *Arch. Microbiol.* **132**, 41-46, (1982a).

Conrad, R. and Seiler, W. Arid soils as a source of atmospheric carbon monoxide. *Geophys. Res. Lett.* **9**, 1353-1356, (1982b).

Conrad, R. and Seiler, W. Influence of temperature, moisture, and organic carbon on the flux of H_2 and CO between soil and atmosphere: Field studies in subtropical regions. *J. Geophys. Res.* **90**, 5699-5709, (1985a).

Conrad, R. and Seiler, W. Destruction and production rates of carbon monoxide in arid soils under field conditions. In *Planetary Ecology*. Caldwell, D.E. and Brierley, J.A. (Eds), Van Nostrand Reinhold, New York. 112-119, (1985b).

Conrad, R. and Seiler, W. Characteristics of abiological carbon monoxide formation from soil organic matter, humic acids and phenolic compounds. *Environ. Sci. Technol.* **19**, 1165-1169, (1985c).

Conrad, R. and Thauer, R.K. Carbon monoxide production by *Methanobacterium thermoautotrophicum*. *FEMS Microbiol. Lett.* **20**, 229-232, (1983).

Conrad, R, Meyer, O. and Seiler, W. Role of carboxydobacteria in consumption of atmospheric carbon monoxide by soil. *Appl. Environ Microbiol.* **42**, 211-215, (1981).

Conrad, R, Schutz, H. and Seiler, W. Emission of carbon monoxide from submerged rice fields into the atmosphere. *Atmos. Environ.* **22**, 821-823, (1988).

Cotton, F.A. and Wilkinson, G. *Advanced Inorganic Chemistry: A Comprehensive Text (4th Edition)* John Wiley and Sons, New York. (1980).

Crooke, W.M. and Simpson, W.E. Determination of NH_4^+ in Kjeldahl digests of crops by an automated procedure. *J. Sci. Fd. Agric.* **22**, 9-10, (1970).

Crutzen, P.J. and Zimmermann, P.H. The changing photochemistry of the troposphere. *Tellus.* **43AB**, 136-151, (1991).

Crutzen, P.J., Heidt, L.E., Krasnec, J.P., Pollock, W.H. and Seiler, W. Biomass burning as a source of atmospheric gases CO , H_2 , N_2O , NO , CH_3Cl and COS . *Nature.* **282**, 253-256, (1979).

Daniel, C. Use of half-normal plots in interpreting factorial two-level experiments. *Technometrics.* **1**, 311-341, (1959).

Daniels, L., Fuchs, G., Thauer, R.K. and Zeikus, J.G. Carbon monoxide oxidation by methanogenic bacteria. *J. Bacteriol.* **132**, 118-126, (1977).

Derwent, R.G., Collins, W.J. and Simmonds, P.G. Ozone and carbon monoxide measurements at a remote maritime location, Mace Head Ireland, from 1990-1992. *Atmos. Environ.* **28**, 2623-2637, (1994).

Dianov-Klokov, V.I. and Yurganov, L.N. A spectroscopic study of the global space-time distribution of atmospheric CO . *Tellus.* **33**, 262-273, (1981).

Diekert, G., Hansch, M. and Conrad, R. Acetate synthesis from 2 CO_2 in acetogenic bacteria: is carbon monoxide an intermediate? *Arch. Microbiol.* **138**, 224-228, (1984).

Diekert, G., Schrader, E. and Harder, W. Energetics of CO formation and CO oxidation in cell suspensions of *Acetobacterium woodii*. *Arch. Microbiol.* **144**, 386-392, (1986).

Doddridge, B.G., Dickerson, R.R., Spain, T.G., Oltmans, S.J. and Novelli, P.C. Carbon monoxide measurements at Mace Head, Ireland. *NASA Conference Publication No. 3266*. 134-137, (1994).

Drury, D.J. Formic acid. In *The Kirk-Othmer Encyclopedia of Chemical Technology Volume 11*. Kroschwitz, J.I. and Howe-Grant, M. (Eds.) Wiley Interscience, New York. 951-958, (1994).

Duggin, J.A. and Cataldo, D.A. The rapid oxidation of atmospheric CO to CO_2 by soils. *Soil Biol. Biochem.* **17**, 469-474, (1985).

- Eikmanns, B, Fuchs, G. and Thauer, R.K. Formation of carbon monoxide from CO₂ and H₂ by *Methanobacterium thermoautotrophicum*. *Eur. J. Biochem.* **146**, 149-154, (1985).
- Evans, W.F.J. and Puckrin, E. An observation of the greenhouse radiation associated with carbon monoxide. *Geophys. Res. Lett.* **22**, 925-928, (1995).
- Fan, S.M, Wofsy, S.C, Bakwin, P.S, Jacob, D.J, Anderson, S.M, Keabian, J.B, McManus, J.B, and Kolb, C.E. Micrometeorological measurements of CH₄ and CO₂ exchange between the atmosphere and subarctic tundra. *J. Geophys. Res.* **97**, 16627-16643, (1992).
- Ferenci, T. The non-growth oxidation of carbon monoxide by *Pseudomonas methanica* and its relevance to studies of methane. In *Microbial Production and Utilization of Gases, (H₂, CH₄, CO)*. Schlegel, H.G, Gottschalk, G. and Pfennig, N. E (Eds), Goltze K.G. Gottingen. 371-378, (1976).
- Fishman, J. and Crutzen, P.J. The origin of ozone in the troposphere. *Nature.* **274**, 855-858, (1978).
- Förstel, H. and Jansen, B. Simultaneous measurements of H₂ and CO deposition velocities into soil. In *Transport and Transform of Pollutants in the Troposphere*. Borrell, P; Borrell, P.M and Seiler, W. (Eds.), Academic Publishing. 135-137, (1991).
- Frye, R.J, Welsh, D, Berry, T.M, Stevenson, B.A. and McCallum. T. Removal of contaminant organic gases from air in closed systems by soil. *Soil Biol. & Biochem.* **24**, 607-612, (1992).
- Funk, D.W, Pullman, E.R, Peterson, K.M, Crill, P.M. and Billings, W.D. Influence of water table on carbon dioxide, carbon monoxide, and methane fluxes from taiga bog microcosms. *Glob. Biogeochem. Cycles.* **8**, 271-278, (1994).
- Galbally, I.E. and Roy, C.R. Destruction of ozone at the earth's surface. *Quart. J. Roy. Met. Soc.* **106**, 599-620, (1980).
- Garcia-Diaz, A. and Phillips, D.T. *Principles of Experimental Design and Analysis*. Chapman and Hall, London. (1995).
- Garland, J.A. and Brost, R.A. Radiative cooling effects within and above the nocturnal boundary layer. *J. Atmos. Sci.* **38**, 2730-2746, (1981).
- Garland, J.A. and Derwent, R.G. Destruction at the ground and the diurnal cycle of ozone and other gases. *Quart. J. Roy. Met. Soc.* **105**, 169-183, (1979).

Garratt, J.R. *The Atmospheric Boundary Layer*. Cambridge University Press, Cambridge. (1992).

Gosink, T.A. and Kelley, J.J. Carbon monoxide evolution from arctic surfaces during spring thaw. *J. Geophys. Res.* **84**, 7041, (1979).

Greenberg, J.P, Zimmerman, P.L, Heidt, L. and Pollock, W. Hydrocarbon and CO emissions from biomass burning in Brazil. *J. Geophys. Res.* **89**, 1350-1354, (1984).

Greenberg, J.P, Zimmerman, P.L, and Haagenson, P. Tropospheric hydrocarbon and CO profiles over the US West Coast and Alaska. *J. Geophys. Res.* **95**, 14015-14026, (1990).

Greenberg, J.P, Zimmerman, P.L, Pollock, W.F, Lueb, R.A. and Heidt, L.E. Diurnal atmospheric methane, non-methane hydrocarbons and carbon monoxide at Mauna Loa. *J. Geophys. Res.* **97**, 10395-10413, (1992).

Haan, D. Martinerie, P. and Raynaud, D. Ice core data of atmospheric carbon monoxide over Antarctica and Greenland during the last 200 years. *Geophys. Res. Lett.* **23**, 2235-2238 (1996).

Hargreaves, K.J, Fowler, D, Storeton-West, R.L, and Duyzer, J.H The exchange of nitric oxide, nitrogen dioxide and ozone between pasture and the atmosphere. *Environ. Pollut.* **75**, 53-59, (1992).

Hargreaves, K.J, Skiba, U, Fowler, D, Arah, J, Wienhold, F.G, Klemetsson, L. and Galle, B. Measurement of nitrous oxide emission from fertilised grassland using micrometeorological techniques. *J. Geophys. Res.* **99**, 16569-16574, (1994).

Harriss, R.C. and Sebach, D.I. Methane flux in forested freshwater swamps of the southeastern United States. *Geophys. Res. Lett.* **8**, 1002-1004, (1981).

Harriss, R.C, Sachse, G.W, Hill, G.F, Wade, L.O. and Gregory, G.L. Carbon monoxide over the Amazon Basin during the wet season. *J. Geophys. Res.* **95**, 16927-16932, (1990a).

Harriss, R.C, Garstang, M, Wofsy, S.C, Beck, S.M, Bendura, R.J, Coelho, J.R.B, Drewry, J.W, Hoell J.M Jr, Matson, P.A, McNeal, R.J, Molion, L.C.B, Navarro, R.L, Rabine, V. and Snell, R.L. The Amazon boundary layer experiment. *J. Geophys. Res.* **95**, 16721-16736, (1990b).

Heichel, G.H. Removal of carbon monoxide by field and forest soils. *J. Environ. Qual.* **2**, 419-423, (1973).

- Hendrickson, O.Q. and Kubiseski, T. Soil microbial activity at high levels of carbon monoxide. *J. Environ. Qual.* **20**, 675-678, (1991).
- Hickey, R.F, Vanderweilen, J. and Switzenbaum, M.S. Production of carbon monoxide during methanogenesis on acetate and methanol. *Biotechnol. Lett.* **9**, 63-66, (1987).
- Ingersoll, R.B, Inman, R.B. and Fisher, W.R. Soil's potential as a sink for atmospheric carbon monoxide. *Tellus.* **26**, 151-159, (1974).
- Inman, R.E. and Ingersoll, R.B. Uptake of carbon monoxide by soil fungi. *J. Air Poll. Control Assoc.* **21**, 646-647, (1971).
- Inman, R.E, Ingersoll, R.B. and Levy, E.A. Soil: a natural sink for carbon monoxide. *Science.* **172**, 1229-1231, (1971).
- Isaksen, I.S.A. and Hov, Ø. Calculation of trends in the tropospheric concentrations of O₃, OH, CO, CH₄, and NO. *Tellus.* **39B**, 271-285, (1987).
- Jacob, D.J. and Wofsy, S.C. Budgets of reactive nitrogen, hydrocarbons, and ozone over the Amazon forest during the wet season. *J. Geophys. Res.* **95**, 16737-16754, (1990).
- Joglekar, H.S, Samant, S.D. and Joshi, J.B. Kinetics of wet air oxidation of phenol and substituted phenols *Water Resources.* **25**, 135-145, (1991).
- Jones, R.D. and Morita, R.Y. Carbon monoxide oxidation by chemolithotrophic ammonium oxidisers. *Can. J. Microbiol.* **29**, 1545-1551, (1983).
- Jones, R.D. and Morita, R.Y. Effect of inhibitors on carbon monoxide and methane oxidation by ammonium oxidisers *Can. J. Microbiol.* **30** 1276-1278, (1984).
- Jones, R.D, Morita, R.Y. and Griffiths, R.P. Method for estimating *in situ* chemolithotrophic ammonium oxidation using carbon monoxide oxidation. *Marine Ecol.* **17**, 259-269, (1984).
- Kalembasa, S.J. and Jenkinson, D.S. A comparative study of titrimetric and gravimetric methods for the determination of organic carbon in soil. *J. Sci. Fd. Agric.* **24**, 1085-1090, (1973).
- Khalil, M.A.K. Decline in atmospheric carbon monoxide raises questions about its cause. *Eos.* **76**, 353-354, (1995).

- Khalil, M.A.K. and Rasmussen, R.A. CO in the Earth's atmosphere: increasing trend. *Science*. **224**, 54-56, (1984).
- Khalil, M.A.K. and Rasmussen, R.A. CO in the Earth's atmosphere: indications of a global increase. *Nature*. **332**, 242-245, (1988).
- Khalil, M.A.K. and Rasmussen, R.A. The global cycle of carbon monoxide: trends and mass balance. *Chemosphere*. **20**, 227-242, (1990a).
- Khalil, M.A.K. and Rasmussen, R.A. Atmospheric carbon monoxide: latitudinal distribution of sources. *Geophys. Res. Lett.* **17**, 1913-1916, (1990b).
- Khalil, M.A.K. and Rasmussen, R.A. Global decrease in atmospheric carbon monoxide concentration. *Nature*. **370**, 639-641, (1994).
- Khalil, M.A.K, Rasmussen, R.A, Wang, M-X and Ren, L. Emissions of trace gases from Chinese rice fields and biogas generators: CH₄, N₂O, CO, CO₂ chlorocarbons and hydrocarbons. *Chemosphere*. **20**, 207-226, (1990).
- Kirchoff, V.W.J.H. and Marinho, E.V.A. Surface carbon monoxide measurements in Amazonia. *J. Geophys. Res.* **95**, 16933-16943, (1990).
- Küsel, K. and Drake, H.L. Effects of environmental parameters on the formation and turnover of acetate by forest soils. *Appl. Environ. Microbiol.* **61**, 3667-3675, (1995).
- Levy, H. (II) Tropospheric budgets for methane, carbon monoxide and related species. *J. Geophys. Res.* **78**, 5325-5332, (1973).
- Liebl, K.H. and Seiler, W. CO and H₂ destruction at the soil surface. In *Microbial Production and Utilization of Gases, (H₂, CH₄, CO)*. Schlegel, H.G; Gottschalk, G. and Pfennig, N. E (Eds), Goltze K.G. Gottingen. 215-229, (1976).
- Logan, J.A, Prather, M.J, Wofsy, S.C. and McElroy, M.B. Tropospheric chemistry: a global perspective. *J. Geophys. Res.* **86**, 7210-7254, (1981).
- MAFF. Soil texture (85) system and pesticide use. *Pamphlet 3001*. Ministry of Agriculture, Fisheries and Food (Publications), Alnwick, UK. (1985).
- Mak, J.E, Brenninkmeijer, C.A.M. and Manning, M.R. Evidence for a missing carbon monoxide sink based on tropospheric measurements of ¹⁴CO. *Geophys. Res. Lett.* **19**, 1467-1470, (1992).

- Marenco, A. and Delaunay, J.C. Experimental evidence of natural sources of CO from measurements in the troposphere. *J. Geophys. Res.* **85**, 5599-5613, (1980).
- Matthews, E. and Fung, I. Methane emission from natural wetlands: global distribution, area, and environmental characteristics of sources *Glob. Biogeochem. Cycles*. **1**, 61-86, (1987).
- McConnell, J.C, McElroy, M.B. and Wofsy, S.C. Natural sources of atmospheric CO. *Nature*. **233**, 187-188, (1971).
- Miller, J.C. and Miller J.N. *Statistics for Analytical Chemistry*. Halsted Press, Chichester, (1988).
- Miyahara, S. and Takahashi, H. Carbon monoxide evolution during auto- and enzymatic oxidation of phenols. *J. Biochem.* **69**, 231-233, (1971).
- Müller, J-F. Geographical distribution and seasonal variation of surface emissions and deposition velocities of atmospheric trace gases. *J. Geophys. Res.* **97**, 3787-3804, (1992).
- Monteith, J.L, and Unsworth, M.H. *Principles of Environmental Physics*. Edward Arnold, London, (1990).
- Meyer, O. Metabolism of aerobic carbon monoxide-utilizing bacteria. In *Microbial Gas Metabolism. Mechanistic, Metabolic and Biotechnological Aspects*. Poole, R.K and Dow, C.S. (Eds), Academic Press, London, 131-151, (1985).
- Nedwell, D.B. and Watson, A. Methane production, oxidation, and emission in a UK ombrotrophic peat bog: influence of sulphate from acid rain. *Soil Biol. Biochem.* **27**, 893-903, (1995).
- Novelli, P.C, Elkins, J.W and Steele, L.P. The development of a gravimetric reference scale for measurements of atmospheric carbon monoxide. *J. Geophys. Res.* **96**, 13109-12121, (1991).
- Novelli, P.C, Masarie, K.A, Tans, P.P. and Lang, P.M. Recent changes in atmospheric carbon monoxide. *Science*. **263**, 1587-1590, (1994).
- Parrish, D.D, Trainer, M, Buhr, M.P, Watkins, B.A. and Fehsenfeld, F.C. Carbon monoxide concentrations and their relation to concentration of total reactive oxidised nitrogen at two rural U.S. sites. *J. Geophys. Res.* **96**, 9309-9320, (1991).

Prather, M, Derwent, R, Ehhalt, D, Fraser, P, Sanhueza, E, and Zhou, X. Other trace gases and atmospheric chemistry. In *Climate Change 1994: Radiative Forcing of Climate Change and an Evaluation of the IPCC IS92 Emission Scenarios*. Houghton, J.T; Meira Filho, L.G, Bruce, J, Lee, H, Callander, B.A, Haites, E, Harris, N, and Maskell, K. (Eds.). Cambridge University Press, Cambridge. 73-126, (1995).

Rinsland, C.P and Levine, J.S. Free tropospheric CO concentrations in 1950-1951 deduced from IR total column amount measurements. *Nature*. **318**, 250-254, (1985).

Ritter, J.A, Lenschow, D.H, Barrick, J.D.W, Gregory, G.L, Sachse, G.W, Hill, G.F. and Woerner, M.A. Jr. Airborne flux measurements and budget estimates of trace species over the Amazon Basin during the GTE/ABLE 2B expedition. *J. Geophys. Res.* **95**, 16875-16886, (1990).

Ritter, J.A, Barrick, J.D.W, Sachse, G.W, Gregory, G.L, Woerner, M.A, Watson, C.E, Hill, G.F. and Collins, J.E. Jr. Airborne flux measurements of trace species in the Arctic boundary layer. *J. Geophys. Res.* **97**, 16601-16625, (1992).

Ritter, J.A, Barrick, J.D.W, Watson, C.E, Sachse, G.W, Gregory, G.L, Anderson, B.E, Woerner, M.A. and Collins, J.E. Jr. Airborne boundary layer flux measurements of trace species over Canadian boreal forest and northern wetland regions. *J. Geophys. Res.* **99** 1671-1685, (1994).

Robbins, R.C, Borg, K.M. and Robinson, E. Carbon monoxide in the atmosphere. *J. Air Poll. Control Assoc.* **18**, 106-110, (1968).

Robbins, R.C, Cavanagh, L.A. and Salas, L.J. Analysis of ancient atmospheres. *J. Geophys. Res.* **78**, 5341-5344, (1973).

Samuels, M. *Statistics for the Life Sciences*. Dellen Publishing Company, Riverside, New Jersey, (1989).

Sanhueza, E, Donoso, L, Scharffe, D. and Crutzen, P.J. Carbon monoxide fluxes from natural, managed, or cultivated savannah grasslands. *J. Geophys. Res.* **99**, 16421-16427, (1994a).

Sanhueza, E, Cárdenas, L, Donoso, L. and Santana, M. Effect of plowing on CO₂, CO, CH₄, N₂O, and NO fluxes from tropical savannah soils. *J. Geophys. Res.* **99**, 16429-16434, (1994b).

Scharffe, D, Hao, W.M, Donoso, L, Crutzen, P.J. and Sanhueza, E. Soil fluxes and atmospheric concentration of CO and CH₄ in the northern part of the Guayana Shield, Venezuela. *J. Geophys. Res.* **95**, 22475-22480, (1990).

Schuepp, P.H; Leclerc, M.Y; Macpherson, J.I and Desjardins, R.L. Footprint predictions of scalar fluxes from analytical solutions of differential equations. *B-L Meteor.* **50** 355-373 (1990).

Seiler, W. The cycle of atmospheric CO. *Tellus.* **26**, 116-135, (1974).

Seiler, W. and Fishman, J. The distribution of carbon monoxide and ozone in the free troposphere. *J Geophys. Res.* **86**, 7255-7265 (1981).

Seiler, W. and Junge, C. Carbon monoxide in the atmosphere. *J. Geophys. Res.* **75**, 2217-2226, (1970).

Seiler, W. and Junge, C. Entwicklung eines Messverfahrens zur Bestimmung kleiner Mengen Kohlenmonoxid (CO). *Meteorol. Rundschau.* **20**, 175-176, (1967).

Seiler, W. and Zankl, H. Man's impact in the atmospheric carbon monoxide cycle. In *Environmental Biogeochemistry*. Nriagu, J.O. (Ed.), Ann Arbor Science Publishers Inc. 25-37, (1976)

Seiler, W, Liebl, K.H, Stöhr, W.T. and Zakosek, H. CO- und H₂- Abbau in Böden. *Z. Pflanzenernähr. Bodenkd.* **140**, 257-272, (1977).

Seiler, W, Giehl, H. and Roggendorf, P. Detection of carbon monoxide and hydrogen by conversion of mercury oxide to mercury vapor. *Atmos. Technol.* **12**, 40-45, (1980).

Seiler, W, Giehl, H, Brunke, E-G. and Halliday, E. The seasonality of CO abundance in the southern hemisphere. *Tellus.* **36B**, 219-231, (1984).

Shine, K.P, Derwent, R.G, Wuebbles, D.J. and Morcrette, J-J. Radiative forcing of climate. In *Climate Change: the IPCC Scientific Assessment*. Houghton, J.T; Jenkins, V.J and Ephraums, J.J. (Eds.) Cambridge University Press, Cambridge. 41-68, (1990).

Sinha, A. and Toumi, R. A comparison of climate forcings due to chlorofluorocarbons and carbon monoxide *Geophys. Res. Lett.* **23**, 65-68, (1996).

Smith, K.A, Bremner, J.M. and Tabatabai, M.A. Sorption of gaseous atmospheric pollutants by soils. *Soil Sci.* **116**, 313-319, (1973).

Smith, K.A, Robertson, G.P, and Melillo, J.M. Exchange of trace gases between the terrestrial biosphere and the atmosphere in the midlatitudes.

Global Atmospheric-Biospheric Chemistry. Prinn, R.G. (Ed.) Plenum Press, New York, 179-203, (1994a).

Smith, K.A, Clayton, H, Arah, J.R.M, Christensen, S, Ambus, P, Fowler, D, Hargreaves, K. J, Skiba, U, Harris, G.W, Wienhold, F.G, Klemetsson, L. and Galle, B. Micrometeorological and chamber methods for measurement of nitrous oxide fluxes between soils and the atmosphere: Overview and conclusions. *J. Geophys. Res.* **99**, 16541-16548, (1994b).

Smith, K.A, Clayton, H, McTaggart, I.P, Thomson, P.E, Arah, J.R.M. and Scott, A. The measurement of nitrous oxide emission from soil by using chambers. *Phil. Trans. Roy. Soc. London A.* **351**, 327-338, (1995).

Spratt, H.G. and Hubbard, J.S. Carbon monoxide metabolism in roadside soils. *Appl. Environ. Microbiol.* **41**, 1192-1201, (1981).

Statistics for Industry. *Applied Statistics for Research Scientists* Manual for course presented at ICI Chemicals and Polymers, Wilton. Statistics for Industry, Victoria Ave, Knaresborough, Yorks. (1990a).

Statistics for Industry. *Design of Experiments* Manual for course presented at ICI Chemicals and Polymers, Runcorn. Statistics for Industry, Victoria Ave, Knaresborough, Yorks. (1990b).

Stewart, J.B and Thom, A.S Energy budgets in pine forest. *Quart. J. Roy. Met. Soc.* **99**, 154-170, (1973).

Streitwieser, A. Jr. and Heathcock, C.H. *Introduction to Organic Chemistry*. Macmillan Publishing Co. Inc, New York. (1981).

Stull, R.B. *An Introduction to Boundary Layer Meteorology*. Kluwer Academic Publishers, Dordrecht, (1993).

Swinerton, J.W; Linnebo, V.J. and Lamontagne, R.A. The ocean: A natural source of carbon monoxide. *Science*. **167**, 984-986, (1970).

Sze, N.D. Anthropogenic CO emissions: Implications for the atmospheric CO-OH-CH₄ cycle. *Science*. **195**, 673-675, (1977).

Tarr, M.A, Miller, W.L. and Zepp, R.G. Direct carbon monoxide photoproduction from plant matter. *J. Geophys. Res.* **100**, 11403-11413, (1995).

Thompson, A.M. and Cicerone, R.J. Atmospheric CH₄, CO and OH from 1860 to 1985. *Nature*. **321**, 148-150, (1986a).

Thompson, A.M. and Cicerone, R.J. Possible perturbation of CO, CH₄, and OH. *J. Geophys. Res.* **91**, 10853-10864, (1986b).

Tseng, J. and Huang, C.P. Mechanistic aspects of the photocatalytic oxidation of phenol in aqueous solution. *ACS Symposium Series*. **422**, 12-39, (1990).

Tyler, S.C, Lowe, D.C, Dlugokencky, E, Zimmerman, P.R. and Cicerone, R.J. Methane and carbon monoxide emissions from asphalt pavement: measurements and estimates of their importance to global budgets. *J. Geophys. Res.* **95**, 14007-14014, (1990).

Vance, E.D, Brookes, P.C. and Jenkinson, D.S. An extraction method for measuring soil microbial biomass C. *Soil Biol. & Biochem.* **19**, 703-707, (1987).

Wang, V. and Shaw, J.H. Variations in the abundance of atmospheric carbon monoxide near the ground. *J. Appl. Met.* **9**, 180-182, (1969).

Watson, C.E, Fishman, J. and Reichle, H.G. Jr. The significance of biomass burning as a source of carbon monoxide and ozone in the southern hemisphere tropics: A satellite analysis. *J. Geophys. Res.* **95**, 16443-16450, (1990).

Watson, R.T, Rodhe, H, Oeschger, H. and Siegenthaler, U. Greenhouse gases and aerosols. In *Climate Change: the IPCC Scientific Assessment*. Houghton, J.T; Jenkins, V.J and Ephraums, J.J. (Eds.). Cambridge University Press, Cambridge. 1-40, (1990).

Weinstock, B. Carbon monoxide: Residence time in the atmosphere. *Science*. **166**, 224-225, (1969).

Wofsy, S.C, McConnell, J.C. and McElroy, M.B. Atmospheric CH₄, CO and CO₂. *J. Geophys. Res.* **77**, 4477-4493, (1972).

World Resources Institute. *World Resources 1992-1993*. Oxford University Press, Oxford. (1992).

Wyngaard, J.C. Modelling the planetary boundary layer - extension to the stable case. *B-L Meteor.* **9**, 441-460, (1975).

Publications arising from this thesis

Journal papers

Moxley, J.M and Cape, J.N. Depletion of carbon monoxide from the nocturnal boundary layer. *Atmospheric Environment* **31** 1147-1155, (1997).

Moxley, J.M. and Smith, K.A. Oxidation of atmospheric CO by soils: field and laboratory studies of soil factors affecting oxidation rates. *Soil Biology and Biochemistry*, In Press (1997)

Moxley, J.M and Smith, K.A. CO production by some Scottish soils. Submitted to *Tellus* (1997).

Other

Moxley, J.M; Smith, K.A; and Cape, J.N. "Carbon Monoxide Exchanges Between Soils and the Atmosphere." Poster presentation at the TIGER programme progress meeting, Grange over Sands, Feb. 1996.

Moxley, J.M; Smith, K.A; and Cape, J.N. Carbon Monoxide Exchanges Between Soils and the Atmosphere. Poster presentation at the European Geophysical Society Conference, Hamburg, April 1995. Abstract in *Annales Geophysicae* Supplement II to Vol 13. P C399. 1995

Moxley, J.M; Smith, K.A; and Cape, J.N. Carbon Monoxide Exchanges Between Soils and the Atmosphere. Presentation at the TIGER programme progress meeting, Grange over Sands, Feb. 1995.

Dobbie, K.E; Moxley, J.M; and Smith, K.A. "Comparison of Woodland and Agricultural Soils as Sinks for Methane and Carbon Monoxide." Poster presentation

at the Greenhouse Gas Balance in Forestry Conference, Royal Geographic Society,
London. Nov 1994.